Examensarbete
LITH-ITN-ED-EX--07/001--SE

Investigation of alternative current measurements in high-voltage applications

Jens Holmgren

2007-01-17

Linköpings universitet
TEKNISKA HÖGSKOLAN

Department of Science and Technology
Linköpings Universitet
SE-601 74 Norrköping, Sweden

Institutionen för teknik och naturvetenskap
Linköpings Universitet
601 74 Norrköping

LITH-ITN-ED-EX--07/001--SE

Investigation of alternative current measurements in high-voltage applications

Examensarbete utfört i elektronikdesign
vid Linköpings Tekniska Högskola, Campus Norrköping

Jens Holmgren

Handledare Christer Sjöberg
Examinator Lars Backström

Norrköping 2007-01-17

Avdelning, Institution
Division, Department

Institutionen för teknik och naturvetenskap

Department of Science and Technology

Datum
Date

2007-01-17

Språk
Language

☐ Svenska/Swedish
☒ Engelska/English

☐ _____

Rapporttyp
Report category

Examensarbete
☐ B-uppsats
☐ C-uppsats
☒ D-uppsats

☐ _____

ISBN

ISRN **LITH-ITN-ED-EX--07/001--SE**

Serietitel och serienummer
Title of series, numbering

ISSN

URL för elektronisk version

Titel
Title

Investigation of alternative current measurements in high-voltage applications

Författare
Author

Jens Holmgren

Sammanfattning
Abstract

ABB:s MACH2 system uses a number of currents to ignite thyristors for AC/DC-trassformation and they are measured for control and protection. The measurement methods used today has major drawbacks. Two alternative techniques are investigated, one based on the Hall-Effect (HED) and the other based on Anisotropic Magnetoreistanse (AMR), both techniques sensing the magnetic field produced by currents in a conductor. The HED hawe low sensitivity so some kind of flux concentrators is needed. This adds volume, costs and complexity to the device. The AMR technique is much more sensitive than the HED. Unfortunately AMR are also much more sensitive for high over currents that may damage the devise, and they are not as common on te market. By testing linearity, step response and frequency dependency for some components, my conclusion is that HED components with toroidal flux concentrators utilizing magnetic feedback (Closed Loop, CL) may be used in this particular application. A drawback with CL are that they, when measuring sharp edged step signals, suffer from overshoots at the output that might activate the over current protection.

Nyckelord
Keyword

ABB,HVDC,current measurements,strömmätning,high power,högspänning,kraftöverföring,AC,DC,MACH2,Hall-Effect,Anisotropic Magnetoreistanse,Magnetoreistanse,magnetic field,magnetfält,flux concentrators,flödeskonsentrator,linearity,lingäritet,step response,steg

Master Thesis

INVESTIGATION OF
ALTERNATIVE CURRENT MEASUREMENTS
IN
HIGH-VOLTAGE APPLICATIONS

Carried out at ABB Power Technologies AB, Ludvika

By Jens Holmgren

Linköping University, ITN Campus Norrköping

Supervisor: Christer Sjöberg
Examiner: Lars Backström

ABSTRACT

The MACH2 controlling and protection system are used to operate a number of thyristors to transform AC current to DC current, or reverse. The MACH2 measures a number of currents to calculate when to ignite the thyristors and to protect the overall system from power components. These current measurements are currently done with a current transformer or a shunt resistor with an isolation amplifier. Both these methods has major drawbacks, it is not possible to measure DC currents with the transformer technique and with the shunt there is a problem with high current density through the conductors on the Printed Circuit Board (PSB), in addition to that the isolation amplifier are unlinear at low currents.

Two alternative measuring techniques are investigated in this thesis, devises based on the well-known Hall-Effect (HED) and devises based on Anisotropic Magnetoreistanse (AMR), both techniques uses the magnetic field produced by currents in a conductor to indirectly measure the current. The HED technique is well established for current measurements but with low sensitivity some kind of flux concentrator is needed to concentrate the magnetic field through the sensor. This adds volume, costs and some complexity to the device. The AMR technique is much more sensitive than the HED and do not need flux concentrators. Unfortunately these components are also much more sensitive for mistreatment and high over currents may damage the devise permanently. Also, current measurement devises based on AMR are not as common as those based on HED.

By testing the linearity, step response and frequency dependency for some different components on the market, my conclusion is that HED components with toroidal flux concentrators utilizing magnetic feedback (so called closed loop devises, CL) may be used in this particular application. A possible major drawback with CL are that they, when measuring sharp edged step signals, suffer from overshoots at the output that might activate the over current protection if no special care is taken.

PREFACE

Winter 2005. My first professional contact with ABB in Ludvika as a “thesis-project-searching”- student was with Johan Mood at the “Labour Market Day” at Umeå University, Uniaden 05. After a while talking about working at ABB I gave him an informal thesis application and moved on, knowing that I most likely would not get a project this time either. A couple of weeks later I get a call from Roland Siljeström who suggested a project about investigating alternative current measurement techniques. I promised to think about it and call him in a couple of weeks. Unfortunately, a pleasant summer can play tricks with your time perception, and the weeks turned to about tree months. Nevertheless, I called him and we decided to go forward with the project.

I started my work in autumn of 2005. Despite that I did take some longer breaks for Christmas, two unrelated courses and to work as a janitor for tree weeks, a total of 11 weeks, I have manage to complete my work and thesis report at spring of 2006. It has been an instructive time with many new experiences about practical investigation.

/The Author

TABLE OF CONTENTS

LIST OF FIGURES

LIST OF EQUATIONS

ACKNOWLEDGMENTS

I want to give great thanks to my supervisor Christer Sjöberg for all help, support and patience with all my questions. I also want to thank my examiner Lars Backström for helping me with the administrative work related to this thesis and my final examination, Head of Department Lars Lindgren for having me as a thesis worker, Hans Björklund for suggesting the project, Roland Siljeström for offering it to me, Johan Mood for convey my thesis application to Roland, Professor Mats Fahlman for helping me with some quantum physic theories and all colleagues at the department for all their help.

BACKGROUND AND PURPOSE

The department (TC) at ABB Power Technologies AB (PTPS) where the thesis is carried out at is responsible for the computer platform MACH2, a control and protection system for HVDC Stations. This system is built up with modules for flexibility and easy maintenance. For the MACH2 system to be able to work, measurements of the system to be controlled and protected are necessary. Special measurement boards are used to achieve these measurements.

In many applications the measured quantity is a high current with nominal values (I_n) that varies depending on method used. Today there are mainly two methods, through current transformers or shunt resistor with an isolation amplifier. The measurement signal is transformed from analogue to digital in order to be communicated between modules in the MACH2 system. One aspect that restricts the accuracy is the fix number of bits that is available, i.e. digital resolution.

For the transformer method an I_n of 1A or 5A, and maximum values of approximately $25*I_n$, are measured. The measured current is led directly to the transformer with no contact to the PCB. The analogue measurement signal for this method is modulated so that high accuracy is established up to $3*I_n$, see Figure 1. The over currents are allowed to be $100*I_n$ for 1s without any damage. Due to the nature of transformers isolation between input and output is achieved. Upper bandwidth limit is approximately in the order of 2 - 20kHz 3dB 1:st order, depending of specifications. With this method DC currents cannot be measured.

In the applications where shunts are used, only lower currents are measured with a typical maximum current of 360mA, some special boards goes as high as maximum continuous current 7A and 20A for 5s. The measured current is led through routs on the PCB to the shunt and if the over current is exceeded the PCB may suffer permanent damage due to high current density. To achieve isolation between input and output an isolation amplifier is used. For this method the bandwidth is DC to 4 - 24kHz 3dB 2:nd order and the transconductans is linear for the entire input interval. Mainly DC currents are measured with this method.

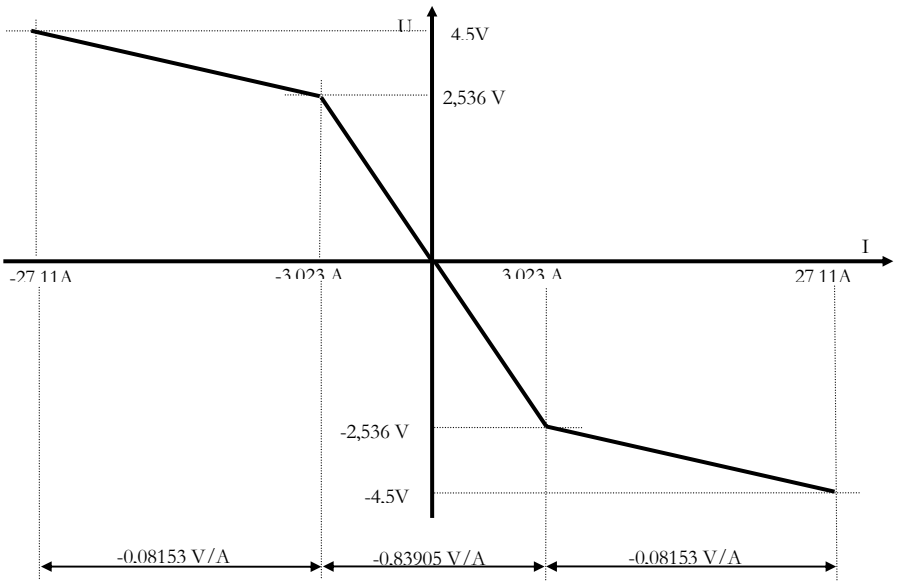

Figure 1: Example transconductans in transformer-method. All values are peak values.

There is a request to find a method that can be used for both AC and DC and both low and reasonably high currents so that only one or a few different measuring boards is needed to cope with the demands of MACH2 in various implementations. This would make the system cheaper and ease maintenance. The general object of this thesis is to investigate the possibility to realise this request and to investigate various methods that might be engaged in the MACH2 system.

METHOD AND DELIMITATIONS

There exist a number of different current measurement methods available on the market today, but when it comes to accuracy, linearity, measurement range, speed and durability VS costs, there are mainly four basic methods of interest: through current transformers, shunt resistors, Hall-effect sensors and anisotropic magnetoresistive current sensors.

For the thesis not to be unwieldy, I limited the investigations to primarily two methods: Hall-effect sensors and anisotropic magnetoresistive current sensors. The methods used today in the MACH2 system are quite well known for the applications, so only comparisons to these will be performed.

The different measurements I perform for this thesis are linearity measurements, step response, frequency dependency and some temperature stability and magnetic field sensitivity. The two later is only arbitrary tested due to difficulties to produce adequate tests.

The linearity measurements are carried out to find if the components of interest is enough linear also for sufficiently low currents. Some components are so unlinear that I therefore discarded them from further tests.

I used step response analysis to investigate speed (rise-time, time-delay), stability and overshoots. High overshoots may cause the over-current protection system to be activated even if the current are not high enough for that to occur.

Frequency dependency is important for the signal not to be distorted. As mentioned a bandwidth from DC to 20-25kHz 3dB 1:st order is desirable, and all tested components has a bandwidth >100kHz.

HALL-EFFECT DEVICES

The Hall-effect was discovered by Edwin Herbert Hall in 1879 and has consequently been known for over one hundred years, but has only been put to noticeable use in the last three decades. With the mass production of semiconductors, it became feasible to use the Hall-effect in high volume products. Today, Hall-effect devices are included in many products, ranging from computers to sewing machines, automobiles to aircraft, and machine tools to medical equipment.[1]

Theory

The ideas of Hall-Effect Devices (HED) are built upon the principals on interaction between moving charges and magnetic fields. When a charged object is mowing with a component of movement perpendicular to a magnetic field, it will perceive a force perpendicular to both that direction of movement and magnetic field acting on it. This force is called the *Lorentz force* and is expressed as

$$\vec{F} = Q(\vec{v} \times \vec{B}) \qquad \text{Eq. 1: } \textit{Lorentz force.}$$

were $\vec{F}$, $\vec{v}$ and $\vec{B}$ are vectors of magnetic force, velocity of object and magnetic flux density respectively, Q is the electric charge of the object. If $\vec{v}$ and $\vec{B}$ is perpendicular to each other their contribution to $\vec{F}$ will be perpendicular to both $\vec{v}$ and $\vec{B}$.

In a HED the charged objects is a current of either electrons or holes (here holes are considered as objects) led through a thin plate of conducting material. With no magnetic field present the current of electrons or holes is distributed evenly in the plate, as shown in Figure 2. If a magnetic field is

present the electrons or holes drift in the direction of $\vec{F}$, and there results a voltage difference V_h between the sides of the sensor, as shown in Figure 3. This voltage V_h is found to be proportional to the current through the plate.

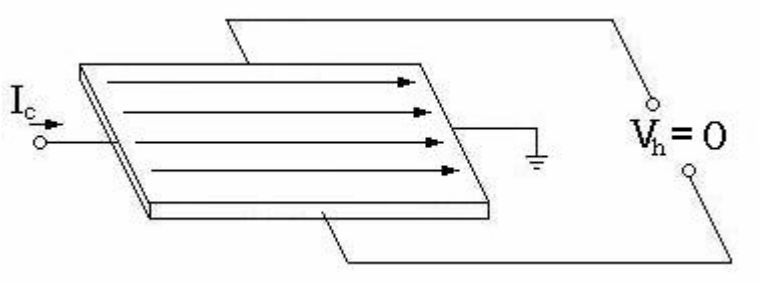

Figure 2: Illustration of Hall-effect. $\vec{B} = 0$.[1]

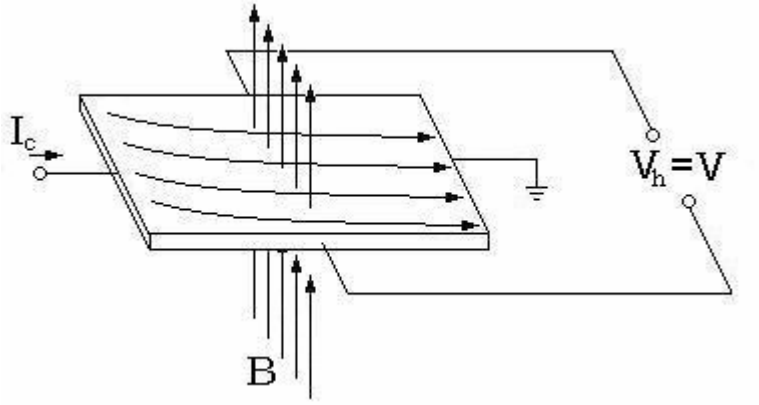

Figure 3: Illustration of Hall-effect. $\vec{B} \neq 0$.[1]

In general the plate can be of any conducting material, but the drift velocity $\vec{v}$ of the electrons and holes depends on the mobility (μ)[1] of the plate material and V_h gets proportionally bigger for higher drift velocities. Therefore semiconductors, which often have higher mobility, are utilized in Hall probes rather then conductors, which have somewhat lower mobility. For example, intrinsic silicon has a mobility of $1600\,cm^2/Vs$ (electrons) and silver (a very god conductor; high conductivity) has a mobility of $56\,cm^2/Vs$ [2].

One great characteristic of the HED is that it cannot get harmed by high magnetic fields. Since the sensors for practise use requires signal conditioning, the over all output will most likely saturate according to the

[1] Not to be confused with conductivity (σ)

conditioning circuit, not according to the HED itself. Another positive characteristic is that magnetic polarity is detected straightforward, i.e. changed polarity means opposite electron drift and reversed V_h.

Unfortunately the sensor suffers from some less desirable characteristic, as the piezoresistance effect and the temperature drift. The piezoresistance effect is a change in resistance proportional to strain. It is possible to minimise this effect by using two (or more) adjacent sensors with different orientation. By summing the outputs eliminates the signal due to stress.[1] The temperature is affecting sensitivity due to resistance change, and with a unchanged supply voltage the current (i.e. number of charged objects) will change. A simple way to deal with the temperature dependence is to use for example a thermistor, with a resistance/temperature coefficient opposite that of the sensor, in series with the output. This will keep the current trough the sensor unchanged. An offset voltage is also present if the voltage is measured at each terminal of the HED according to ground. This voltage is the same at each terminal and is terminated since the output is taken as a differential voltage between the terminals. The sensitivity of the sensor is ratiometric, witch means that the sensitivity is dependent of the supply voltage (V_s) and, for HED:s, increases proportionally with V_s. This is simply due to Ohm's law and higher voltage means more electrons to drift.

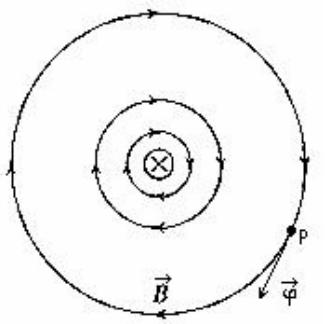

Figure 4: Magnetic field lines around a conductor.
Current going in to the paper.

Current Sensors

If a current is led through a conductor, it will induce a magnetic field around the conductor. This field is proportional to the current and inversely

proportional to the distance from the conductor, see Figure 4. The magnetic field follows the relationship (in vacuum or air)

$$\overrightarrow{B_{I_p}} = \frac{\mu_0 I_p}{2\pi r}\vec{\varphi}$$

Eq. 2: *Magnetic flux density around a straight circular conductor.[3]*

Were

$$\vec{\varphi} = \frac{\vec{I}}{\left|\vec{I}\right|} \times \frac{\vec{r}}{\left|\vec{r}\right|}$$

Eq. 3: *Azimuthal unit vector.*

is the unit vector pointing in the azimuthal direction at a point P, at a distance r from the centre of the conductor. $\mu_0 \equiv 4\pi * 10^{-7}\, Vs/Am$ is the permeability of free space. A HED placed in the magnetic field of a conductor, perpendicular to $\vec{B}_{I_p}$, will induce a measurable voltage $V_h \neq 0$ and the current in the conductor can be determined. But even though silicon is used the sensitivity is not that very high, only in the order of $0{,}1\, \mu V_h / V_s / \mu T$ (V_s is the supply voltage). For that reason a number of measures are taken to increase the sensitivity depending on how the Hall sensor will be used. One general thing to do for practical usage is to simply amplify V_h. Additionally there are a number of aggravating issues making the accuracy of the determination low. For example, different kinds of noise will have great impact on the measurement due to the low sensitivity of the sensor, V_h depends highly on the distance from the conductor and it is unprotected from external magnetic fields.

In the case of current measurements a very common technique to deal with the downsides of the HED is to use steal cores as flux concentrators, as described later in a separate section. Another technique is to use Integrated Magnetic Concentrator (IMC) sensors. This technique also utilises flux concentrators but in a less expensive and less bulky manner. This will also be discussed later.

ANISOTROPIC MAGNETORESISTIVE SENSORS

The magnetoresistive effect was first described by William Thompson, Lord Kelvin, in 1856. But as in the case of HED it took over a hundred years to make the magnetoresistive effect commercially useful and cost-effective due to the development of thin film technology. Today these devices are used in a variety of applications as disk drive read heads, electric compasses, vehicle detection, current measurements and movement detection. In this thesis focus are laid on anisotropic magnetoresistive devises.

Theory

There are a number of different kinds of devises that utilizes materials and/or material configurations that possess magnetoresistive properties, but with different underlying theories for it. What they all have in common is that a change in resistance is present when object to a magnetic field. A common variant for industrial use are anisotropic magnetoresistive (AMR) sensors. The basic theory of AMR is fairly complicated and not fully understood by scientists, and to describe it in detail are far beyond the scope of this thesis. Nevertheless I will mention some features that are fundamental to the phenomena.

The main part of the actual AMR sensors is small stripes of thin film ferromagnetic materials, usually permalloy ($Ni_{81}Fe_{19}$). Ferromagnets exhibit four properties of great importance; two of them are directly related to their band structure.

The first property is an odd number of electrons in the outer shells of the atom. This is a necessary condition for the material to be magnetic. For atoms with an even number of electrons the magnetic moments of the individual electrons cancels out due to the fact that electrons come in pairs with the same energy but with different orbital direction and spin. These materials do not posses magnetic properties. For atoms with odd number of electrons there is an electron “left over” and that gives the atom a magnetic

moment. Here we have the magnetic materials. Magnetic materials can be divided into subgroups with different magnetic properties depending on relative orientation of the magnetic moments. The group of interest here are ferromagnets. In these materials the magnetic moments tend to align to each other in such a way that the total energy of the system get as low as possible. If all, or at least the majority, of the magnetic moments in a ferromagnetic sample were aligned in the same direction, we would have a magnetic flux outside the sample as in Figure 5A. This configuration does not offer the lowest energy of the system for most of the ferromagnetic materials. Instead, lowest system energy is most often obtained by configurations with separate, internally aligned domains. The magnetic orientation (magnetization) of each domain is such that closed loops of magnetization are obtained, hence no magnetic flux outside is present as in Figure 5B.

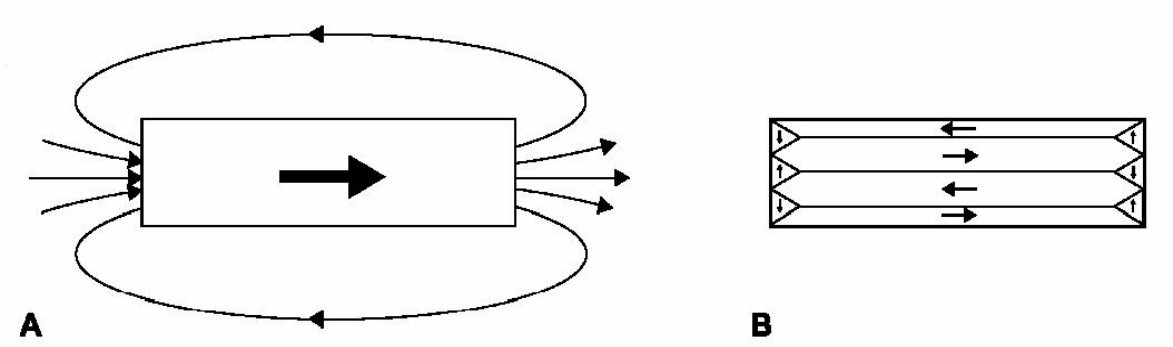

Figure 5: A - Magnetic moments are all aligned. B – Aligned as magnetic domains. Highly simplified drawings.[7]

The magnetization is also affected by the crystal lattice of the material; it is coupled to the axis of the lattice. Less energy is required for directions of magnetization in certain directions, called easy axis, and more energy are required for other directions, hard axis. Most domains are aligned to the easy axis if no external field is present, as the bigger domains in Figure 5B. In thin film samples the easy axis become parallel to the surface of the film due to boundary conditions. If the width of the thin film sample is narrow enough it will act as a single domain with unidirectional magnetisation, and act once again as Figure 5A.

It is possible to alter the magnetization by applying an external magnetic field $\vec{B}_{ex}$ through the material. What happens is that $\vec{B}_{ex}$ affects the magnetic moment of the individual electrons. Most of them align to the easy axis in the direction closest to the direction of $\vec{B}_{ex}$, and the corresponding domains grow while antiparallel domains shrinks. If $\vec{B}_{ex}$ gets stronger all domains first align to the easy axis, then starts to rotate towards the direction of $\vec{B}_{ex}$. When $\vec{B}_{ex}$ gets strong enough and the magnetization is parallel to $\vec{B}_{ex}$, no more change of magnetic moment will occur; it is saturated. If $\vec{B}_{ex}$ is removed the magnetization will return to a multi domain configuration but with some magnetic flux remaining. The strength of that flux depends strongly on the specific material used. If a strong flux remains, the material is said to be a hard magnet, soft magnet if the flux is weak. In ARM devices ultra soft magnets are used.

The second important property of ferromagnetic materials is their so-called transition metal properties, which means their valence electrons are present in more than one energy band. Ferromagnetic materials have two overlapping energy bands for their electrons close to the Fermi energy E_F, the s and d band. The conductivity of the material is a combination of the conductivity of s band and d band, as $\sigma = \sigma_s + \sigma_d$. The σ_s and σ_d are inversely proportional to the effective electron mass (m^*) of their corresponding bands and $m_d^* >> m_s^*$ due to the narrow d band, as seen in the schematic Figure 6. Hence $\sigma \approx \sigma_s$.[17]

The third special ferromagnetic feature is that the energy levels of the s and d bands are different for electrons with up-spin (↑) then for those with down-spin (↓), so called spin-split bands, Figure 6. The two spin states is relatively independent of each other and a current through the material can approximately be seen as two separate, parallel currents with different polarisation.[17]

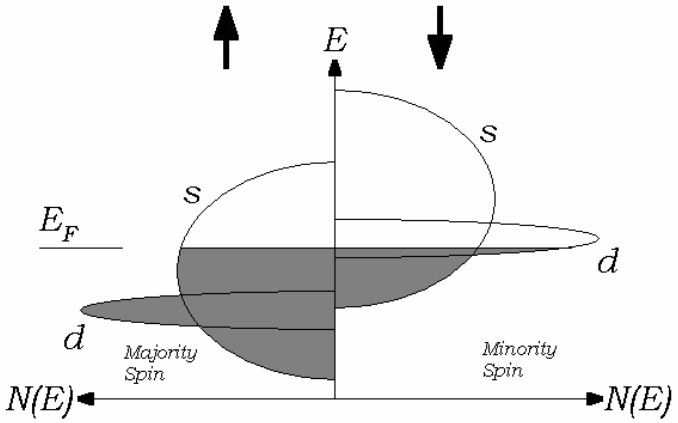

Figure 6: Spin-split bands of ferromagnets.

The spin with the larger density of states $N(E)$ at E_F will be the majority carrier. When conduction electrons in ferromagnets are moving through the material it is mainly by $s \to s$ or $s \to d$ transitions (i.e. electrons jumping between energy states; within s band, or from s to d band). As a result of the higher amount of free energy states of the d band for the majority carriers ($\downarrow$), more $s \to d$ transitions are present, decreasing the conductivity for $\downarrow$, still $\sigma_\downarrow > \sigma_\uparrow$ due to $N(E_F)_\downarrow > N(E_F)_\uparrow$ and for currents $I_\downarrow > I_\uparrow$. Consequently the current passing through a ferromagnetic material is polarised to some extent. If it is possible to reduce the number of $s \to d$ transitions $\sigma_\downarrow$ will increase and hence resistance will decrease[17]. The spin-split properties also contribute to the magnetization properties, according to the different amount of $\downarrow$-electrons and $\uparrow$- electrons at a certain energy level.

The fourth property, and in this context the most important, is the by scientists not yet fully understood relationship between magnetisation and conductivity. If a current is driven through the material parallel to the magnetization, the probability for $s \to d$ transitions is higher than if the current was driven perpendicular to the magnetization. Hence, the conductance is lower for the parallel case then for the perpendicular. Using, for this thesis a more convenient property, resistance, it is found that the relationship follows a mathematical model expressed as

$$\frac{\Delta R(\theta)}{R} = \frac{\Delta R}{R}_{\max} * \cos^2\theta$$ Eq. 4: *Anisotropic relationship.[18]*

were $\frac{\Delta R(\theta)}{R}$ is the change of resistance relative to zero-field-resistance, $\frac{\Delta R}{R}_{\max}$ is the maximum change of resistance and θ is the angel between magnetisation and current, Figure 7. This direction-dependency is giving it its name, ANISOTROPIC magnetoresistance.

As mentioned above, if the resistor has small dimensions with a thickness in the order of 150-400 $\mathring{A}$, a width of 10-50 μm and length of 0,2-1 mm the zero-field-resistance will be high and it will have a unidirectional magnetisation. Both high resistance and unidirectional magnetisation is favourable for the anisotropic characteristic of the AMR. To improve it further the stripes is produced while subject to a high magnetic field to assure that the easy axis is along the mechanical length of the stripe. By this, a magnetization of the stripe will create a high resistance along the easy axis and hence along the mechanical length.

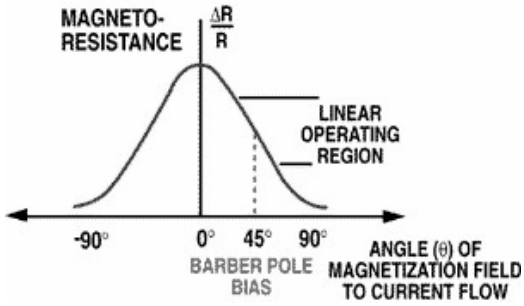

Figure 7: Magnetoresistance of a simple sensor.[9]

Current Sensors

If a primary current I_p is flowing in a external conductor above or below the stripe and a secondary current I_s is driven through the stripe, both parallel (or antiparallell) to the mechanical length of the stripe, a magnetic field H_p are induced by I_p that affects the magnetization direction of the material that in turn decreases the resistance and hence the voltage over the stripe, see Figure 7. In its simpliest form an AMR cannot sense direction of currents (magnetic fields), they have poor temperature characteristics, limited

linearity, magnetic memory and wide range of sensitivity between devises. But by taking a number of measures greate improvements can be made.[12]

The easiest way to greatly improve some of the features is by use of so-called barber poles. These are small, highly conductive stripes placed over the permalloy at an angel of $\pm 45^\circ$ to the magnetization as in Figure 8. The current then takes the easiest path through the devise by minimize the transition length in the highly resistive permalloy. In this way the angel between current and magnetization is biased to $\pm 45^\circ$, were the $\frac{\Delta R(\theta)}{R}$ has its linearity range and it is now possible to determine direction of I_p. Depending on the sign of biasing, the $\frac{\Delta R(\theta)}{R}$ is a positive or negative function over the linear range. One drawback when using barber poles, is that the effective length of the permalloy is reduced, i.e. $\Delta R(\theta)$, and hence sensitivity decreases.

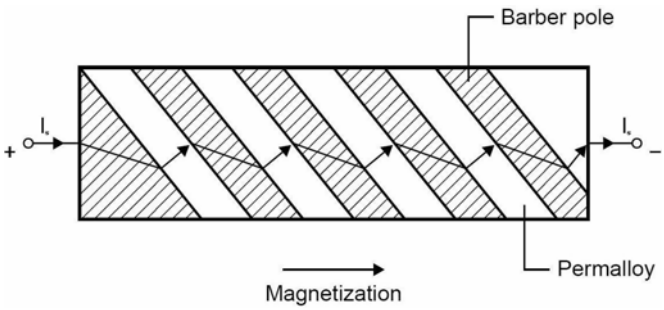

Figure 8: Barber pole configuration.[10]

Temperature dependents and device sensitivity differences are still discouraging. By connecting four resistors in a Wheatstone bridge these properties can be substantially reduced. They are connected close to each other and manufactured in the same process so that the sensitivities are as matched as possible. Further trimming of the bridge can be done by trimming-resistors during the production to reduce offset voltage. Thanks to the close connection the resistors are affected by the same temperature and magnetic fields. A principal drawing of a Wheatstone bridge is shown in Figure 9.

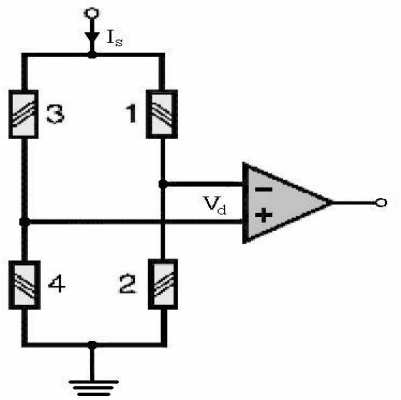

Figure 9: Wheatstone bridge. I_p passing vertically above (or below) the resistors. Observe barber pole direction.[11]

The output is taken as a differential voltage V_d between the two voltage dividers 1-2 and 3-4 that divide the bridge voltage V_b according to resistance proportions. The resistances in Figure 9 are oriented in such a way that if 1 and 4 is increased by a magnetic field 2 and 3 decreases. If the temperature changes, the resistance of all four will change with the same rate but V_d stays the same. In this way the temperature dependency becomes highly reduced.

If configured as in Figure 9 the device can be highly integrated and used to measure currents in a straight, remote conductor, but it requires external shielding. If the orientation of the resistors is altered so that 1 changes accordingly to 3 and 2 accordingly to 4, and letting I_p pass first over 1-2 and then back over 2-4, as in Figure 10, the devise becomes almost immune to moderate external magnetic fields. For example if an external field is present that increases the resistance in 1 and 3 and decreases the resistance in 2-4, both potential levels connected to the OP will decrease, but V_d stays the same. With this configuration the behaviour of the AMR current sensing devise has god characteristics but the primary conductor must be fixed as a U-turn and relatively close to the AMR so that the magnetic field from one conductor passage not interferes with the field from the other through corresponding resistor pairs.

Unfortunately, if affected by high magnetic fields, the magnetization of the permalloy stripes may be disoriented and the overall performance of the devise are deteriorated or it may even start to malfunction. This holds for external fields to, even if the configuration in Figure 10 is used. In that configuration the net affect of an external field does not affect V_d initially, but the magnetization of the resistors are still twisted and the linearity range is decreasing. For sufficiently high external fields the permalloy becomes saturated and the devise stops working properly. The temperature dependency are not completely reduced either, there is still a drift in offset and sensitivity due to temperature. But there is hope.

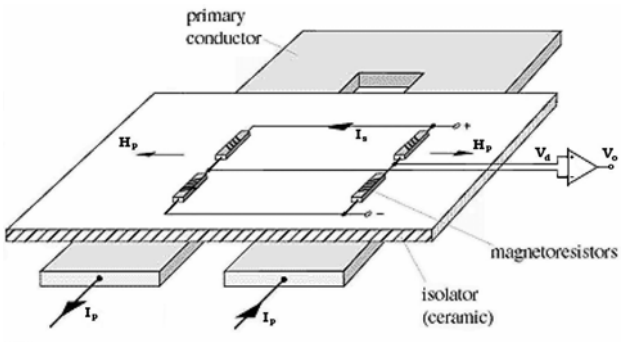

Figure 10: Wheatstone bridge. External fields have almost no impact.[11]

Magnetization Set/Reset

To avoid deterioration due to external fields, one may restore the magnetization of the permalloy stripes by pulsing a strong magnetic field through them in the direction of the easy axis, and taking the measurement between pulses. A current pulse $I_{s/r}$ through a properly oriented coil or strap may achieve this magnetic field. Depending on the sign of this current the magnetization becomes parallell (set) or anti parallell (reset) to the original direction from manufacture, see Figure 11. If the magnetization is set-pulsed only, problems with deteriorating properties are diminished. But by taking advantage of the ability to reset the magnetization even features like offset and temperature offset drift can be coped with.

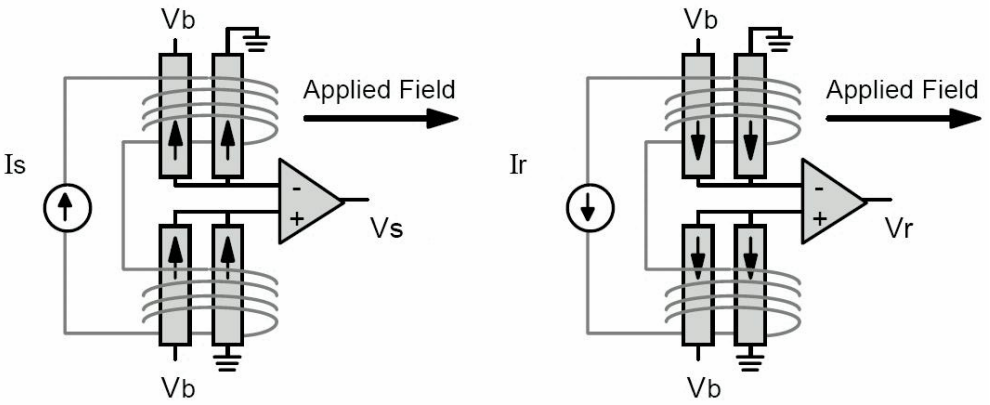

Figure 11: Set/Reset magnetization.[14]

If one compares the measurement from a bridge after a set-pulse with the value after a reset-pulse, the only difference should be the sign. This is since when altering direction of magnetization the angle between magnetization and barber poles, and hence the one between magnetization and current, are changed and as a result $\frac{\Delta R(\theta)}{R}$ becomes $\frac{-\Delta R(\theta)}{R}$. In Figure 12 an example of set and reset measurements are illustrated.

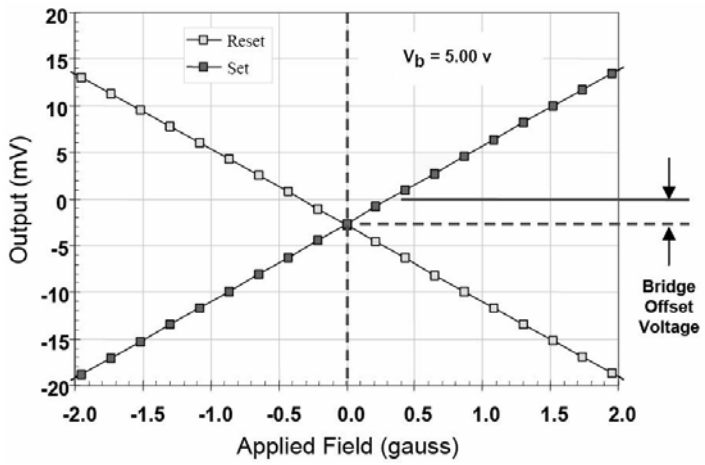

Figure 12: Set/reset output for the same applied field.[13]

As seen above the difference between output values for set and reset at the same applied fields are not just the sign but also a level shift, the offset, is present. The offset of an AMR device are not influenced by the magnetization and for that reason the offset portion of the output value stays the same, both in magnitude and sign. This indicates a grate opportunity to manipulate the offset in a desirable manner.

If the AMR device is put to set and reset mode in a cyclic manner as in Figure 13, one could use V_s and V_r to erase the offset almost completely, if desirable. This can be realised in several different ways. For example if a microprocessor is used V_s and the subsequent V_r can be stored and used to calculate

$$V_s - V_r = 2 * S * H_{applied} = V_o$$ Eq. 5: *Offset cancellation by microprocessor.*

or

$$V_s + V_r = 2 * V_{os}$$ Eq. 6: *Offset detection by microprocessor.*

$S\left[mV/V/Oe\right]$ is the sensitivity of the devise.

Another technique is electronic feedback were V_o are passed through a low pass filter, only letting V_{os} through, and connected to one of the inputs of the first differential amplifier, were V_d and V_{os} sums up like

$$V_d - V_{os} = S * H_{applied} + V_{os} - V_{os} = S * H_{applied} = V_o$$ Eq. 7: *Offset cancellation by electronic feedback.*

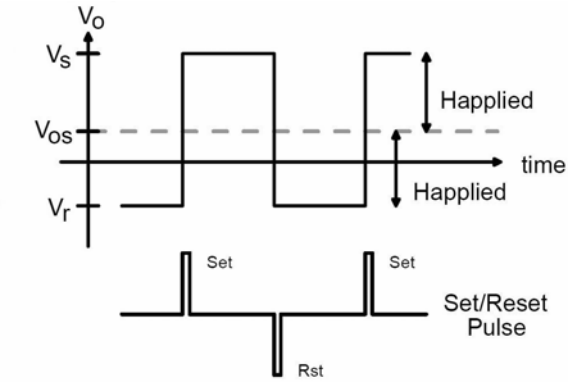

Figure 13: Set/reset pulse sequence.[14]

The offset and its temperature dependents of the AMR device is not only due to the AMR bridge but also to subsequent electronics and by using the set/reset technique the AMR device acquires great offset and temperature characteristics. It is possible to improve device characteristics even more by magnetic feedback using an offset strap formed as a coil near the resistors, more about this in the next section.

Unfortunately when using set/reset techniques the bandwidth of the devise may be reduced sufficiently due to the sampling characteristics and the Nyqvist criterion. But if the offset is known through measurements in zero magnetic field environment the offset may be reduced by using a trim resistor parallel to one leg of the bridge. A less labour intensive technique is to use the coil shaped offset strap mentioned above to produce a static magnetic field to compensate for the known offset. It is also possible to use the offset strap to compensate for known static external fields. Using the trim resistor or the offset strap do reduce the offset, but compensating for temperature variations becomes more difficult then using set/reset techniques.

Feedback

By adding a high gain, negative feedback circuit like the one in Figure 14 the output of the amplifier is connected magnetically to the input by driving a current I_c through conductors placed parallel and in near vicinity of the resistors, creating a compensating magnetic field $H_c = -H_p$ through the resistors. Hence the magnetization of the resistors are left unchanged and $V_d = 0$. Now I_c is a scaled version of I_p and by driving it through a high accuracy shunt resistor V_o is obtained. In a set/reset configuration the offset strap mentioned earlier may be used instead of the compensation conductors, in combination with offset cancellation.

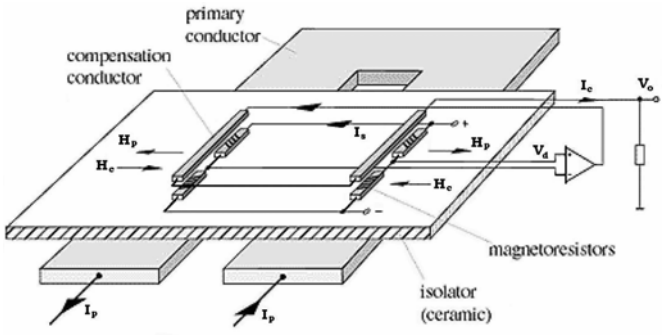

Figure 14: Wheatstone bridge. Feedback circuit (Set/Reset circuit is excluded).[11]

Like this the device becomes much more robust according to strong H_p fields. Not only that, the linearity range and accuracy increases sufficiently and by altering the shunt resistors different resolution and current ranges may be obtained without altering amplifier or bridge location.

FLUX CONCENTRATORS

When it comes to magnetic current measurements, flux concentrators of highly permeable material with low remanence (e.g. ferrite or silicon steal) are often used to concentrate the magnetic field surrounding the conductor upon which the measurement is performed.[4] In this section a brief description of the theory, benefits and drawbacks of this technique are described.

Toroidal Cores

When utilizing flux concentrators in magnetic current measurements a toroidaly shaped ring with an air gap for the sensor is the presently most common application, see Figure 15

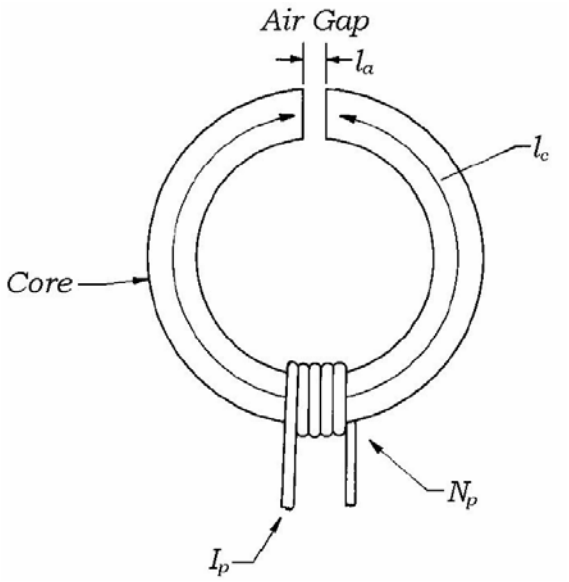

Figure 15: Toroidal flux concentrator.[1]

where l_a is the width of the air gap (m), l_c is the mean length of the core (m) and I_p is the primary current to be measured going through a coil with N_p turns (counted at the inner diameter of the core). If the air gap is narrow compared to the cross sectional area of the core, the flux density in the gap will be the same as in the core, and expressed as

$$B_a = \frac{\mu_0 \mu_c}{l_c + \mu_c l_a} N_p I_p$$

$$-B_{sat} \le B_a \le B_{sat}$$

Eq. 8: *Magnetic flux density in toroidal core with a narrow gap.[2]*

where μ_c is the relative permeability, a unitless material quantity of the core. When core materials are affected by a magnetic flux, there internal magnetic domains line up in the direction of the field and the material is magnetized. If the field is strong enough, all of the domains will line up and then the magnetization of the core will not increase further; it is saturated. This happens when the magnetic flux density retches $\pm B_{sat}$.

Unfortunately, as with all physical objects, cores of any material are not ideal components but highly unlinear and possess a number of infuriating properties. One of those is due to eddy currents, which is circulating currents inside the core induced by changing magnetic fields. This current is proportional to the square of the frequency, and a common method to minimize it is to use laminated or sintered cores. Still, eddy currents are a source of frequency restriction in flux concentration applications.

Core materials suffer from hysteresis characteristics in the relation between the magnetizing field H (in this case $H = \mu_0^{-1} N_p B_{I_p}$) induced by the current and magnetic flux density B inside the core. Therefore it is desirable to use a material with a narrow loop. See Figure 16, were B_r is the remanence $(H = 0)$ and H_c is the coercive force that resets B to zero.

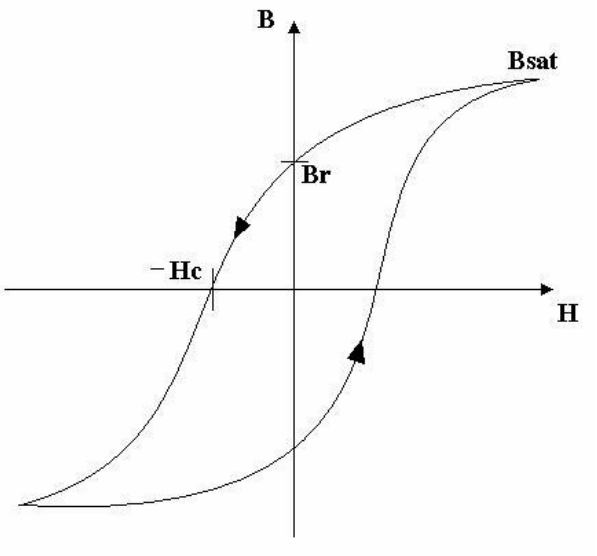

Figure 16: Hysteresis loop.

Most core materials used for magnetic current sensors exhibit very narrow hysteresis loops (low H_c) and errors involving hysteresis is rather minor (e.g. ferrite ~1%), and they are also quite linear between the knees (were they saturate). Power dissipation due to eddy currents and hysteresis phenomena are also very small for these materials, practically they can be neglected.[3][6]

If very high magnetic DC field influences the core, it may get permanently magnetized in some extent and an offset field in the gap, and so at the sensor output as well, will be present. The core material is also affected by temperature. Higher temperatures reduce $\pm B_{sat}$ and the core goes to saturation earlier. This may reduce the measuring range in certain current measuring applications.

Open Loop Current Sensors

By placing a magnetic sensing device in the gap of a toroidal core, it will be affected by a much stronger magnetic field then by placing it in free space in the near vicinity of a conductor without flux concentrator. This configuration is called open loop (OL), for reasons that will come evident in the next section.

A positive effect of OL is that the overall sensitivity and accuracy of the devise becomes greater. By wrapping the conductor several times around the core an even higher sensitivity is accomplished; the magnetic fields of single turns add together in the core. A second order effect is that with higher sensitivity noise will have reduced impact on the output signal. The cross sectional area of the core is not critical as long as it covers the sensor placed in the gap.

The location of the conductor in the hole of the torus is not critical as in the case of free space, practically almost no lack of accuracy due to relative geometrical mismatch between conductor and the sensor will occur. In the case of multiple turns of the conductor, there will be a minor effect due to the way it is wrapped and the best way to decrease this effect is to wrap it uniformly over the whole length of the core.

Not only does the sensitivity and geometrical relaxation increase with the use of a core, the effect of external magnetic fields decreases significantly due to the fact that these fields rather go around inside the core then pas over the gap, as shown in Figure 17. By moderately increase the gap the external fields over the sensor will be suppressed even more, but the sensitivity will decrease as well.

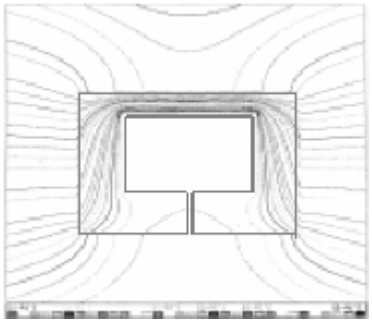

Figure 17: External field in core.[5]

The unlinear properties and other negative aspects affecting the performance of the core will distort the measured signal, but not in a devastating manner as long as moderate signal strengths and frequencies are measured. The

benefits VS drawbacks of using cores, in for the application well suited materials, depend on the application and the sensor technology used.

Closed Loop Current Sensors

As mentioned earlier there are limitations to the accuracy, sensitivity, operational range, and frequency limits of the OL sensors, even if they may have much better performance characteristics then basic sensors without flux concentrators. But these sensors offer a possibility to feedback a current from the output to the input, so called closed loop (CL), through a compensation coil winded around the core, as in Figure 18. The current and coil are scaled to produce a reverse magnetic field to the field produced by the measured current. The fields add together and the result is a zero field in the core.

The secondary current I_s producing this reverse magnetic field can be much lower then the primary current I_p simply by letting the number of turns on the secondary side, N_s be much higher then on the primary side, N_p. This reduces the power consumption of the CL.

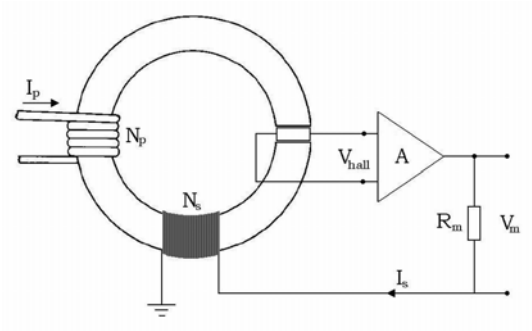

Figure 18: Closed Loop

The relation between currents and number of turns may be expressed like

$$\frac{I_s}{I_p} = \frac{N_p}{N_s}$$ *Eq. 9: Transformation Ratio.*

and I_s is therefore a scaled image of I_p. With a configuration like in Figure 18 the output signal is not an amplified version of V_{hall} as in OL, but a measure of the feedback current I_s passing through a high-accuracy shunt-resistor R_m, and $V_{hall} \approx 0$ because of the zero field in the core.

Thanks to the CL configuration, bad affects as eddy currents and hysteresis can be neglected as long as the frequency not exceeds the bandwidth of the feedback circuitry and V_{hall} not causes it to saturate. Therefore the bandwidth of the overall CL current sensor is often much grater then for OL current sensors. The linear range is also broadened substantially, and is primarily restricted by the amplifier; it gets saturated when its output reaches the supply voltage. The wider linear range is due to that the feedback does not allow the core to go in to saturation, and a second order consequence is that the temperature dependency of $\pm B_{sat}$ has no affect on the performance. It is not only the linear range that benefit on the zero magnetic field, the overall linearity itself also gets much better.

Unfortunately an offset level on I_s is present because of both sensor and amplifier offsets, and they also drift with temperature. This is the reason why $V_{hall} \approx 0$ instead of $V_{hall} = 0$. If the CL current sensor is not powered up the core may, like other flux concentrators, exhibit a permanent magnetic offset if affected by a high magnetic DC field. The total offset is most often restricted to a couple of hundreds or tenth of mA.

When using flux concentrators the benefits and drawbacks must be compared with the characteristics of the sensor used. In this thesis HED and AMR sensors are subject to investigation, and their characteristics differs to some extent. HED sensors have much lower sensitivity but they can be exposed to extremely high magnetic fields without damage. Using HED together with flux concentrators is very beneficial in analogue output current measurements. Thanks to the high sensitivity of AMR sensors they do not need flux concentrators, and there are other techniques available for

shielding from external fields, as mentioned. The high sensitivity and restricted magnetic durability of AMR sensors makes flux concentrators even unsuitable.

Compared to many other sensors OL and CL are bulky and CL are more expensive and consumes higher supply currents then many contending techniques, and this must be balanced with their benefits. There are though alternatives available on the market were the flux concentrators are small and integrated with the sensor, so called IMC.

Integrated Magnetic Concentrators

As is described in earlier sections toroidal cores are common as flux concentrators in current measurement. But there are less bulky alternatives. Actually, with proper design small pieces of highly permeable materials can be integrated with the sensor and the overall components become much smaller, so called Integrated Magnetic Concentrators (IMC). There exist several different implementation techniques for these concentrators, and most often the manufacturers do not reveal how it is done on specific components. Therefore I will only present two basic techniques of interest to give the reader some idea on benefits and downsides of IMC principals. As mentioned before the sensors that most often make use of concentrators are HED:s and therefore I refer to them in this section, but it is of course possible to use AMR's to.

In Figure 19 basic arrangements of the two techniques are shown. In A the HED is placed in the flux passing between two concentrator stripes. It is also possible to use only one stripe and place the HED close to it. The HED are perpendicular to the applied field. In B the concentrators has a total length of approximately a couple of mm's with a thickness and gap width in the order of couples of hundreds of mm's, and the flux are measured by HED pairs in the near vicinity of the narrow gap were the field lines are vertical. Here the HED:s are parallel to the applied field. A variant of the configuration in B uses one concentrator with the HED:s on each end. The reason why two

HED:s are used is because the same field passes the sensors in a differential manner and by subtracting the outputs all vertical adjacent fields passing the sensors as common mode signals are cancelled out.[8] By these configurations small and cheap components are possible to produce. Imagine an electric current going out of this paper through a conductor placed above each sensor, creating the magnetic field shown.

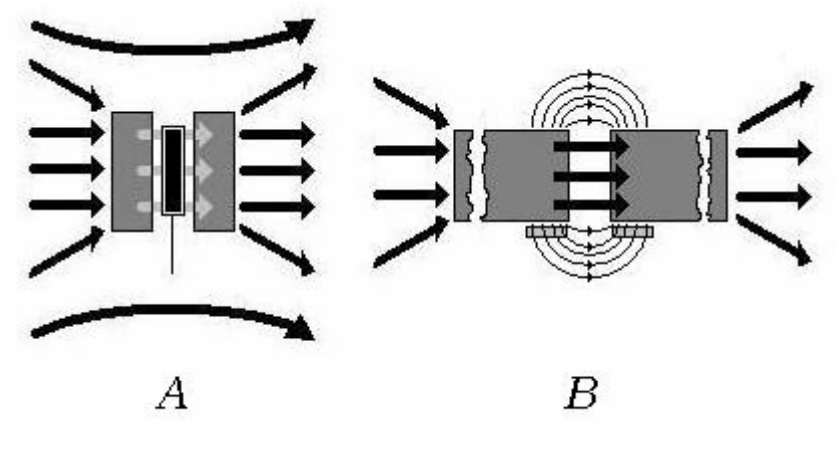

Figure 19: Integrated Magnetic Concentrators.
Dimensions of A and B are not comparable[2].

Both variants can be constructed as lead-through components, were the primary conductor are a part of the component. In this way the conductor is fixed to a certain distance and the accuracy are therefore not affected by mismatch. They may also be shielded quite easily. On the other hand they will be fixed to a certain measurement range due conductor dimensions and saturation of conformation electronics.

By excluding the conductor, more flexible components are archived. Different current ranges can be measured by placing the external conductor at a distance corresponding to required current range and resolution. Extremely high currents can be measured, but with pretty poor resolution though. External conductor measurements are in general more sensitive to adjacent fields and may need external shielding, and mismatch between component and conductor may be a source of inaccuracy.

[2] The configuration in Figure 19 B is developed by GMW Associates.

PREPARATIONS

To better understand the theories presented in Chapter 2 and how real components with their un-ideal characteristics work, some measurements are performed. These measurements are carried out in an application specific manner according to MACH2 system requirements so that the results may be used in future designs.

Selection of Components

When I selected components to be measured I first tried to choose components that could measure the highest levels of currents measured today, i.e. ~25*5A. Not all components of interest did have this ability, but they had other characteristics of high interest. For example, components with different input range, but equal output range (e.g. 0-5V) have different resolution (sensitivity) and by combining components, more accurate measurements can be obtained. Recall that for the MACH2 system a higher accuracy and resolution are desired for $0-3*I_n$ then for the rest of the range. All components chosen are bidirectional, i.e. can measure both strength and direction of the current, and are more or less linear over the whole range. The sensitivity is often slightly dependent on temperature, and I tried to find components with low temperature dependence.

It was also desirable that the components could withstand high over currents in levels of ~$100*I_n$ (i.e. 100*5A) for a shorter period of time (~1s) without getting harmed or permanently affected otherwise. Unfortunately many components of interest do not endure that kind of over currents according to their data sheets or it is not specified. In spite of that I carried out measurements on their tolerance for high currents in order to se if they still could be used in these applications.

Many components suffer from offset levels that affects the overall behaviour of the measuring circuit, but as long as these levels are stable they can be dealt with quite easily. Unfortunate these levels are often temperature dependent and then it becomes more complicated. I tried to find components that have low offset and low offset temperature dependence.

Other important aspects I looked at in order to be able to make correct conclusions about whether or not a certain measurement technique can be used in our applications are linearity, accuracy, reaction time, rise time and bandwidth. The component bandwidth are sufficient if it is >40kHz, but most components has a bandwidth of ~100—200kHz.

I also performed some measurements on simple components that did not qualify to be used in the MACH2 system but could give a certain understanding on basic ideas.

Different Component Techniques

There are mainly three basic component techniques that I utilize in this report. First there is the most common one for current measurements today, that make use of HED-sensors and toroidal cores, both in open and closed loop configurations. With this technique you get high isolation between input and output, it is easy to reconfigurate the sensitivity on the measuring circuit by simply add or remove turns to the input winding and there is no insertion losses. But, they are bulky, expensive and they may exhibit offset change due to permanent magnetization of the core after high current spikes.

The second technique is a cheaper, more “back to basic” configuration. Here you fixate the conductor at a specified distance to a small sensor and measure the magnetic field more straightforward. It provides high input/output isolation. The sensors, that can be of both HED and MRS type, may have flux concentrators, but they are small and integrated in the same IC as the actual sensor. Some of them are not harmed, but saturated by high fields, but then you can place them at a different distance to the conductor.

The accuracy of the overall circuit may suffer from geometrical mismatch between sensor and conductor, and it may need external shielding from adjacent fields. I discovered that the sensitivity and ability to measure low currents was quite inadequate on the components I had chosen. They are primarily produced as position detectors, and as such they should detect higher magnetic fields then the low fields induced around a conductor with a current lower than 1A. According to the application specific nature of this thesis, the difficulties to measure low currents and geometrical mismatch problems, I decided not to do any full-scale measurements and discarded these components from further testing.

Both techniques mentioned have high electronic and thermal isolation between input and output. The third technique though has quite high electronic isolation to, but the thermal isolation is quite insufficient. Here the measured current is led through the component itself, and the component is dimensioned for a predefined maximum current. If the current exceeds this maximum, the current density might cause such a heat so the component will be permanently damaged or destroyed. The advantages of this technique are that the components are simple, cheap and easy to mount and they do not suffer from geometrical mismatch. They are also quite often well shielded from adjacent fields internally.

TEST CONFIGURATIONS

Linearity

I made some measurements with a series of DC-currents between 50mA to 25A to investigate the linearity, especially for low currents. For low currents I used a current generator, VARIREF VF-12 that could deliver a maximum current of 120mA with high accuracy. For medium currents I used an OMICRON CMC 256-6, which has a lower accuracy for low currents. Unfortunately, the VARIREF VF-12 could not deliver currents bidirectional, so I was forced to alter the circuit contacts to alter direction of current. This

may have affected the measurements slightly by contact glitches. For the components with toroidal cores (referred to as OL and CL, se Chapter 3) I led the current through the sensor twice, which doubles the flux passing through the HED. By this it was possible to use the VARIREF VF-12 up to (virtually) 240mA for these components. Throughout this chapter when talking about low currents and medium currents the intervals 50mA-240mA and 0,5A-25A are intended respectively.

Unfortunately it was not possible to do accurate measurements for higher currents (up to 125A). The OMICRON CMC 256-6 can according to the specifications deliver up to 75A, but only under certain circumstances and during a very short time, therefore I did no measurements for higher currents. The most interesting interval though are from 0A to 3*5A=15A, see Chapter 1.

All measurements were carried out with the same procedure:

- Power up. No I_p to observe the offset and possible offset drift.
- High I_p (altering direction), then again no I_p. To se if the offset is affected by measured current.
- Current measurements. Started with lowest currents, for both current directions. Then successively rising the current: 50mA, -50mA, 60mA, -60mA, 70mA …
- As the current gets higher, I increase the increments.
- After the measurements are done, the offset is noted, and the average value between before and after measurements are used when I compare components.

I made three (two for CL, one for OL) separate measuring series for each component: 50mA-120mA and 130mA-240mA (50mA-240mA for CL and OL) with 10mA increment and 0,5A-25A with 0,5A increment up to 10A, then 2,5A increment up to 25A. For OL I only made one series, 50mA-240mA, due to the relatively bad linearity at low currents, se “Results-Linearity”.

As power source I used an ELECTRONIC MEASUREMENTS INC. 40205 in low current measurements, even if I used the OMICRON CMC 256-6 as current generator for the 130-240mA interval on the ACS754K and AMR

components. For medium currents I used the OMICRON CMC 256-6 as both current generator and power source.

I used MS Excel for calculations and comparison of measured data. To be able to compare different components to each other, I first subtracted the noted offset from measured values. Thereafter I calculated trendlines for each component using linear regression analysis and fine-tuned the offsets so that all the trendlines intercepted zero output at zero input. I did this offset-tuning separately for each of the three (two) series I specified above.

To find the linearity I calculated it relative to the trendlines as

$$\varepsilon_L(I_p) = \frac{M(I_p) - S_t * I_p}{S_t * I_n} * 100$$ Eq. 10: *Linearity calculation.*

were $\varepsilon_L(I_p)$ is the %-linearity at I_p, $M(I_p)$ is the measured value at I_p (offset subtracted) and S_t is the slope of the trendline. I_n is the nominal current for the measurement boards used in the MACH2 system. In this way the result can be directly compared with the maximum allowed unlinearity of the measurement boards. On these boards the unlinearity should be better then $\pm 0{,}2\%$ of their nominal value. For instance if a card with $I_n = 1A$ would make use of one of the components tested in this thesis as a transducer, the linearity-chart (Appendix C) for that component need to be enclosed within $\pm 0{,}2\%$. With other I_n than 1A, only divide the values in Table 4 by I_n.

I also arbitrary tested the sensitivity to external magnetic fields by moving a strong permanent magnet in the near vicinity of the component. I found that the magnet affected all components. Even so, the magnetic field from the magnet is many times as strong as from realistic nearby circuitry.

By using a heating blower I tried to test the offset temperature drift, but according to different types of housing, imprecise air temperature and

adjacent load resistor (also affected) it was difficult to get comparable results. The offset did change slightly for all components, though.

Step response

A waveform generator, Hewlett Packard 33120A, are used to produce a square-formed wave with a frequency of 100Hz. Unfortunately this waveform generator could only deliver a bidirectional peak-to-peak current of 0,358A (0,179A to –0,179A). Even though this current is low it is sufficient to detect step response characteristics for most of the components. Both output and input are viewed with the Tektronix TDS 3054, the later over a 5ohm resistance. The configuration is otherwise the same as for the linearity measurements, which means that the step is doubled for OL and CL components.

Frequency dependency

To find out how the components of interest handles different signal frequencies I used a two-channel network signal analyser with one output channel and two input channels, SRS Model SR780. On it's output it could deliver a voltage-signal and sweep the frequency from zero to 102,4 kHz. For the current to be sufficiently high I used an amplifier, Sentec ACM1 that resulted in a current of approximately 2 A depending on load, i.e. a 4,7 ohm wire-wound power resistor + the test object.

For the amplifier and power resistor not to influence the measurements I connected channel one on the signal analyser over the power resistor (input) and channel two to the output terminals on the test object (output). By this the only difference in frequency contents would be that of the test object, in comparison with connecting channel one directly to the output channel. The result is presented as amplitude and phase in decibel, dBV(Hz), and degrees, deg(Hz), respectively. The configuration is otherwise the same as for the linearity measurements.

RESULTS

All figure cross-references in this section are referring to either Appendix C, D or E.

Linearity

In Appendix C the results of the linearity measurements are presented. First the results are presented in table form with the actual measured values, Table 1. The second table, Table 2, contains the results with offset subtracted and after that the deviation from trendlines in volts are presented, Table 3. In the last table the deviation is presented in percentage relative the expected output if a $I_n = 1A$ current where measured, see Eq. 10 and Table 4. The offset adjusted table and the linearity table are also presented in a number of charts. In Figure 26 and Figure 27 the values from Table 2 are drawn. At a first glance at Figure 26 all components seams to be quite linear, even if only medium currents are shown. Also in the smaller interval, Figure 27, it is still hard to observe any unlinearity. Only two components, CSLA2DG-1 and 2, are unlinear enough so that it can be visually observed by comparing the slope for positive currents with the slope for negative currents. It is necessary to use the calculated linearity to be able to make any conclusions.

As mentioned in the section "Test Configurations" I performed three (two) measuring series using different current generators and power supplies. At first I tried to combine the results from these series in the same charts, but unfortunately they do not "fit" due to slightly different V_{cc} (ratiometric, se Chapter 2) and accuracy on I_p. Therefore all linearity analyse need to be done separately for low currents and medium currents. Furthermore, the results on the low current measurements for the ACS754K and AMR components are as mentioned earlier two separate series, with the VARIREF VF-12 up to 120mA and the OMICRON CMC 256-6 up to 240mA but with the same power sourse. Even so, I decided to treat them as one series,

because when studying the low current linearity charts for these components there is only a slight difference between them, se Figure 30. This difference is most apparent for the ACS754K.

In Figure 28 the linearity for low currents are displayed. As seen there are rather big differences between components. To make it more visibly I separated the low current series in two charts. One for components with unlinearity above 0,5% (Figure 31) and one for unlinearity below 0,5% (Figure 32). In Figure 31 we find the OL components and ACS754K, which in fact also is an open loop HED component but without toroidal core. The CL and AMR components are displayed in Figure 32. Another aspect to consider is the fluctuation of the linearity. A component with high fluctuation in the linearity illustrates a more noisy output then other components with lower fluctuation. As one can se it is a relatively big difference both in linearity and fluctuation (noise). The noise may be possible to reduce by filtering, but that would add more electronics to the signal path slowing it down and maybe distort the signal. The high unlinearity and noise of the OL in addition to the principal similarities to CL motivated to discard them from further investigation and reduce the number of components for the step response and frequency dependency measurements. As seen in Table 1 I also, for the same reasons, chose not to compete the linearity measurements for the OL. The principal differences to the CL are the reason why I kept the ACS754K. I found it interesting to investigate them further even with their higher unlinearity and noise.

In Figure 29 the linearity for medium currents are displayed. According to the decision to discard OL components they are not present. As seen the ACS754K suffers from much poorer linearity then the CL and AMR components. In Figure 33 I have taken away the ACS754K to better see the behaviour of the CL and AMR. Now we can se that they follow different trends, polynomials. The NT-50 behaves as a fourth-order, the CLN-100 and CLSM-100 follows a second-order and the CSNT651 follows a third-order polynomial. In Figure 34 I collected all components that has linearity better

than 1% for medium currents. Here it is seen that LA100-P follows a sixth-order and that CMR-25 also follows a third-order polynomial. Most likely these different trends depends on the amplifiers and other electronics following the actual sensor. It is a quite big difference between CSNT651-1 and CSNT651-2. I cannot give a good explanation for this, but it shows that two components of the same model are not identical and may perform slightly different.

To be usable in the MACH2 implementation a linearity better than 0,2% up to $3*I_n$ are required. If $I_n = 1A$ only the LA100-P and CMR-25 can be used according to these linearity measurements. The same components can be used for $I_n = 360mA$ (0,072%/0,36=0,2%). If $I_n = 5A$ also CLSM-100 and CLN-100 can be used (1%/5=0,2%).

Looking at linearity and noise, there are three components with prominent test results: LA 100-P, CLSM 100 and CMR-25. Linearity-charts with these are shown in Figure 34 and Figure 35. Note a low current linearity better than 0,15% for LA 100-P and CLSM 100 and 0,05% for CMR-25 (except some deviating values). At higher currents the series are more fluctuating (possible due to the OMICRON CMC 256-6), but the trends for LA 100-P and CMR-25 are within +/-0,2% up to 3*1A and up to 3*5A all three components are within +/-1% (1%/5=0,2%). Unfortunately the over current durability for transducers used in the MACH2 system should be better than $100*I_n$ for 1s and the maximum DC current allowed for CMR-25 are 40A. By this the CMR-25 may only be used when $I_n \leq 0{,}4A$. The LA 100-P and CLSM 100 may only be used when $I_n \geq 0{,}75A$ (0,15%/0,75=0,2%). But if only one component are to be used in all implementations, it may in fact be possible to externally trim the linearity for a certain current interval, an hence it may be possible to use most components even with I_n=360mA. It is still preferable to have as linear components as possible, so that wider intervals may be measured. It may also be possible to combine components, e.g. one CL with a nominal

current closer to the I_n for the measurement board and with a great linearity for the $3*I_n$ interval, and another CL (or a cheaper OL) with nominal current close to $25*I_n$ for that interval. This example is possible thanks to the greate over current protection the CL and OL components exhibit even for rather small nominal currents.

Step response

In Appendix D the results of the step response measurements are presented as prints from the Tektronix TDS 3054.

For the ACS754KCB I needed to measure the response relative a reference voltage due to that the zero-output from the ACS754KCB is 2,5V and it is not possible to get a reasonable resolution on the Tektronix TDS 3054 at that voltage level. If compared with the rest of the components the output of the ACS754KCB seams to be noisy. If that has to do with the reference source are hard to tell, but while collecting data for the linearity measurements the values on the voltmeter did fluctuate more than average, indicating noisy output. In Figure 36, Figure 37 and Figure 38 the results for the ACS754KCB are shown. Either with or without the noise it is clear that if compared with the other components it is rather slow. It takes about $8-10\mu s$ to reach 90% of final value.

Even though discarded from further investigation, the HAS 50-S are included for comparison. One difference from the CL is the size of the overshoot. On the HAS 50-S it is small and does not exceed the final value, as seen in Figure 48 to Figure 50. Another difference is that the transient oscillation is stronger for the CL. Both these differences are due to the succeeding electronics. For the closed loop circuitry to work satisfactory, i.e. be able to suppress fast events in the flux concentrator, it must be very fast, close to instable. With that comes the overshoot and oscillation. In the MACH2 system it is important that overshoots not exceed over current protection levels. If they do the MACH2 may interpret it as an over current and shut the primary current down. This is the major disadvantage for using

CL sensors. But for the overshoots to occur the primary current need to change rapidly, as in the case with steps, but the currents to be measured change somewhat slower and may not cause excessive overshoot if CL sensors are used. The CL with the lowest overshoot is the CLN 100 with a 2% overshoot while the CSLM 100 and LA 100-P has an overshoot of about 19% and 30% respectively. The oscillation is not as crucial as the overshoot but with a fast settle it is possible to get a faster accurate reading. The LA 100 has a settling time of $30\mu s$ while the CLN 100 and CSLM 100 has a settling time of $80\mu s$. The results for the CL components are shown in Figure 39 to Figure 47

The rise time for the CL is much faster than for the ACS754KCB. The slowest CL is CLN 100 with a $2-3\mu s$ rise time, about half the time of the OL HAS 50-S. The CSLM 100 and LA 100-P has the fastest rise times in the test with $160ns$ and $400ns$ respectively.

For the AMR component NT-50, Figure 51 to Figure 53, the rise time is $1{,}6-2{,}0\mu s$ and comparable to the CLN 100. It has an overshoot of 28%, about the same as for the LA 100-P. The CMR-25 has also a rise time of about $2\mu s$ but it is hard to tell about the overshoots, as seen in Figure 54 to Figure 56 the initial part of the print are highly fluctuating. This kind of fluctuation is also apparent for the ACS754KCB and HAS 50-S. If it is component specific or caused by external influence are hard to tell at this stage but may become clear in more thorough investigations in the future.

I find out that the prints for the CMR-25-3 differed from the CMR-25-1 and –2 in that the CMR-25-3 did not transfer DC currents. This can be seen in Figure 57 and Figure 61 were the square wave from the Hewlett Packard 33120A are folly visible. For the CMR-25-3 the levels drop in a logarithmic manner indicating lack of DC component. When I tested the sensitivity of external magnetic fields I used the CMR-25-3 and I tested it in a rather harsh manner. This is probably the reason for the erroneous behaviour,

most likely due to disorientated magnetisation in the resistance stripes mentioned in Chapter 2.

Frequency dependency

In appendix E the results of the frequency sweep are presented. The numbers in dB and deg in the image text are the difference between start value and stop value in each chart. As for the step response I included the HAS 50-S for comparison.

The amplitude chart shows how the component influences the output level for various inputs with the same amplitude but different frequency. If this behaviour is well defined it is rather simple to compensate. The phase charts show how signals with different frequencies are phase shifted differently when passed through the component. As long as it is linear there will be no need for compensation. As an example, if the phase acts like

$$-\omega t_d$$ Eq. 11: *Linear phase behaviour.*

were t_d are a positive constant, and

$$I_{in} = \hat{I}_{in1}\cos(\omega_1 t) + \hat{I}_{in2}\cos(\omega_2 t)$$ Eq. 12: *Input signal.*

then

$$I_{out} = \hat{I}_{out1}\cos(\omega_1 t - \omega_1 t_d) + \hat{I}_{out2}\cos(\omega_2 t - \omega_2 t_d) = \\ = \hat{I}_{out1}\cos(\omega_1[t - t_d]) + \hat{I}_{out2}\cos(\omega_2[t - t_d])$$ Eq. 13: *Time-delayed output.*

Hence, all signal components are time–delayed the same and therefore no distortion due to phase shift are present.

The phase for all components starts at 0 deg except for the ACS754KCB-150 that starts at 180 deg, se Figure 62 and Figure 63. This is probably due to a mistake during connection of the component by alternated polarity at the input or output. This will not have an effect on the results other then adding

180 deg to the phase. The ACS754KCB-150 has an amplitude characteristic that has a 13 dB difference between highest and lowest value. This is far more then the component with the second highest difference, the HAS 50-S (Figure 70 and Figure 71) with 3,5 dB. 13 dB corresponds to a twenty times lowering, while 3,5 dB only corresponds to about a halving. The phase are quite linear but also rather high, about 230 deg compared with 72 deg for the HAS 50-S.

The components with the most complicated behaviour are the CL. For all of them something happens around 15-20 kHz. This can be seen in Figure 64 to Figure 69, Figure 72 and Figure 73. Except for the LA 100-P (Figure 72 and Figure 73) both the amplitude and phase are rather linear but the amplitude makes a significant lowering at 15-20 kHz with a corresponding step in the phase shift. The LA 100-P acts somewhat different. It has a zero phase up to 20 kHz and there after it declines linearly about 30 deg to 100 kHz. The amplitude starts low and increases quadratic to 30 kHz and from there it declines linearly to 100 kHz. The shape of the amplitude for LA 100-P may be complicated to compensate for, if that would be necessary. The HAS 50-S act similar to the CL components but without the amplitude lowering. This implies that it is caused by the feedback circuitry, i.e. amplifier and secondary coil. Also, the HAS 50-S has about tree times steeper phase chart witch means that the time-delay are about tree times higher for the HAS 50-S than for the CL components.

The amplitude characteristics for NT-50 (Figure 74 and Figure 75) differ from the other components by having a more quadratic shape. This may, as for the LA 100-P, be somewhat complicated to compensate for. The phase shift are in the same order as for the HAS 50-S but starts quadratic the first 10 kHz, but it is close to zero and may be treated in that way.

The frequency characteristics for the CMR-25 (Figure 76 and Figure 77) is also rather similar to the CL, but as in the case with the HAS 50-S, without the amplitude lowering and phase step. The total phase-shift are tough much better than the HAS 50-S and somewhat better than the CL, i.e. lesser

time-delay, but at about 1 kHz both amplitude and phase fluctuates for a 300 Hz period. The reason for this is not clear. In Figure 78 and Figure 79 the characteristics for the CMR-25-3 are shown. As in the case with step response the charts with CMR-25-1 and CMR-25-3 differs from each other. Here we can see that for CMR-25-3 low frequency currents are not passing through but for frequencies above 300 Hz they act rather similar. This was expected since the step response investigations show a lack of DC transition. Recall the explanation for the erroneous step response.

The components with the lowest amplitude and phase differences in the test interval are CSLM 100, LA 100-P and CMR-25. The amplitude difference is for all three below a $\sqrt{2}$-times lowering and the phase is 27 deg for the CL and 20 deg for CMR-25. These three components did also perform best results in the linearity measurements.

Observations

Here I list some observations about components I did during my tests.

HAS 50-S	a little noisy and the output has some floating tendency.
BB-150	the output has some floating tendency.
CSNT651	the offset voltage slightly wanders.
LA 100-P	the offset voltage wanders least among CL.
CLSM-100	the output does not float much.
CLN-100	the offset voltage descend a rather long time after powered on.
CMR-25	very little noise, sensitive for external magnetic fields (offset “memory”) and noticeable hysteresis. Sensitive, measure <1 mA.
NT-50	sensitive for external magnetic fields, offset takes time to become stable.

The most important characteristic for the transducers in the MACH2 current measurement application is their linearity at low currents. Based on that I decided not to continue with further investigation of some components that did not perform according to the demands on linearity. These components are the Open Loop Hall-Effect Devices (OL HED) with toroidal flux concentrators. Also the OL HED named ACS754KCB-150 did not perform satisfactory but since they are rather different from the other components I decided to carry out the other tests to, but also in the step response measurements and frequency dependency tests the ACS754KCB-150 did not perform satisfactory.

I found that the component with the best characteristics is the CMR-25 based on Anisotropic Magnetoresistance (AMR). It is the far most linear component among those tested here and it has god frequency behaviour. Unfortunately it can only manage up to 40 A without damage and therefore, according to the $100 * I_n$ over current protection, it can only be used in the MACH2 system for $I_n < 400\,mA$.

The most serious alternative for current measurements in these applications is the Closed Loop HED. The technique is well known and it exist a great amount of alternatives on the market when it comes to nominal current, accuracy, linearity, speed and price. They also endure high over currents and they are mechanically durable. Another advantage is the ability to control the sensitivity by adjusting how many times the current passes through the component, i.e. number of turns around the toroidal core. The major disadvantage CL may have in this application is the overshoot discovered in the step response measurements. As mentioned it may cause the MACH2 system to detect false over currents and activate protection procedures. Another disadvantage may be the amplitude lowering and phase step seen in the frequency dependency tests. The transducers need to have a

bandwidth of 40-50 kHz and the lowering and step appears at 15-20 kHz, but it might be possible to compensate it externally.

The second AMR component, the NT-50, act rather similar to the less performing CL components, the linearity is not as god as for the LA 100-P or CLSM 100. It is less bulky then the CL, but since the current is led through the component it is not possible to alter the sensitivity as in the case with CL and it is more sensitive for high currents.

Among the components tested here the LA 100-P is the best candidate to be used in this application and the CLSM 100 may also be an alternative. The LA 100-P is linear enough to handle $I_n \geq 0{,}75A$, but components in the same family (LEM LA xx) with lower nominal currents may be used for lower currents.

The CL endure high over currents as mentioned, but they only deliver accurate output values up to about 1,5 times their nominal current, therefore it may be necessary to combine components. As mentioned earlier an alternative is to use two HED components; one to measure low currents with high accuracy and the other one for medium and high currents. Correct values are detected even if the low current component saturate.

Compared with the current transformers used today the CL components are somewhat more complicated and may have a less well-defined effect on the signal. On the other hand they manage DC and low frequency currents, a quality that I think greatly overcomes less desirable aspects. The shunt resistor is in it self the best and most linear method, but there is two major drawbacks related to it. First, there is no electric isolation between input and output, and to establish this isolation amplifiers are used adding unlinearity at low currents and making the overall measurements slower. The second drawback is the problem to transfer high currents through the thin metal conductors at the PCB to the shunt resistor, i.e. high current density. This is the major reason why shunt resistors are only used in low current applications so far. The CL components are electrically isolated between

input and output by galvanic isolation and thereby no isolation amplifiers are required. Also since the primary current are led through the hole in the toroidal core by a sufficiently thick conductor, the problem with high current density is solved.

By looking at the results of the measurements and tests carried out for this thesis my conclusions about alternative current measuring techniques for the MACH2 system are that I do think that with careful selection and thorough testing the CL HED technique is possible to engage in this application. Other techniques based on the Hall-Effect tested here are not suited manly due to insufficient linearity. The AMR techniques may be possible to engage, but the insufficient amount of components on the market makes it hard to find suitable candidates.

Here I list the suppliers, components and type of sensor. I also note down the supply voltage (Vcc), load resistance (Rload), and coil turns (Np, for OL and CL HED) that I used. ACS754xCB-150 needed a capacitor between Vcc and GND (Ccc). For detailed information and data sheets, please refer to each companies webpage.

Allegro MicroSystems, Inc.
115 Northeast Cutoff
Worcester, MA 01606
USA
Tel: +1 508 853 5000
www.allegromicro.com
Sensors:

A1301 and A1302	HED Position sensor, discarded from detailed measurements. Vcc=5V
ACS754xCB-150	Lead-through HED current sensor. Vcc=5V, Rload =100Kohm, Ccc=0,1uF

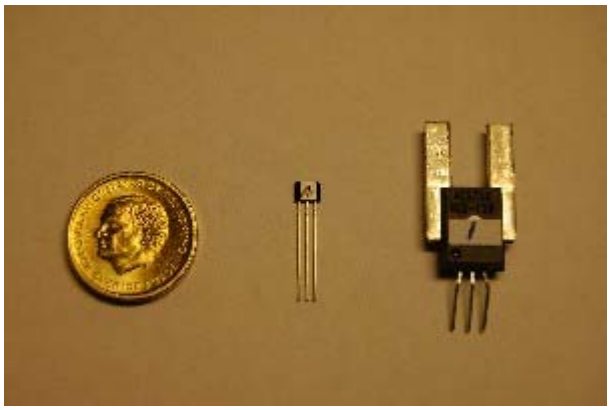

Figure 20: Left, A1301 and A1302 look the same. Right, ACS754xCB-150.

Honeywell Sensing and Control
11 West Spring Street
Freeport, IL 61032
USA
Tel: +1 815 235 6847
http://content.honeywell.com/sensing
Sensors:

CSLA2DGI	OL HED current sensor with toroidal core. Vcc=8V, Rload =10Kohm, Np=2. Quantity: 2
CSNT651	CL HED current sensor with toroidal core. Vcc=+/-15V, Rload =125ohm, Np=2 Quantity: 2

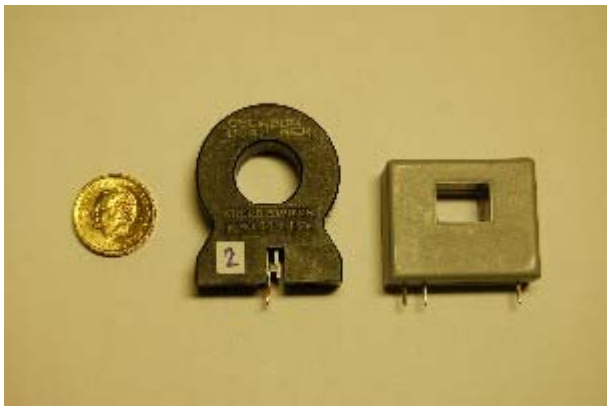

Figure 21: From left CSLA2DGI and CSNT651.

Figure 22: The flux concentrator and sensor circuit separated.
Observe the gap in the toroidal core and the
HAL sensor; the small white square.

LEM Holding SA
8, chemin des Aulx
CH-1228 Plan-les-Ouates, Genève
Switzerland
Tel: + 41 022 706 11 11
www.lem.com
Sensors:

HAS 50-S	OL HED current sensor with toroidal core. Vcc=+/-15V, Rload =120Kohm, Np=2 Quantity: 1
LA 100-P	CL HED current sensor with toroidal core. Vcc=+/-15V, Rload =125ohm, Np=2 Quantity: 1

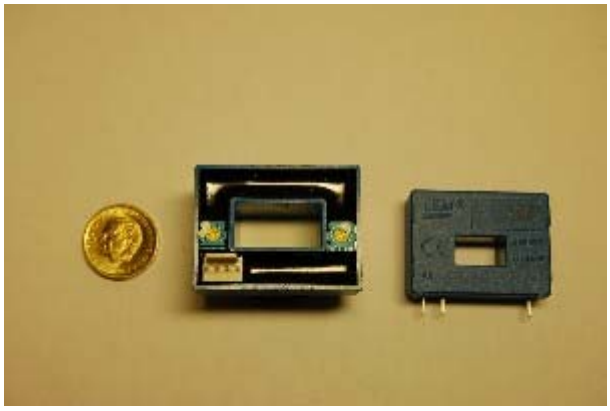

Figure 23: From left HAS 50-S and LA 100-P.

Sypris Test & Measurement
6120 Hanging Moss Road
Orlando, FL 32807
USA
Tel: +1 407 678 6900
www.fwbell.com
Sensors:

BB-150	OL HED current sensor with toroidal core. Vcc=+/-15V, Rload =10Kohm, Np=2 Quantity: 1
CLN 100	CL HED current sensor with toroidal core. Vcc=+/-15V, Rload =75ohm, Np=2 Quantity: 1
CLSM 100	CL HED current sensor with toroidal core. Vcc=+/-15V, Rload =75ohm, Np=2 Quantity: 1
CMR-25 (also at Honeywell, CSNX25)	AMR current sensor combined with an ASIC. Vcc=5V, Rload =27ohm, Np=1 (of 3 possible) Quantity: 3
NT-50 (also at Sensitec, CMS2050)	AMR current sensor. Vcc=+/-15V, Rload =100Kohm Quantity: 3

Figure 24: From left BB-150, CLN 100, CLSM 100, CMR-25 and NT-50

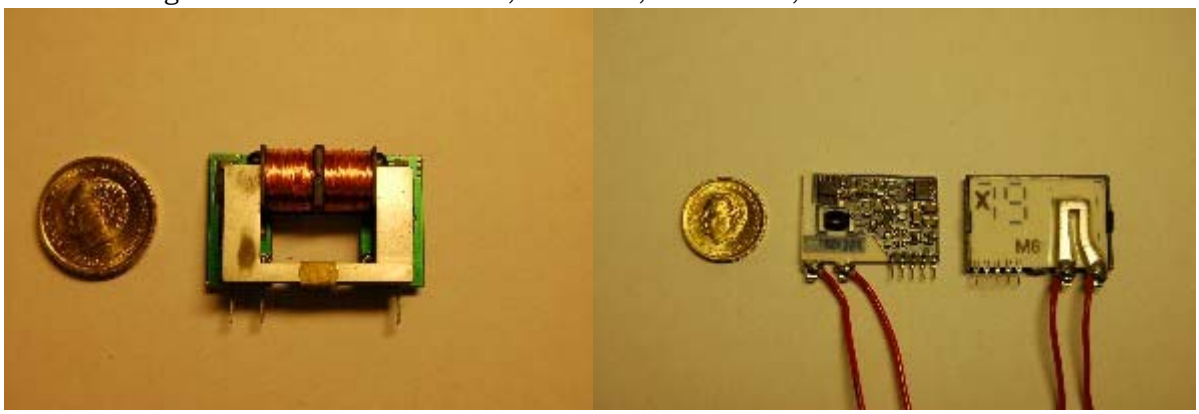

Figure 25: Left, CLSM 100 opend. Observe the feedback coil.
Right, back and inside of NT-50.

VARIREF VF-12

Current and voltage precision generator. Used as a current generator for low current linearity measurements. Contact: www.semitronic.com

ELECTRONIC MEASUREMENTS INC. 40205

Current and voltage generator. Used as a power source for Vcc in the low current linearity measurements and for step response measurements. Contact: http://www.lambda-emi.com

OMICRON CMC 256-6

Computer operated test apparatus, with separate outputs and inputs for both currents and voltages. Used both as a current generator and power source for medium current linearity measurements (up to 25A). Contact: http://www.omicron.at

Hewlett Packard 33120A (Agilent 33120A)

Waveform generator to produce square-formed waves in step response measurements. Contact: www.agilent.com

Stanford Research Systems Model SR780

Two-channel network signal analyzer for the frequency dependency measurements. Contact: www.thinksrs.com

Sentec ACM1

Amplifier used to amplify the output from the SRS SR780 in frequency dependency measurements. Contact: Non

KEITHLEY 196 SYSTEM DMM

Multimeter to measure component output signals. Used for linearity measurements. Contact: www.keithley.com

Tektronix TDS 3054

Digital oscilloscope with ability to save screen shots to investigate step response, AC and frequency behaviour. Contact: www.tektronix.com

For detailed information about each apparatus, please refer to contact websites, all valid 2006-03-27.

	Linearity - Low and Medium Currents																	
	CSLA2DG.1	CSLA2DG.2	HAS 50.S	BB.150	CSNT651.1	CSNT651.2	LA100.P	CLSM.100	CLN.100	ACS754KCB.150.PSF.1	ACS754K.2	ACS754K.3	CMR.25.1	CMR.25.2	CMR.25.3	NT.50.1	NT.50.2	NT.50.3
Vs (V)	8,00	8,00	+/-15,00	+/-15,00	+/-15,00	+/-15,00	+/-15,00	+/-15,00	+/-15,00	5,00	5,00	5,00	5,00	5,00	5,00	+/-15,00	+/-15,00	+/-15,00
RL (ohm)	10000	10000	120000	10000	125	125	100	74,97	74,97	100000	100000	100000	27	27	27	100000	100000	100000
Np	2	2	2	2	2	2	2	2	2	---	---	---	1*	1*	1*	---	---	---
Voff (=V)	3,9987	3,981	0,0153	-0,0098	-0,0042	-0,0011	0,0045	0,0012	-0,001	2,4981	2,5011	2,4999	-0,00014	0,00015	-0,00011	-0,0025	-0,0076	0,0034
Voff (=V),Ip=<0,24A	---	---	---	---	---	---	---	---	---	2,496	2,4983	2,4985	0,00003	-0,000134	0,00008	-0,002	-0,0059	0,0031
Voff (=V),Ip=<25A					-0,005	-0,0007	0,0044	0,007	-0,0014	2,4954	2,4984	2,4977	-0,00002	-0,000474	0,00011	0,0004	-0,0028	0,0029
Intercept	3,999005	3,980398	0,015000	-0,009635	-0,004128	-0,000888	0,004518	0,001275	-0,001275	2,498144	2,501194	2,499963	-0,000144	0,000150	-0,000112	-0,002319	-0,007606	0,00335
Intercept	---	---	---	---	---	---	---	---	---	2,4960875	2,498366667	2,498425	3,5833E-05	-0,00013042	9,20833E-05	-0,0018375	-0,00620417	0,002975
Intercept	---	---	---	---	-0,00431923	-0,000675	0,003296154	0,006759615	-0,00095385	2,495273077	2,497753846	2,497055769	1,0385E-05	-0,00043308	0,000137885	0,00160962	-0,00179038	0,00393653

Ip (A) \ Vo (V)																		
Ip	**CSLA2DG.1**	**CSLA2DG.2**	**HAS 50.S**	**BB.150**	**CSNT651.1**	**CSNT651.2**	**LA100.P**	**CLSM.100**	**CLN.100**	**ACS754KCB.150.PSF.1**	**ACS754K.2**	**ACS754K.3**	**CMR.25.1**	**CMR.25.2**	**CMR.25.3**	**NT.50.1**	**NT.50.2**	**NT.50.3**
25					1,5552	1,5606	1,2451	0,9447	1,869	2,8295	2,827	2,8326	0,33723	0,33681	0,33745	1,2514	1,2442	1,2491
22,5					1,3989	1,4044	1,1209	0,8509	1,6821	2,7962	2,7942	2,7988	0,3035	0,30293	0,3037	1,1273	1,1204	1,1262
20					1,2425	1,2482	0,9966	0,757	1,495	2,7627	2,7618	2,7652	0,26977	0,26918	0,26994	1,0027	0,9966	1,0021
17,5					1,086	1,0919	0,8724	0,6631	1,3078	2,7293	2,7292	2,7315	0,23604	0,23547	0,2362	0,8777	0,8723	0,8781
15					0,9303	0,9359	0,7484	0,5694	1,1211	2,6959	2,6963	2,6977	0,20233	0,20178	0,20248	0,7526	0,7479	0,7537
12,5					0,7738	0,7798	0,6242	0,4757	0,9342	2,6623	2,6633	2,6641	0,1686	0,16806	0,16874	0,6276	0,6232	0,629
10					0,6178	0,6236	0,5001	0,3819	0,7472	2,6288	2,6301	2,6305	0,13486	0,13434	0,135	0,5024	0,4984	0,5041
9,5					0,5866	0,5925	0,4753	0,3632	0,7099	2,6221	2,6235	2,6238	0,12812	0,1276	0,12826	0,4771	0,4734	0,4789
9					0,5554	0,5612	0,4504	0,3444	0,6725	2,6154	2,6169	2,6171	0,12138	0,12086	0,12151	0,4519	0,4484	0,454
8,5					0,5243	0,53	0,4256	0,3256	0,6352	2,6087	2,6104	2,6104	0,11463	0,11412	0,11477	0,4267	0,4232	0,429
8					0,493	0,4987	0,4007	0,3068	0,5978	2,602	2,6037	2,6037	0,10789	0,10738	0,10803	0,4015	0,3983	0,4036
7,5					0,4619	0,4675	0,3759	0,2881	0,5604	2,5953	2,5972	2,597	0,10115	0,10065	0,10129	0,3765	0,3732	0,3788
7					0,4307	0,4362	0,351	0,2693	0,523	2,5887	2,5906	2,5903	0,09441	0,0939	0,09454	0,3512	0,348	0,3536
6,5					0,3995	0,405	0,3262	0,2505	0,4856	2,582	2,584	2,5837	0,08766	0,08716	0,0878	0,3262	0,3229	0,3285
6					0,3684	0,3737	0,3013	0,2317	0,4482	2,5754	2,5774	2,577	0,08093	0,08043	0,08106	0,301	0,2975	0,3034
5,5					0,3372	0,3424	0,2765	0,2129	0,4108	2,5687	2,5708	2,5703	0,07419	0,07369	0,07432	0,2758	0,2725	0,2784
5					0,3061	0,3112	0,2517	0,1942	0,3735	2,5621	2,5642	2,5637	0,06744	0,06695	0,06757	0,2506	0,2473	0,2532
4,5					0,275	0,2799	0,2268	0,1754	0,336	2,5554	2,5577	2,5569	0,06071	0,06022	0,06084	0,2257	0,2225	0,2282
4					0,244	0,2487	0,202	0,1567	0,2987	2,5486	2,5511	2,5503	0,05396	0,05347	0,05409	0,2007	0,1975	0,2031
3,5					0,213	0,2176	0,1771	0,1379	0,2613	2,5421	2,5445	2,5436	0,04721	0,04673	0,04734	0,1755	0,1722	0,1779
3					0,1819	0,1862	0,1522	0,1191	0,2238	2,5354	2,538	2,537	0,04046	0,03998	0,04059	0,1505	0,1472	0,153
2,5					0,151	0,1599	0,1274	0,1004	0,1864	2,5289	2,5314	2,5303	0,03372	0,03325	0,03385	0,1255	0,1222	0,128
2					0,1201	0,1239	0,1027	0,0816	0,1491	2,5223	2,5249	2,5237	0,02698	0,02651	0,02711	0,1004	0,097	0,1029
1,5					0,089	0,0925	0,0778	0,0628	0,1116	2,5156	2,5184	2,5171	0,02024	0,01977	0,02036	0,0753	0,0722	0,0779
1					0,0581	0,0613	0,0629	0,044	0,0742	2,509	2,512	2,5104	0,0135	0,01304	0,01363	0,0502	0,0472	0,0529
0,5					0,0274	0,0302	0,0281	0,0253	0,0369	2,5026	2,5055	2,5037	0,00675	0,00629	0,00688	0,0253	0,0222	0,0279
0,24	4,0031	3,9839	0,0332	-0,0001	0,0107	0,0141	0,0164	0,0103	0,0165	2,4992	2,5016	2,5014	0,00327	0,0031	0,00333	0,01	0,0057	0,0148
0,23	4,0029	3,9838	0,0325	-0,0006	0,0101	0,0135	0,0159	0,0099	0,0157	2,4991	2,5014	2,5013	0,00313	0,00297	0,00319	0,0095	0,0051	0,0141
0,22	4,0028	3,9837	0,0307	-0,0009	0,0095	0,0129	0,0154	0,0095	0,015	2,499	2,5012	2,5011	0,003	0,00283	0,00306	0,009	0,0046	0,0137
0,21	4,0026	3,9835	0,0304	-0,0011	0,0089	0,0122	0,0149	0,0092	0,0143	2,4989	2,5011	2,501	0,00286	0,00269	0,00292	0,0086	0,0041	0,0134
0,2	4,0024	3,9834	0,0296	-0,0016	0,0082	0,0116	0,0144	0,0088	0,0136	2,4987	2,501	2,501	0,00273	0,00256	0,00278	0,0082	0,0038	0,0129
0,19	4,0022	3,9834	0,0289	-0,002	0,0076	0,011	0,0139	0,0084	0,0128	2,4985	2,5009	2,5009	0,00259	0,00242	0,00264	0,0077	0,0032	0,0124
0,18	4,0019	3,9832	0,0284	-0,0023	0,007	0,0104	0,0134	0,008	0,0121	2,4984	2,5006	2,5008	0,00246	0,00229	0,00252	0,0072	0,0028	0,0119
0,17	4,0018	3,9831	0,0276	-0,0029	0,0063	0,0097	0,0129	0,0076	0,0114	2,4982	2,5005	2,5007	0,00232	0,00216	0,00238	0,0068	0,0024	0,0115
0,16	4,0017	3,983	0,0268	-0,0033	0,0057	0,0091	0,0125	0,0073	0,0107	2,498	2,5004	2,5006	0,00219	0,00202	0,00225	0,0063	0,0019	0,011
0,15	4,0015	3,9829	0,0259	-0,0037	0,0052	0,0085	0,012	0,0069	0,0099	2,4979	2,5003	2,5004	0,00205	0,00188	0,00211	0,0058	0,0014	0,0105
0,14	4,0013	3,9827	0,0251	-0,0039	0,0045	0,0079	0,0115	0,0065	0,0092	2,4978	2,5002	2,5004	0,00192	0,00175	0,00197	0,0053	0,001	0,01
0,13	4,0011	3,9826	0,0243	-0,0042	0,0039	0,0072	0,011	0,0061	0,0085	2,4976	2,5	2,5003	0,00178	0,00162	0,00184	0,0047	0,0005	0,0096
0,12	4,0009	3,9825	0,024	-0,0049	0,0033	0,0066	0,0105	0,0058	0,0077	2,4997	2,5028	2,5015	0,00147	0,00176	0,0015	0,0037	-0,0016	0,0093
0,11	4,0007	3,9824	0,023	-0,0053	0,0027	0,006	0,01	0,0054	0,007	2,4996	2,5026	2,5013	0,00134	0,00163	0,00137	0,0033	-0,0021	0,0088
0,1	4,0005	3,9822	0,0224	-0,0058	0,0021	0,0053	0,0095	0,005	0,0063	2,4994	2,5025	2,5013	0,0012	0,0015	0,00124	0,0027	-0,0026	0,0083
0,09	4,0003	3,9821	0,0213	-0,0062	0,0015	0,0047	0,009	0,0047	0,0055	2,4993	2,5024	2,5011	0,00107	0,00136	0,0011	0,002	-0,0032	0,0078
0,08	4,0001	3,9819	0,021	-0,0065	0,0009	0,004	0,0085	0,0043	0,0048	2,4991	2,5022	2,501	0,00093	0,00123	0,00097	0,0017	-0,0036	0,0073
0,07	3,9999	3,982	0,0206	-0,007	0,0003	0,0034	0,008	0,0039	0,0041	2,499	2,5021	2,5008	0,0008	0,00109	0,00083	0,0011	-0,0041	0,0069
0,06	3,9997	3,9819	0,0198	-0,0075	-0,0003	0,0028	0,0075	0,0035	0,0034	2,4989	2,5019	2,5007	0,00067	0,00096	0,0007	0,0007	-0,0046	0,0063
0,05	3,9995	3,9817	0,0189	-0,0078	-0,001	0,0021	0,007	0,0031	0,0027	2,4988	2,5018	2,5006	0,00053	0,00082	0,00056	0,0002	-0,0051	0,0058
-0,05	3,9979	3,9802	0,0117	-0,0118	-0,0072	-0,0041	0,002	-0,0006	-0,0048	2,4975	2,5005	2,4994	-0,00082	-0,00052	-0,00079	-0,0048	-0,0101	0,0005
-0,06	3,9978	3,9799	0,0112	-0,0123	-0,0078	-0,0047	0,0016	-0,001	-0,0056	2,4974	2,5004	2,4992	-0,00095	-0,00066	-0,00092	-0,0054	-0,0106	0,0004
-0,07	3,9977	3,9796	0,0102	-0,0126	-0,0085	-0,0053	0,001	-0,0013	-0,0064	2,4973	2,5003	2,4991	-0,00109	-0,00079	-0,00106	-0,0058	-0,0111	-0,0002
-0,08	3,9975	3,9793	0,0092	-0,013	-0,009	-0,0059	0,0005	-0,0017	-0,0071	2,4971	2,5002	2,499	-0,00122	-0,00093	-0,00119	-0,0062	-0,0116	-0,0005
-0,09	3,9974	3,9791	0,0083	-0,0133	-0,0097	-0,0065	0	-0,0021	-0,0079	2,497	2,5001	2,4988	-0,00136	-0,00106	-0,00132	-0,0069	-0,0121	-0,0011
-0,1	3,9973	3,9789	0,0076	-0,0137	-0,0104	-0,0071	-0,0004	-0,0025	-0,0087	2,4969	2,4998	2,4987	-0,00149	-0,0012	-0,00146	-0,0073	-0,0126	-0,0016
-0,11	3,9972	3,9788	0,0069	-0,0141	-0,0109	-0,0078	-0,001	-0,0029	-0,0095	2,4967	2,4998	2,4985	-0,00163	-0,00133	-0,00159	-0,0078	-0,0131	-0,0021
-0,12	3,9971	3,9785	0,0063	-0,0144	-0,0116	-0,0084	-0,0014	-0,0032	-0,0102	2,4966	2,4997	2,4984	-0,00176	-0,00146	-0,00173	-0,0083	-0,0136	-0,0026
-0,13	3,9969	3,9782	0,0055	-0,0149	-0,0122	-0,009	-0,0019	-0,0036	-0,0109	2,4943	2,4966	2,4969	-0,00172	-0,00188	-0,00166	-0,0082	-0,0125	-0,0034
-0,14	3,9968	3,9781	0,0045	-0,0152	-0,0128	-0,0096	-0,0024	-0,004	-0,0117	2,4942	2,4966	2,4967	-0,00185	-0,00201	-0,00179	-0,0087	-0,0131	-0,0039
-0,15	3,9966	3,9779	0,0038	-0,0154	-0,0134	-0,0102	-0,0029	-0,0043	-0,0124	2,4941	2,4964	2,4966	-0,00196	-0,00215	-0,00193	-0,0092	-0,0136	-0,0044
-0,16	3,9965	3,9777	0,0033	-0,0159	-0,0141	-0,0108	-0,0034	-0,0047	-0,0133	2,494	2,4963	2,4964	-0,00212	-0,00228	-0,00206	-0,0098	-0,0141	-0,0048
-0,17	3,9963	3,9775	0,0026	-0,0163	-0,0147	-0,0115	-0,0039	-0,0051	-0,014	2,4939	2,4961	2,4963	-0,00226	-0,00242	-0,0022	-0,0102	-0,0146	-0,0055
-0,18	3,9962	3,9773	0,0014	-0,0165	-0,0153	-0,0121	-0,0044	-0,0055	-0,0148	2,4938	2,496	2,4961	-0,00239	-0,00255	-0,00233	-0,0108	-0,0153	-0,0059
-0,19	3,996	3,9771	0,0007	-0,017	-0,0159	-0,0127	-0,0049	-0,0059	-0,0156	2,4937	2,4959	2,4961	-0,00252	-0,00269	-0,00247	-0,0114	-0,0157	-0,0064
-0,2	3,9959	3,9768	-0,0001	-0,0175	-0,0165	-0,0133	-0,0054	-0,0062	-0,0163	2,4936	2,4958	2,4958	-0,00265	-0,00282	-0,0026	-0,0119	-0,0162	-0,007
-0,21	3,9958	3,9766	-0,0012	-0,0179	-0,0171	-0,0139	-0,0059	-0,0066	-0,0171	2,4935	2,4957	2,4955	-0,00279	-0,00295	-0,00273	-0,0124	-0,0168	-0,0074
-0,22	3,9956	3,9764	-0,0013	-0,0184	-0,0178	-0,0146	-0,0064	-0,007	-0,0179	2,4933	2,4955	2,4954	-0,00292	-0,00309	-0,00287	-0,013	-0,0174	-0,0081
-0,23	3,9955	3,9762	-0,002	-0,0187	-0,0184	-0,0152	-0,0069	-0,0073	-0,0186	2,4932	2,4954	2,4953	-0,00306	-0,00322	-0,003	-0,0135	-0,0178	-0,0086
-0,24	3,9953	3,976	-0,003	-0,019	-0,0189	-0,0158	-0,0074	-0,0077	-0,0194	2,4932	2,4953	2,4952	-0,0032	-0,00336	-0,00314	-0,0141	-0,0183	-0,009
-0,5					-0,0346	-0,0322	-0,0215	-0,0122	-0,0379	2,4893	2,4925	2,4907	-0,00673	-0,00717	-0,0066	-0,0248	-0,0278	-0,022
-1					-0,0657	-0,0633	-0,0464	-0,0309	-0,0773	2,4827	2,4859	2,4842	-0,01347	-0,01391	-0,01334	-0,0498	-0,0527	-0,047
-1,5					-0,0967	-0,0945	-0,0712	-0,0497	-0,1127	2,4761	2,4793	2,4776	-0,02021	-0,02065	-0,02009	-0,0747	-0,0776	-0,0719
-2					-0,1278	-0,1257	-0,0961	-0,0684	-0,1502	2,4695	2,4727	2,4709	-0,02695	-0,02738	-0,02682	-0,0997	-0,1026	-0,0968
-2,5					-0,1589	-0,1568	-0,1208	-0,0871	-0,1875	2,4628	2,466	2,4644	-0,03369	-0,03412	-0,03356	-0,1245	-0,1274	-0,1217
-3					-0,1901	-0,1881	-0,1458	-0,1059	-0,225	2,456	2,4594	2,4578	-0,04043	-0,04086	-0,04031	-0,1494	-0,1523	-0,1465
-3,5					-0,2212	-0,2192	-0,1705	-0,1246	-0,2624	2,4494	2,4527	2,4512	-0,04717	-0,04759	-0,04705	-0,1745	-0,1772	-0,1715
-4					-0,2523	-0,2504	-0,1953	-0,1434	-0,2999	2,4426	2,446	2,4444	-0,05391	-0,05432	-0,05379	-0,1993	-0,202	-0,1962
-4,5					-0,2835	-0,2816	-0,2202	-0,1621	-0,3373	2,436	2,4393	2,4378	-0,06065	-0,06106	-0,06054	-0,2242	-0,2269	-0,2212
-5					-0,3147	-0,3128	-0,245	-0,1808	-0,3747	2,4293	2,4327	2,431	-0,0674	-0,06781	-0,06729	-0,2491	-0,2519	-0,2459
-5,5					-0,3459	-0,344	-0,2698	-0,1996	-0,4121	2,4225	2,426	2,4243	-0,07414	-0,07455	-0,07403	-0,2739	-0,2768	-0,2707
-6					-0,3771	-0,3752	-0,2947	-0,2183	-0,4496	2,4157	2,4193	2,4176	-0,08089	-0,08129	-0,08078	-0,2987	-0,3011	-0,2956
-6,5					-0,4082	-0,4064	-0,3195	-0,237	-0,487	2,409	2,4126	2,4108	-0,08764	-0,08804	-0,08753	-0,3236	-0,3259	-0,3203
-7					-0,4394	-0,4376	-0,3444	-0,2558	-0,5244	2,4022	2,4058	2,4041	-0,09438	-0,09477	-0,09427	-0,3484	-0,3508	-0,3451
-7,5					-0,4706	-0,4688	-0,3691	-0,2745	-0,5618	2,3954	2,3991	2,3973	-0,10113	-0,10152	-0,10102	-0,3732	-0,3757	-0,3699
-8					-0,5018	-0,5	-0,394	-0,2933	-0,5992	2,3887	2,3923	2,3906	-0,10787	-0,10826	-0,10777	-0,398	-0,4005	-0,3946
-8,5					-0,533	-0,5312	-0,4188	-0,312	-0,6367	2,3819	2,3855	2,3838	-0,11462	-0,11501	-0,11452	-0,4228	-0,4253	-0,4196
-9					-0,5643	-0,5624	-0,4438	-0,3307	-0,6742	2,3751	2,3787	2,377	-0,12137	-0,12175	-0,12126	-0,4475	-0,4502	-0,4445
-9,5					-0,5955	-0,5936	-0,4685	-0,3494	-0,7116	2,3683	2,3719	2,3702	-0,12811	-0,12849	-0,12801	-0,4724	-0,475	-0,4693
-10					-0,6268	-0,625	-0,4934	-0,3682	-0,7492	2,3614	2,3651	2,3634	-0,13486	-0,13523	-0,13476	-0,497	-0,4998	-0,4941
-12,5					-0,783	-0,7811	-0,6175	-0,4619	-0,9364	2,3276	2,3314	2,3296	-0,16857	-0,16892	-0,16847	-0,6216	-0,6248	-0,6185
-15					-0,9398	-0,9373	-0,7419	-0,5557	-1,124	2,2937	2,2971	2,2958	-0,2023	-0,20263	-0,2022	-0,7464	-0,7494	-0,7432
-17,5					-1,0958	-1,0935	-0,8661	-0,6494	-1,3114	2,2596	2,2625	2,2617	-0,23604	-0,23635	-0,23594	-0,8705	-0,8741	-0,8681
-20					-1,2521	-1,2497	-0,9904	-0,7431	-1,4988	2,2256	2,228	2,2277	-0,26979	-0,27007	-0,26968	-0,9953	-0,999	-0,9932
-22,5					-1,4083	-1,4057	-1,1145	-0,8367	-1,6861	2,1915	2,193	2,1934	-0,30352	-0,30377	-0,3034	-1,1203	-1,1246	-1,1187
-25					-1,5646	-1,5619	-1,2387	-0,9304	-1,8735	2,1573	2,1643	2,1592	-0,33728	-0,33757	-0,33715	-1,246	-1,2496	-1,2447

Table 1: Measured data for linearity analysis.
Red numbers correspond to currents produced by the VARIREF VF-12 and black to the OMICRON CMC 256-6. Vcc by the EM 40205 between –0,24A and 0,24A. From +/-0,5A to +/-25A Vcc by the OMICRON.

Ip	CSLA2DG-1	CSLA2DG-2	HAS 50-S	BB-150	CSNT651-1	CSNT651-2	LA100-P	CLSM-100	CLN-100	ACS754KCB-150-PSF-1	ACS754K-2	ACS754K-3	CMR-25-1	CMR-25-2	CMR-25-3	NT-50-1	NT-50-2	NT-50-3
25					1,559519231	1,561275	1,241803846	0,937940385	1,869953846	0,334226923	0,329246154	0,335544231	0,33721962	0,337243077	0,337312115	1,24979038	1,249990385	1,245163462
22,5					1,403219231	1,405075	1,117603846	0,844140385	1,683053846	0,300926923	0,296446154	0,301744231	0,30348962	0,303363077	0,303562115	1,12569038	1,122190385	1,122263462
20					1,246819231	1,248875	0,993303846	0,750240385	1,495953846	0,267426923	0,264046154	0,268144231	0,26975962	0,269613077	0,269802115	1,00109038	0,998390385	0,998163462
17,5					1,090319231	1,092575	0,869103846	0,656340385	1,308753846	0,234026923	0,231446154	0,234444231	0,23602962	0,235903077	0,236062115	0,87609038	0,874090385	0,874163462
15					0,934619231	0,936575	0,745103846	0,562640385	1,122053846	0,200626923	0,198546154	0,200644231	0,20231962	0,202213077	0,202342115	0,75099038	0,749690385	0,749763462
12,5					0,778119231	0,780475	0,620903846	0,468940385	0,935153846	0,167026923	0,165546154	0,167044231	0,16858962	0,168493077	0,168602115	0,62599038	0,624990385	0,625063462
10					0,622119231	0,624275	0,496803846	0,375140385	0,748153846	0,133526923	0,132346154	0,133444231	0,13484962	0,134773077	0,134862115	0,50079038	0,500190385	0,500163462
9,5					0,590919231	0,593175	0,472003846	0,356440385	0,710853846	0,126826923	0,125746154	0,126744231	0,12810962	0,128033077	0,128122115	0,47549038	0,475190385	0,474963462
9					0,559719231	0,561875	0,447103846	0,337640385	0,673453846	0,120126923	0,119146154	0,120044231	0,12136962	0,121293077	0,121372115	0,45029038	0,450190385	0,450063462
8,5					0,528619231	0,530675	0,422303846	0,318840385	0,636153846	0,113426923	0,112646154	0,113344231	0,11461962	0,114553077	0,114632115	0,42509038	0,424990385	0,425063462
8					0,497319231	0,499375	0,397403846	0,300040385	0,598753846	0,106726923	0,105946154	0,106644231	0,10787962	0,107813077	0,107892115	0,39989038	0,400090385	0,399863462
7,5					0,466219231	0,468175	0,372603846	0,281340385	0,561353846	0,100026923	0,099446154	0,099944231	0,10113962	0,101083077	0,101152115	0,37489038	0,374990385	0,374863462
7					0,435019231	0,436875	0,347703846	0,262540385	0,523953846	0,093426923	0,092846154	0,093244231	0,09439962	0,094333077	0,094402115	0,34969038	0,349790385	0,349663462
6,5					0,403819231	0,405675	0,322903846	0,243740385	0,486553846	0,086726923	0,086246154	0,086644231	0,08764962	0,087593077	0,087662115	0,32459038	0,324690385	0,324563462
6					0,372719231	0,374375	0,298003846	0,224940385	0,449153846	0,080126923	0,079646154	0,079944231	0,08091962	0,080863077	0,080922115	0,29939038	0,299290385	0,299463462
5,5					0,341519231	0,343075	0,273203846	0,206140385	0,411753846	0,073426923	0,073046154	0,073244231	0,07417962	0,074123077	0,074182115	0,27419038	0,274290385	0,274463462
5					0,310419231	0,311875	0,248403846	0,187440385	0,374453846	0,066826923	0,066446154	0,066644231	0,06742962	0,067383077	0,067432115	0,24899038	0,249090385	0,249263462
4,5					0,279319231	0,280675	0,223603846	0,168640385	0,336953846	0,060126923	0,059946154	0,059844231	0,06069962	0,060653077	0,060702115	0,22409038	0,224290385	0,224263462
4					0,248319231	0,249375	0,198703846	0,149940385	0,299653846	0,053326923	0,053346154	0,053244231	0,05394962	0,053903077	0,053952115	0,19909038	0,199290385	0,199163462
3,5					0,217319231	0,218175	0,173803846	0,131140385	0,262253846	0,046826923	0,046746154	0,046544231	0,04719962	0,047163077	0,047202115	0,17389038	0,173990385	0,173963462
3					0,186219231	0,186875	0,148903846	0,112340385	0,224753846	0,040126923	0,040246154	0,039944231	0,04044962	0,040413077	0,040452115	0,14889038	0,148990385	0,149063462
2,5					0,155319231	0,160575	0,124103846	0,093640385	0,187353846	0,033626923	0,033646154	0,033244231	0,03370962	0,033683077	0,033712115	0,12389038	0,123990385	0,124063462
2					0,124419231	0,124575	0,099403846	0,074840385	0,150053846	0,027026923	0,027146154	0,026644231	0,02696962	0,026943077	0,026972115	0,09879038	0,098790385	0,098963462
1,5					0,093319231	0,093175	0,074503846	0,056040385	0,112553846	0,020326923	0,020646154	0,020044231	0,02022962	0,020203077	0,020222115	0,07369038	0,073990385	0,073963462
1					0,062419231	0,061975	0,049603846	0,037240385	0,075153846	0,013726923	0,014246154	0,013344231	0,01348962	0,013473077	0,013492115	0,04859038	0,048990385	0,048963462
0,5					0,031719231	0,030875	0,024803846	0,018540385	0,037853846	0,007326923	0,007746154	0,006644231	0,00673962	0,006723077	0,006742115	0,02369038	0,023990385	0,023963462
0,24	0,004095	0,0035025	0,0182	0,009535	0,0148275	0,0149875	0,0118825	0,009025	0,017775	0,0031125	0,003233333	0,002975	0,00323417	0,003230417	0,003237917	0,0118375	0,011904167	0,011825
0,23	0,003895	0,0034025	0,0175	0,009135	0,0142275	0,0143875	0,0113825	0,008625	0,016975	0,0030125	0,003033333	0,002875	0,00309417	0,003100417	0,003097917	0,0113375	0,011304167	0,011125
0,22	0,003795	0,0033025	0,0157	0,008735	0,0136275	0,0137875	0,0108825	0,008225	0,016275	0,0029125	0,002833333	0,002675	0,00296417	0,002960417	0,002967917	0,0108375	0,010804167	0,010725
0,21	0,003595	0,0031025	0,0154	0,008535	0,0130275	0,0130875	0,0103825	0,007925	0,015575	0,0028125	0,002733333	0,002575	0,00282417	0,002820417	0,002827917	0,0104375	0,010304167	0,010425
0,2	0,003395	0,0030025	0,0146	0,008035	0,0123275	0,0124875	0,0098825	0,007525	0,014875	0,0026125	0,002633333	0,002575	0,00269417	0,002690417	0,002687917	0,0100375	0,010004167	0,009925
0,19	0,003195	0,0030025	0,0139	0,007635	0,0117275	0,0118875	0,0093825	0,007125	0,014075	0,0024125	0,002533333	0,002475	0,00255417	0,002550417	0,002547917	0,0095375	0,009404167	0,009425
0,18	0,002895	0,0028025	0,0134	0,007335	0,0111275	0,0112875	0,0088825	0,006725	0,013375	0,0023125	0,002233333	0,002375	0,00242417	0,002420417	0,002427917	0,0090375	0,009004167	0,008925
0,17	0,002795	0,0027025	0,0126	0,006735	0,0104275	0,0105875	0,0083825	0,006325	0,012675	0,0021125	0,002133333	0,002275	0,00228417	0,002290417	0,002287917	0,0086375	0,008604167	0,008525
0,16	0,002695	0,0026025	0,0118	0,006335	0,0098275	0,0099875	0,0079825	0,006025	0,011975	0,0019125	0,002033333	0,002175	0,00215417	0,002150417	0,002157917	0,0081375	0,008104167	0,008025
0,15	0,002495	0,0025025	0,0109	0,005935	0,0093275	0,0093875	0,0074825	0,005625	0,011175	0,0018125	0,001933333	0,001975	0,00201417	0,002010417	0,002017917	0,0076375	0,007604167	0,007525
0,14	0,002295	0,0023025	0,0101	0,005735	0,0086275	0,0087875	0,0069825	0,005225	0,010475	0,0017125	0,001833333	0,001975	0,00188417	0,001880417	0,001877917	0,0071375	0,007204167	0,007025
0,13	0,002095	0,0022025	0,0093	0,005435	0,0080275	0,0080875	0,0064825	0,004825	0,009775	0,0015125	0,001633333	0,001875	0,00174417	0,001750417	0,001747917	0,0065375	0,006704167	0,006625
0,12	0,001895	0,0021025	0,009	0,004735	0,0074275	0,0074875	0,0059825	0,004525	0,008975	0,00155625	0,00160625	0,0015375	0,00161438	0,00161	0,001611875	0,00601875	0,00600625	0,00594375
0,11	0,001695	0,0020025	0,008	0,004335	0,0068275	0,0068875	0,0054825	0,004125	0,008275	0,00145625	0,00140625	0,0013375	0,00148438	0,00148	0,001481875	0,00561875	0,00550625	0,00544375
0,1	0,001495	0,0018025	0,0074	0,003835	0,0062275	0,0061875	0,0049825	0,003725	0,007575	0,00125625	0,00130625	0,0013375	0,00134438	0,00135	0,001351875	0,00501875	0,00500625	0,00494375
0,09	0,001295	0,0017025	0,0063	0,003435	0,0056275	0,0055875	0,0044825	0,003425	0,006775	0,00115625	0,00120625	0,0011375	0,00121438	0,00121	0,001211875	0,00431875	0,00440625	0,00444375
0,08	0,001095	0,0015025	0,006	0,003135	0,0050275	0,0048875	0,0039825	0,003025	0,006075	0,00095625	0,00100625	0,0010375	0,00107438	0,00108	0,001081875	0,00401875	0,00400625	0,00394375
0,07	0,000895	0,0016025	0,0056	0,002635	0,0044275	0,0042875	0,0034825	0,002625	0,005375	0,00085625	0,00090625	0,0008375	0,00094438	0,00094	0,000941875	0,00341875	0,00350625	0,00354375
0,06	0,000695	0,0015025	0,0048	0,002135	0,0038275	0,0036875	0,0029825	0,002225	0,004675	0,00075625	0,00070625	0,0007375	0,00081438	0,00081	0,000811875	0,00301875	0,00300625	0,00294375
0,05	0,000495	0,0013025	0,0039	0,001835	0,0031275	0,0029875	0,0024825	0,001825	0,003975	0,00065625	0,00060625	0,0006375	0,00067438	0,00067	0,000671875	0,00251875	0,00250625	0,00244375
-0,05	-0,001105	-0,000198	-0,003300	-0,002165	-0,003073	-0,003213	-0,002518	-0,001875	-0,003525	-0,00064375	-0,00069375	-0,0005625	-0,0006756	-0,00067	-0,00067813	-0,0024813	-0,00249375	-0,00245625
-0,06	-0,001205	-0,000498	-0,003800	-0,002665	-0,003673	-0,003813	-0,002918	-0,002275	-0,004325	-0,00074375	-0,00079375	-0,0007625	-0,0008056	-0,00081	-0,00080813	-0,0030813	-0,00299375	-0,00295625
-0,07	-0,001305	-0,000898	-0,004800	-0,002965	-0,004373	-0,004413	-0,003518	-0,002575	-0,005125	-0,00084375	-0,00089375	-0,0008625	-0,0009456	-0,00094	-0,00094813	-0,0034813	-0,00349375	-0,00355625
-0,08	-0,001505	-0,001098	-0,005800	-0,003365	-0,004873	-0,005013	-0,004018	-0,002975	-0,005825	-0,00104375	-0,00099375	-0,0009625	-0,0010756	-0,00108	-0,00107813	-0,0038813	-0,00399375	-0,00385625
-0,09	-0,001605	-0,001298	-0,006700	-0,003665	-0,005573	-0,005613	-0,004518	-0,003375	-0,006625	-0,00114375	-0,00109375	-0,0011625	-0,0012156	-0,00121	-0,00120813	-0,0045813	-0,00449375	-0,00445625
-0,1	-0,001705	-0,001498	-0,007400	-0,004065	-0,006273	-0,006213	-0,004918	-0,003775	-0,007425	-0,00124375	-0,00139375	-0,0012625	-0,0013456	-0,00135	-0,00134813	-0,0049813	-0,00499375	-0,00495625
-0,11	-0,001805	-0,001598	-0,008100	-0,004465	-0,006773	-0,006913	-0,005518	-0,004175	-0,008225	-0,00144375	-0,00139375	-0,0014625	-0,0014856	-0,00148	-0,00147813	-0,0054813	-0,00549375	-0,00545625
-0,12	-0,001905	-0,001898	-0,008700	-0,004765	-0,007473	-0,007513	-0,005918	-0,004475	-0,008925	-0,00154375	-0,00149375	-0,0015625	-0,0016156	-0,00161	-0,00161813	-0,0059813	-0,00599375	-0,00595625
-0,13	-0,002105	-0,002198	-0,009500	-0,005265	-0,008073	-0,008113	-0,006418	-0,004875	-0,009625	-0,0017875	-0,00176667	-0,001525	-0,0017558	-0,00174958	-0,00175208	-0,0063625	-0,00629583	-0,006375
-0,14	-0,002205	-0,002298	-0,010500	-0,005565	-0,008673	-0,008713	-0,006918	-0,005275	-0,010425	-0,0018875	-0,00176667	-0,001725	-0,0018858	-0,00187958	-0,00188208	-0,0068625	-0,00689583	-0,006875
-0,15	-0,002405	-0,002498	-0,011200	-0,005765	-0,009273	-0,009313	-0,007418	-0,005575	-0,011125	-0,0019875	-0,00196667	-0,001825	-0,0019958	-0,00201958	-0,00202208	-0,0073625	-0,00739583	-0,007375
-0,16	-0,002505	-0,002698	-0,011700	-0,006265	-0,009973	-0,009913	-0,007918	-0,005975	-0,012025	-0,0020875	-0,00206667	-0,002025	-0,0021558	-0,00214958	-0,00215208	-0,0079625	-0,00789583	-0,007775
-0,17	-0,002705	-0,002898	-0,012400	-0,006665	-0,010573	-0,010613	-0,008418	-0,006375	-0,012725	-0,0021875	-0,00226667	-0,002125	-0,0022958	-0,00228958	-0,00229208	-0,0083625	-0,00839583	-0,008475
-0,18	-0,002805	-0,003098	-0,013600	-0,006865	-0,011173	-0,011213	-0,008918	-0,006775	-0,013525	-0,0022875	-0,00236667	-0,002325	-0,0024258	-0,00241958	-0,00242208	-0,0089625	-0,00909583	-0,008875
-0,19	-0,003005	-0,003298	-0,014300	-0,007365	-0,011773	-0,011813	-0,009418	-0,007175	-0,014325	-0,0023875	-0,00246667	-0,002325	-0,0025558	-0,00255958	-0,00256208	-0,0095625	-0,00949583	-0,009375
-0,2	-0,003105	-0,003598	-0,015100	-0,007865	-0,012373	-0,012413	-0,009918	-0,007475	-0,015025	-0,0024875	-0,00256667	-0,002625	-0,0026858	-0,00268958	-0,00269208	-0,0100625	-0,00999583	-0,009975
-0,21	-0,003205	-0,003798	-0,016200	-0,008265	-0,012973	-0,013013	-0,010418	-0,007875	-0,015825	-0,0025875	-0,00266667	-0,002925	-0,0028258	-0,00281958	-0,00282208	-0,0105625	-0,01059583	-0,010375
-0,22	-0,003405	-0,003998	-0,016300	-0,008765	-0,013673	-0,013713	-0,010918	-0,008275	-0,016625	-0,0027875	-0,00286667	-0,003025	-0,0029558	-0,00295958	-0,00296208	-0,0111625	-0,01119583	-0,011075
-0,23	-0,003505	-0,004198	-0,017000	-0,009065	-0,014273	-0,014313	-0,011418	-0,008575	-0,017325	-0,0028875	-0,00296667	-0,003125	-0,0030958	-0,00308958	-0,00309208	-0,0116625	-0,01159583	-0,011575
-0,24	-0,003705	-0,004398	-0,018000	-0,009365	-0,014773	-0,014913	-0,011918	-0,008975	-0,018125	-0,0028875	-0,00306667	-0,003225	-0,0032358	-0,00322958	-0,00323208	-0,0122625	-0,01209583	-0,011975
-0,5					-0,03028077	-0,031525	-0,024796154	-0,01895962	-0,03694615	-0,005973077	-0,00525385	-0,00635577	-0,0067404	-0,00673692	-0,00673788	-0,0264096	-0,02600962	-0,02593654
-1					-0,06138077	-0,062625	-0,049696154	-0,03765962	-0,07634615	-0,012573077	-0,01185385	-0,01285577	-0,0134804	-0,01347692	-0,01347788	-0,0514096	-0,05090962	-0,05093654
-1,5					-0,09238077	-0,093825	-0,074496154	-0,05645962	-0,11174615	-0,019173077	-0,01845385	-0,01945577	-0,0202204	-0,02021692	-0,02022788	-0,0763096	-0,07580962	-0,07583654
-2					-0,12348077	-0,125025	-0,099396154	-0,07515962	-0,14924615	-0,025773077	-0,02505385	-0,02615577	-0,0269604	-0,02694692	-0,02695788	-0,1013096	-0,10080962	-0,10073654
-2,5					-0,15458077	-0,156125	-0,124096154	-0,09385962	-0,18654615	-0,032473077	-0,03175385	-0,03265577	-0,0337004	-0,03368692	-0,03369788	-0,1261096	-0,12560962	-0,12563654
-3					-0,18578077	-0,187425	-0,149096154	-0,11265962	-0,22404615	-0,039273077	-0,03835385	-0,03925577	-0,0404404	-0,04042692	-0,04044788	-0,1510096	-0,15050962	-0,15043654
-3,5					-0,21688077	-0,218525	-0,173796154	-0,13135962	-0,26144615	-0,045873077	-0,04505385	-0,04585577	-0,0471804	-0,04715692	-0,04718788	-0,1761096	-0,17540962	-0,17543654
-4					-0,24798077	-0,249725	-0,198596154	-0,15015962	-0,29894615	-0,052673077	-0,05175385	-0,05265577	-0,0539204	-0,05388692	-0,05392788	-0,2009096	-0,20020962	-0,20013654
-4,5					-0,27918077	-0,280925	-0,223496154	-0,16885962	-0,33634615	-0,059273077	-0,05845385	-0,05925577	-0,0606604	-0,06062692	-0,06067788	-0,2250096	-0,22510962	-0,22513654
-5					-0,31038077	-0,312125	-0,248296154	-0,18755962	-0,37374615	-0,065973077	-0,06505385	-0,06605577	-0,0674104	-0,06737692	-0,06742788	-0,2507096	-0,25010962	-0,24983654
-5,5					-0,34158077	-0,343325	-0,273096154	-0,20635962	-0,41114615	-0,072773077	-0,07175385	-0,07275577	-0,0741504	-0,07411692	-0,07416788	-0,2755096	-0,27500962	-0,27463654
-6					-0,37278077	-0,374525	-0,297996154	-0,22505962	-0,44864615	-0,079573077	-0,07845385	-0,07945577	-0,0809004	-0,08085692	-0,08091788	-0,3003096	-0,29930962	-0,29953654
-6,5					-0,40388077	-0,405725	-0,322796154	-0,24375962	-0,48604615	-0,086273077	-0,08515385	-0,08625577	-0,0876504	-0,08760692	-0,08766788	-0,3252096	-0,32410962	-0,32423654
-7					-0,43508077	-0,436925	-0,347696154	-0,26255962	-0,52344615	-0,093073077	-0,09195385	-0,09295577	-0,0943904	-0,09433692	-0,09440788	-0,3500096	-0,34900962	-0,34903654
-7,5					-0,46628077	-0,468125	-0,372396154	-0,28125962	-0,56084615	-0,099873077	-0,09865385	-0,09975577	-0,1011404	-0,10108692	-0,10115788	-0,3748096	-0,37390962	-0,37383654
-8					-0,49748077	-0,499325	-0,397296154	-0,30005962	-0,59824615	-0,106573077	-0,10545385	-0,10645577	-0,1078804	-0,10782692	-0,10790788	-0,3996096	-0,39870962	-0,39873654
-8,5					-0,52868077	-0,530525	-0,422096154	-0,31875962	-0,63574615	-0,113373077	-0,11225385	-0,11325577	-0,1146304	-0,11457692	-0,11465788	-0,4244096	-0,42350962	-0,42353654
-9					-0,55998077	-0,561725	-0,447096154	-0,33745962	-0,67324615	-0,120173077	-0,11905385	-0,12005577	-0,1213804	-0,12131692	-0,12139788	-0,4491096	-0,44840962	-0,44843654
-9,5					-0,59118077	-0,592925	-0,471796154	-0,35615962	-0,71064615	-0,126973077	-0,12585385	-0,12685577	-0,1281204	-0,12805692	-0,12814788	-0,4740096	-0,47320962	-0,47323654
-10					-0,62248077	-0,624325	-0,496696154	-0,37495962	-0,74824615	-0,133873077	-0,13265385	-0,13365577	-0,1348704	-0,13479692	-0,13489788	-0,4986096	-0,49800962	-0,49803654
-12,5					-0,77868077	-0,780425	-0,620796154	-0,46865962	-0,93544615	-0,167673077	-0,16635385	-0,16745577	-0,1685804	-0,16848692	-0,16860788	-0,6232096	-0,62300962	-0,62243654
-15					-0,93548077	-0,936625	-0,745196154	-0,56245962	-1,12304615	-0,201573077	-0,20065385	-0,20125577	-0,2023104	-0,20219692	-0,20233788	-0,7480096	-0,74760962	-0,74713654
-17,5					-1,09148077	-1,092825	-0,869396154	-0,65615962	-1,31044615	-0,235673077	-0,23525385	-0,23535577	-0,2360504	-0,23591692	-0,23607788	-0,8721096	-0,87230962	-0,87203654
-20					-1,24778077	-1,249025	-0,993696154	-0,74985962	-1,49784615	-0,269673077	-0,26975385	-0,26935577	-0,2698004	-0,26963692	-0,26981788	-0,9969096	-0,99720962	-0,99713654
-22,5					-1,40398077	-1,405025	-1,117796154	-0,84345962	-1,68514615	-0,303773077	-0,30475385	-0,30365577	-0,3035304	-0,30333692	-0,30353788	-1,1219096	-1,12280962	-1,12263654
-25					-1,56028077	-1,561225	-1,241996154	-0,93715962	-1,87254615	-0,337973077	-0,33345385	-0,33785577	-0,3372904	-0,33713692	-0,33728788	-1,2476096	-1,24780962	-1,24863654

Table 2: Measured data for linearity analysis. Offset subtracted.
Red numbers, se Table 1.

Slope, datasheet	16,2	16,2	80	40	62,5	62,5	50	37,485	74,9700
Slope, medium					62,31541933	62,44034908	49,67363133	37,50268199	74,83694338
Slope, low	16,16632444	16,52772074	74,13039014	39,67659138	61,90657084	62,33778234	49,57494867	37,48973306	74,71971253
Ip	**CSLA2DG-1**	**CSLA2DG-2**	**HAS 50-S**	**BB-150**	**CSNT651-1**	**CSNT651-2**	**LA100-P**	**CLSM-100**	**CLN-100**
25					0,001633748	0,000266273	-3,69372E-05	0,000373335	-0,00096974
22,5					0,001122296	0,000167146	-5,28588E-05	0,00033004	-0,00077738
20					0,000510844	6,80183E-05	-0,00016878	0,000186745	-0,00078502
17,5					-0,00020061	-0,00013111	-0,000184702	4,34497E-05	-0,00089266
15					-0,00011206	-3,0236E-05	-6,23833E-07	0,000100155	-0,0005003
12,5					-0,00082351	-2,9364E-05	-1,65455E-05	0,00015686	-0,00030795
10					-0,00103496	-0,00012849	6,75328E-05	0,000113565	-0,00021559
9,5					-0,00107725	-8,3163E-06	0,000104348	0,000164906	-9,7116E-05
9					-0,00111954	-8,8142E-05	4,11642E-05	0,000116247	-7,8644E-05
8,5					-0,00106183	-6,7967E-05	7,79798E-05	6,75877E-05	3,98274E-05
8					-0,00120412	-0,00014779	1,47955E-05	1,89287E-05	5,82991E-05
7,5					-0,00114641	-0,00012762	5,16112E-05	7,02697E-05	7,67708E-05
7					-0,0011887	-0,00020744	-1,15732E-05	2,16107E-05	9,52425E-05
6,5					-0,00123099	-0,00018727	2,52425E-05	-2,7048E-05	0,000113714
6					-0,00117329	-0,00026709	-3,79418E-05	-7,5707E-05	0,000132186
5,5					-0,00121558	-0,00034692	-1,12617E-06	-0,00012437	0,000150658
5					-0,00115787	-0,00032675	3,56895E-05	-7,3025E-05	0,000269129
4,5					-0,00110016	-0,00040657	-2,74948E-05	-0,00012168	0,000187601
4					-0,00094245	-0,0003864	9,32082E-06	-7,0343E-05	0,000306073
3,5					-0,00078474	-0,00036622	-5,38635E-05	-0,000119	0,000324544
3					-0,00072703	-0,00044605	-0,000117048	-0,00016766	0,000243016
2,5					-0,00046932	0,004474127	-8,02322E-05	-0,00011632	0,000261488
2					-0,00021161	-0,0003057	5,65835E-05	-0,00016498	0,000379959
1,5					-0,0001539	-0,00048552	-6,60084E-06	-0,00021364	0,000298431
1					0,000103811	-0,00046535	-6,97852E-05	-0,0002623	0,000316903
0,5					0,000561521	-0,00034517	-3,29695E-05	-0,00021096	0,000435374
0,24	0,000215082	-0,00046415	0,000408706	1,26181E-05	-3,0077E-05	2,64322E-05	-1,54877E-05	2,74641E-05	-0,00015773
0,23	0,000176745	-0,00039888	0,00045001	9,38398E-06	-1,1011E-05	4,98101E-05	-1,97382E-05	2,3614E-06	-0,00021053
0,22	0,000238409	-0,0003336	-0,000608686	6,1499E-06	8,05441E-06	7,31879E-05	-2,39887E-05	-2,2741E-05	-0,00016334
0,21	0,000200072	-0,00036832	-0,000167382	0,000202916	2,71201E-05	-3,4343E-06	-2,82392E-05	5,21561E-05	-0,00011614
0,2	0,000161735	-0,00030304	-0,000226078	9,96817E-05	-5,3814E-05	1,99435E-05	-3,24897E-05	2,70534E-05	-6,8943E-05
0,19	0,000123398	-0,00013777	-0,000184774	9,64476E-05	-3,4748E-05	4,33214E-05	-3,67402E-05	1,95072E-06	-0,00012175
0,18	-1,49384E-05	-0,00017249	5,65298E-05	0,000193214	-1,5683E-05	6,66992E-05	-4,09908E-05	-2,3152E-05	-7,4548E-05
0,17	4,67248E-05	-0,00010721	-2,16632E-06	-1,00206E-05	-9,6617E-05	-9,923E-06	-4,52413E-05	-4,8255E-05	-2,7351E-05
0,16	0,000108388	-4,1936E-05	-6,08624E-05	-1,32546E-05	-7,7551E-05	1,34548E-05	5,05082E-05	2,66427E-05	1,9846E-05
0,15	7,00513E-05	2,33419E-05	-0,000219659	-1,64887E-05	4,15144E-05	3,68326E-05	4,62577E-05	1,54004E-06	-3,2957E-05
0,14	3,17146E-05	-1,1381E-05	-0,000278265	0,000180277	-3,942E-05	6,02105E-05	4,20072E-05	-2,3563E-05	1,42402E-05
0,13	-6,62218E-06	5,38963E-05	-0,000336951	0,000277043	-2,0354E-05	-1,6412E-05	3,77567E-05	-4,8665E-05	6,14374E-05
0,12	-4,49589E-05	0,000119174	0,000104353	-2,6191E-05	-1,2885E-06	6,96612E-06	3,35062E-05	2,6232E-05	8,6345E-06
0,11	-8,32957E-05	0,000184451	-0,000154343	-2,94251E-05	1,77772E-05	3,03439E-05	2,92556E-05	1,12936E-06	5,58316E-05
0,1	-0,000121632	0,000149728	-1,3039E-05	-0,000132659	3,68429E-05	-4,6278E-05	2,50051E-05	-2,3973E-05	0,000103029
0,09	-0,000159969	0,000215005	-0,000371735	-0,000135893	5,59086E-05	-2,29E-05	2,07546E-05	5,0924E-05	5,02259E-05
0,08	-0,000198306	0,000180282	6,95688E-05	-3,91273E-05	7,49743E-05	-9,9523E-05	1,65041E-05	2,58214E-05	9,7423E-05
0,07	-0,000236643	0,00044556	0,000410873	-0,000142361	9,404E-05	-7,6145E-05	1,22536E-05	7,18686E-07	0,00014462
0,06	-0,000274979	0,000510837	0,000352177	-0,000245595	0,000113106	-5,2767E-05	8,00308E-06	-2,4384E-05	0,000191817
0,05	-0,000313316	0,000476114	0,00019348	-0,00014883	3,21715E-05	-0,00012939	3,75257E-06	-4,9487E-05	0,000239014
-0,05	-0,000296684	0,000628886	0,00040652	-0,00018117	2,28285E-05	-9,5611E-05	-3,87526E-05	-5,1335E-07	0,000210986
-0,06	-0,000235021	0,000494163	0,000647823	-0,000284405	4,18943E-05	-7,2233E-05	5,69969E-05	-2,5616E-05	0,000158183
-0,07	-0,000173357	0,00025944	0,000389127	-0,000187639	-3,904E-05	-4,8855E-05	-4,72536E-05	4,92813E-05	0,00010538
-0,08	-0,000211694	0,000224718	0,000130431	-0,000190873	8,00257E-05	-2,5477E-05	-5,15041E-05	2,41786E-05	0,000152577
-0,09	-0,000150031	0,000189995	-2,82649E-05	-9,41068E-05	-9,0862E-07	-2,0996E-06	-5,57546E-05	-9,2402E-07	9,97741E-05
-0,1	-8,83676E-05	0,000155272	1,3039E-05	-9,73409E-05	-8,1843E-05	2,12782E-05	3,99949E-05	-2,6027E-05	4,69713E-05
-0,11	-2,67043E-05	0,000220549	5,43429E-05	-0,000100575	3,72228E-05	-5,5344E-05	-6,42556E-05	-5,1129E-05	-5,8316E-06
-0,12	3,49589E-05	8,58265E-05	0,000195647	-3,80903E-06	-4,3711E-05	-3,1966E-05	3,14938E-05	2,3768E-05	4,13655E-05
-0,13	-3,37782E-06	-4,8896E-05	0,000136951	-0,000107043	-2,4646E-05	-8,5883E-06	2,72433E-05	-1,3347E-06	8,85626E-05
-0,14	5,82854E-05	1,63809E-05	-0,000121745	-1,02772E-05	-5,5801E-06	1,47895E-05	2,29928E-05	-2,6437E-05	3,57598E-05
-0,15	1,99487E-05	-1,8342E-05	-8,04415E-05	0,000186489	1,34856E-05	3,81674E-05	1,87423E-05	4,846E-05	8,29569E-05
-0,16	8,16119E-05	-5,3065E-05	0,000160862	8,32546E-05	-6,7449E-05	6,15452E-05	1,44918E-05	2,33573E-05	-6,9846E-05
-0,17	4,32752E-05	-8,7787E-05	0,000202166	8,00206E-05	-4,8383E-06	-1,5077E-05	1,02413E-05	-1,7454E-06	-2,2649E-05
-0,18	0,000104938	-0,00012251	-0,00026653	0,000276786	-2,9317E-05	8,30082E-06	5,99076E-06	-2,6848E-05	-7,5452E-05
-0,19	6,66016E-05	-0,00015723	-0,000215226	0,000173552	-1,0252E-05	3,16786E-05	1,74025E-06	-5,1951E-05	-0,00012825
-0,2	0,000128265	-0,00029196	-0,000273922	7,03183E-05	8,81417E-06	5,50565E-05	-2,51027E-06	2,29466E-05	-8,1057E-05
-0,21	0,000189928	-0,00032668	-0,000632618	6,70842E-05	2,78799E-05	7,84343E-05	-6,76078E-06	-2,1561E-06	-0,00013386
-0,22	0,000151591	-0,0003614	8,68583E-06	-3,61499E-05	-5,3054E-05	1,81211E-06	-1,10113E-05	-2,7259E-05	-0,00018666
-0,23	0,000213255	-0,00039612	4,99897E-05	6,0616E-05	-3,3989E-05	2,51899E-05	-1,52618E-05	4,76386E-05	-0,00013947
-0,24	0,000174918	-0,00043085	-0,000208706	0,000157382	8,5077E-05	4,85678E-05	-1,95123E-05	2,25359E-05	-0,00019227
-0,5					0,00087694	-0,00030483	4,06618E-05	-0,00020827	0,000472318
-1					0,00093465	-0,00018465	-2,25225E-05	-0,00015693	-0,00150921
-1,5					0,00109236	-0,00016448	1,42932E-05	-0,00020559	0,000509261
-2					0,001150069	-0,0001443	-4,88912E-05	-0,00015425	0,000427733
-2,5					0,001207779	-2,4127E-05	8,79245E-05	-0,00010291	0,000546205
-3					0,001165489	-0,00010395	-7,52598E-05	-0,00015157	0,000464676
-3,5					0,001223198	1,62218E-05	6,15558E-05	-0,00010023	0,000483148
-4					0,001280908	3,63963E-05	9,83715E-05	-0,00014889	0,00040162
-4,5					0,001238618	5,65709E-05	3,51872E-05	-9,7546E-05	0,000420091
-5					0,001196327	7,67454E-05	7,20028E-05	-4,6205E-05	0,000438563
-5,5					0,001154037	9,692E-05	0,000108818	-9,4864E-05	0,000457035
-6					0,001111747	0,000117095	4,56341E-05	-4,3523E-05	0,000375506
-6,5					0,001169456	0,000137269	8,24498E-05	7,81757E-06	0,000393978
-7					0,001127166	0,000157444	1,92655E-05	-4,0841E-05	0,00041245
-7,5					0,001084876	0,000177618	0,000156081	1,04996E-05	0,000430922
-8					0,001042585	0,000197793	9,28968E-05	-3,8159E-05	0,000449393
-8,5					0,001000295	0,000217967	0,000129712	1,31816E-05	0,000367865
-9					0,000958005	0,000238142	-3,34719E-05	6,45225E-05	0,000286337
-9,5					0,000815714	0,000258316	0,000103344	0,000115864	0,000304808
-10					0,000673424	7,84908E-05	4,01595E-05	6,72045E-05	0,00012328
-12,5					0,000261972	7,93636E-05	0,000124238	0,00012391	1,56384E-05
-15					-0,00074948	-1,9764E-05	-9,16839E-05	8,06145E-05	-0,000492
-17,5					-0,00096093	-0,00011889	-0,000107606	0,000137319	-0,00079964
-20					-0,00147238	-0,00021802	-0,000223527	0,000194024	-0,00110729
-22,5					-0,00188383	-0,00011715	-0,000139449	0,000360729	-0,00131493
-25					-0,00239529	-0,00021627	-0,000155371	0,000407434	-0,00162257

Slope, datasheet	13,3	13,3	13,3	13,5	13,5	13,5	50	50	50
Slope, medium	13,40379736	13,28680289	13,40834398	13,4880645	13,48157514	13,48980077	49,9571392	49,89725841	49,89226054
Slope, low	12,73203285	12,96817248	12,93737166	13,4587269	13,44958932	13,46396304	50,0605749	49,95893224	49,5687885
Ip	**ACS754KCB-150-PSF-1**	**ACS754K-2**	**ACS754K-3**	**CMR-25-1**	**CMR-25-2**	**CMR-25-3**	**NT-50-1**	**NT-50-2**	**NT-50-3**
25	-0,000868011	-0,00292392	0,000335631	1,8253E-05	0,000203698	6,70962E-05	0,0008619	-0,00144108	-0,0021430
22,5	-0,000658518	-0,00250691	5,64913E-05	8,3893E-06	2,76363E-05	4,15981E-05	0,00165475	-0,00049793	-0,0003124
20	-0,000649024	-0,0016899	-2,2649E-05	-1,474E-06	-1,8426E-05	6,10006E-06	0,0019476	0,000445216	0,000318251
17,5	-0,000539531	-0,0010729	-0,00020179	-1,134E-05	-2,4488E-05	-9,398E-06	0,00184045	0,000888362	0,00104890
15	-0,000430037	-0,00075589	-0,00048093	-1,202E-06	-1,055E-05	-4,8961E-06	0,0016333	0,001231508	0,00137955
12,5	-0,000520544	-0,00053888	-0,00056007	-1,107E-05	-2,6612E-05	-2,0394E-05	0,00152614	0,001274655	0,00141020
10	-0,000511051	-0,00052188	-0,00063921	-3,093E-05	-4,2674E-05	-3,5892E-05	0,00121899	0,001217801	0,00124085
9,5	-0,000509152	-0,00047847	-0,00063504	-2,69E-05	-4,1887E-05	-3,0992E-05	0,00089756	0,00116643	0,00098698
9	-0,000507253	-0,00043507	-0,00063087	-2,288E-05	-4,1099E-05	-3,6092E-05	0,00067613	0,001115059	0,00103311
8,5	-0,000505354	-0,00029167	-0,00062669	-2,885E-05	-4,0312E-05	-3,1191E-05	0,0004547	0,000863688	0,00097924
8	-0,000503456	-0,00034827	-0,00062252	-2,482E-05	-3,9524E-05	-2,6291E-05	0,00023327	0,000912317	0,00072537
7,5	-0,000501557	-0,00020487	-0,00061835	-2,079E-05	-2,8737E-05	-2,139E-05	0,00021184	0,000760947	0,00067150
7	-0,000399658	-0,00016147	-0,00061418	-1,677E-05	-3,7949E-05	-2,649E-05	-0,0001096	0,000509576	0,00041763
6,5	-0,00039776	-0,00011806	-0,00051001	-2,274E-05	-3,7161E-05	-2,159E-05	-0,000131	0,000358205	0,00026376
6	-0,000295861	-7,4664E-05	-0,00050583	-8,712E-06	-2,6374E-05	-1,6689E-05	-0,0003525	-9,3166E-05	0,00010989
5,5	-0,000293962	-3,1262E-05	-0,00050166	-4,684E-06	-2,5586E-05	-1,1789E-05	-0,0005739	-0,00014454	5,60286E-0
5	-0,000192064	1,21394E-05	-0,00039749	-1,066E-05	-2,4799E-05	-1,6888E-05	-0,0007953	-0,00039591	-0,00019784
4,5	-0,000190165	0,000155541	-0,00049332	3,3702E-06	-1,4011E-05	-1,9881E-06	-0,0007167	-0,00024728	-0,00025171
4	-0,000288266	0,000198942	-0,00038915	-2,603E-06	-2,3224E-05	-7,0877E-06	-0,0007382	-0,00029865	-0,00040558
3,5	-8,63677E-05	0,000242344	-0,00038497	-8,575E-06	-2,2436E-05	-1,2187E-05	-0,0009596	-0,00065002	-0,00065945
3	-8,4469E-05	0,000385745	-0,0002808	-1,455E-05	-3,1648E-05	-1,7287E-05	-0,000981	-0,00070139	-0,00061332
2,5	0,00011743	0,000429147	-0,00027663	-1,052E-05	-2,0861E-05	-1,2387E-05	-0,0010025	-0,00075276	-0,00066719
2	0,000219328	0,000572548	-0,00017246	-6,494E-06	-2,0073E-05	-7,4861E-06	-0,0011239	-0,00100413	-0,00082106
1,5	0,000221227	0,00071595	-6,8285E-05	-2,466E-06	-1,9286E-05	-1,2586E-05	-0,0012453	-0,0008555	-0,00087493
1	0,000323126	0,000959351	-6,4113E-05	1,5609E-06	-8,4982E-06	2,31462E-06	-0,0013668	-0,00090687	-0,0009288
0,5	0,000625024	0,001102752	-5,9941E-05	-4,412E-06	-1,7711E-05	-2,785E-06	-0,0012882	-0,00095824	-0,00098267
0,24	5,68121E-05	0,000120972	-0,00012997	4,0722E-06	2,51523E-06	6,56554E-06	-0,000177	-8,5977E-05	-7,1509E-05
0,23	8,41324E-05	5,06537E-05	-0,0001006	-1,341E-06	7,01112E-06	1,20517E-06	-0,0001764	-0,00018639	-0,00027582
0,22	0,000111453	-1,9665E-05	-0,00017122	3,2467E-06	1,50702E-06	5,8448E-06	-0,0001758	-0,0001868	-0,00018013
0,21	0,000138773	1,00171E-05	-0,00014185	-2,166E-06	-3,9971E-06	4,84428E-07	-7,522E-05	-0,00018721	1,55544E-05
0,2	6,60934E-05	3,96988E-05	-1,2474E-05	2,4213E-06	4,98802E-07	-4,8759E-06	2,5385E-05	1,23802E-05	1,12423E-05
0,19	-6,58624E-06	6,93806E-05	1,68994E-05	-2,991E-06	-5,0053E-06	-1,0236E-05	2,5991E-05	-8,803E-05	6,93018E-06
0,18	2,07341E-05	-0,00010094	4,62731E-05	1,5968E-06	-5,0941E-07	4,40332E-06	2,6597E-05	1,15589E-05	2,61807E-06
0,17	-5,19456E-05	-7,1256E-05	7,56468E-05	-3,817E-06	3,98648E-06	-9,5705E-07	0,0001272	0,000111148	9,8306E-05
0,16	-0,000124625	-4,1574E-05	0,000105021	7,7036E-07	-1,5176E-06	3,68258E-06	0,00012781	0,000110738	9,39938E-05
0,15	-9,73049E-05	-1,1893E-05	3,43943E-05	-4,642E-06	-7,0217E-06	-1,6778E-06	0,00012841	0,000110327	8,96817E-05
0,14	-6,99846E-05	1,77892E-05	0,000163768	-5,51E-08	-2,5258E-06	-7,0382E-06	0,00012902	0,000209916	8,53696E-05
0,13	-0,000142664	-5,2529E-05	0,000193142	-5,468E-06	1,97005E-06	-2,3985E-06	2,9625E-05	0,000209505	0,00018105
0,12	2,84061E-05	5,00693E-05	-1,4985E-05	-6,722E-07	-3,9507E-06	-3,8006E-06	1,1481E-05	1,11781E-05	-4,5046E-06
0,11	5,57264E-05	-2,0249E-05	-8,5611E-05	3,915E-06	5,45175E-07	8,39066E-07	0,00011209	1,07675E-05	-8,8167E-06
0,1	-1,69533E-05	9,43275E-06	4,37628E-05	-1,498E-06	5,04107E-06	5,4787E-06	1,2693E-05	1,03568E-05	-1,3129E-05
0,09	1,0367E-05	3,91145E-05	-2,6863E-05	3,0896E-06	-4,6304E-07	1,18326E-07	-0,0001867	-9,0054E-05	-1,7441E-05
0,08	-6,23126E-05	-3,1204E-05	2,51027E-06	-2,323E-06	4,03285E-06	4,75796E-06	1,3904E-05	9,53542E-06	-2,1753E-05
0,07	-3,49923E-05	-1,5221E-06	-6,8116E-05	2,2641E-06	-1,4713E-06	-6,0241E-07	-8,549E-05	9,12474E-06	7,39348E-05
0,06	-7,67197E-06	-7,184E-05	-3,8742E-05	6,8514E-06	3,02464E-06	4,03722E-06	1,5116E-05	8,71407E-06	-3,0377E-05
0,05	1,96484E-05	-4,2159E-05	-9,3686E-06	1,4387E-06	-2,4795E-06	-1,3232E-06	1,5721E-05	8,30339E-06	-3,4689E-05
-0,05	-7,14836E-06	-4,5341E-05	8,43686E-05	-2,689E-06	2,47947E-06	-4,9268E-06	2,1779E-05	4,19661E-06	2,21894E-05
-0,06	2,0172E-05	-1,566E-05	1,37423E-05	1,8986E-06	-3,0246E-06	-2,8722E-07	-7,762E-05	3,78593E-06	1,78773E-05
-0,07	4,74923E-05	1,40221E-05	4,3116E-05	-3,514E-06	1,47125E-06	-5,6476E-06	2,299E-05	3,37526E-06	-8,6435E-05
-0,08	-2,51874E-05	4,37038E-05	7,24897E-05	1,0732E-06	-4,0329E-06	-1,008E-06	0,0001236	2,96458E-06	0,00010925
-0,09	2,13296E-06	7,33855E-05	1,86345E-06	-4,34E-06	4,63039E-07	3,63167E-06	-7,58E-05	2,5539E-06	4,94097E-06
-0,1	2,94533E-05	-9,6933E-05	3,12372E-05	2,4769E-07	-5,0411E-06	-1,7287E-06	2,4807E-05	2,14322E-06	6,2885E-07
-0,11	-4,32264E-05	3,2749E-05	-3,9389E-05	-5,165E-06	-5,4517E-07	2,91093E-06	2,5413E-05	1,73255E-06	-3,6833E-06
-0,12	-1,59061E-05	6,24307E-05	-1,0015E-05	-5,778E-07	3,95072E-06	-2,4494E-06	2,6019E-05	1,32187E-06	-7,9954E-06
-0,13	-0,000132336	-8,0804E-05	0,000156858	-6,199E-06	-1,1367E-06	-1,7681E-06	0,00014537	0,000198828	6,89425E-05
-0,14	-0,000105015	4,88775E-05	8,6232E-05	-1,612E-06	3,35917E-06	2,87149E-06	0,00014598	9,84172E-05	6,46304E-05
-0,15	-7,76951E-05	-2,1441E-05	0,000115606	2,2976E-05	-2,1449E-06	-2,4889E-06	0,00014659	9,80065E-05	6,03183E-05
-0,16	-5,03747E-05	8,24093E-06	4,49795E-05	-2,437E-06	2,35096E-06	2,15075E-06	4,7192E-05	9,75958E-05	0,000156008
-0,17	-2,30544E-05	-6,2077E-05	7,43532E-05	-7,85E-06	-3,1531E-06	-3,2096E-06	0,0001478	9,71851E-05	-4,8306E-05
-0,18	4,26591E-06	-3,2396E-05	3,7269E-06	-3,262E-06	1,34274E-06	1,43001E-06	4,8403E-05	-0,00010323	4,73819E-05
-0,19	3,15862E-05	-2,7139E-06	0,000133101	1,3248E-06	-4,1614E-06	-3,9304E-06	-5,099E-05	-3,6362E-06	4,30698E-05
-0,2	5,89066E-05	2,69678E-05	-3,7526E-05	5,912E-06	3,34531E-07	7,09274E-07	-5,039E-05	-4,0469E-06	-6,1242E-05
-0,21	8,62269E-05	5,66496E-05	-0,00020815	4,9932E-07	4,83042E-06	5,3489E-06	-4,978E-05	-0,00010446	3,44456E-05
-0,22	1,35472E-05	-1,3669E-05	-0,00017878	5,0866E-06	-6,7368E-07	-1,1465E-08	-0,0001492	-0,00020487	-0,00016987
-0,23	4,08676E-05	1,6013E-05	-0,0001494	-3,261E-07	3,82221E-06	4,62817E-06	-0,0001486	-0,00010528	-0,00017418
-0,24	0,000168188	4,56947E-05	-0,00012003	-5,739E-06	-1,6819E-06	-7,322E-07	-0,000248	-0,00010569	-7,8491E-05
-0,5	0,000728822	0,001389555	0,000348403	3,6426E-06	3,86449E-06	7,01577E-06	-0,001431	-0,00106099	-0,00099041
-1	0,00083072	0,001432957	0,000552575	7,6699E-06	4,65206E-06	1,19162E-05	-0,0014525	-0,00101236	-0,00104428
-1,5	0,000932619	0,001476358	0,000656747	1,1697E-05	5,43963E-06	6,81653E-06	-0,0013739	-0,00096373	-0,00099815
-2	0,001034518	0,00151976	0,000660919	1,5724E-05	1,62272E-05	2,17169E-05	-0,0013953	-0,0010151	-0,00095202
-2,5	0,001036416	0,001463161	0,000865091	1,9752E-05	1,70148E-05	2,66173E-05	-0,0012168	-0,00086647	-0,00090589
-3	0,000938315	0,001506563	0,000969263	2,3779E-05	1,78023E-05	2,15177E-05	-0,0011382	-0,00081784	-0,00075976
-3,5	0,001040214	0,001449964	0,001073435	2,7806E-05	2,85899E-05	2,64181E-05	-0,0012596	-0,00076921	-0,00081363
-4	0,000942113	0,001393365	0,000977607	3,1833E-05	3,93775E-05	3,13184E-05	-0,0010811	-0,00062058	-0,0005675
-4,5	0,001044011	0,001336767	0,001081779	3,5861E-05	4,0165E-05	2,62188E-05	-0,0010025	-0,00057195	-0,00062137
-5	0,00104591	0,001380168	0,000985951	2,9888E-05	3,09526E-05	2,11192E-05	-0,0009239	-0,00062332	-0,00037524
-5,5	0,000947809	0,00132357	0,000990123	3,3915E-05	3,17402E-05	2,60196E-05	-0,0007453	-0,00057469	-0,00022911
-6	0,000849707	0,001266971	0,000994295	2,7942E-05	3,25278E-05	2,092E-05	-0,0005668	7,39351E-05	-0,00018298
-6,5	0,000851606	0,001210373	0,000898467	2,197E-05	2,33153E-05	1,58204E-05	-0,0004882	0,000222564	6,3155E-05
-7	0,000753505	0,001053774	0,000902639	2,5997E-05	3,41029E-05	2,07207E-05	-0,0003096	0,000271193	0,00020928
-7,5	0,000655403	0,000997176	0,000806811	2,0024E-05	2,48905E-05	1,56211E-05	-0,0001311	0,000319823	0,00035541
-8	0,000657302	0,000840577	0,000810983	2,4051E-05	2,5678E-05	1,05215E-05	4,7498E-05	0,000468452	0,00040154
-8,5	0,000559201	0,000683978	0,000715155	1,8079E-05	1,64656E-05	5,4219E-06	0,00022607	0,000617081	0,00054767
-9	0,000461099	0,00052738	0,000619327	1,2106E-05	1,72532E-05	1,03223E-05	0,00050464	0,00066571	0,00059380
-9,5	0,000362998	0,000370781	0,000523499	1,6133E-05	1,80407E-05	5,22266E-06	0,00058321	0,000814339	0,00073993
-10	0,000164897	0,000214183	0,000427671	1,016E-05	1,88283E-05	1,23047E-07	0,00096178	0,000962969	0,00088606
-12,5	-0,00012561	-0,00026881	0,00014863	2,0297E-05	3,27662E-05	1,4625E-05	0,00125462	0,000706115	0,00121671
-15	-0,000516117	-0,0013518	-0,00013061	1,0433E-05	2,6704E-05	9,12688E-06	0,00134747	0,000849261	0,00124737
-17,5	-0,001106623	-0,0027348	-0,00070975	-9,431E-06	1,06418E-05	-6,3712E-06	0,00214032	0,000892407	0,00107802
-20	-0,00159713	-0,00401779	-0,00118889	-3,929E-05	-5,4203E-06	-2,1869E-05	0,00223317	0,000735553	0,00070867
-22,5	-0,002187636	-0,00580078	-0,00196803	-4,916E-05	-1,4825E-06	-1,7367E-05	0,00212602	-0,0001213	-6,0676E-05
-25	-0,002878143	-0,00128377	-0,00264717	-8,902E-05	-9,7545E-06	-4,2865E-05	0,00131886	-0,00037816	-0,00133003

Table 3: Measured data for linearity analysis. Deviation from trendline in volts.
Red numbers, se Table 1.

Ip	CSLA2DG-1	CSLA2DG-2	HAS 50-S	BB-150	CSNT651-1	CSNT651-2	LA100-P	CLSM-100	CLN-100	ACS754KCB-150-PSF-1	ACS754K-2	ACS754K-3	CMR-25-1	CMR-25-2	CMR-25-3	NT-50-1	NT-50-2	NT-50-3
Slope, datasheet	16,2	16,2	80	40	62,5	62,5	50	37,485	74,9700	13,3	13,3	13,3	13,5	13,5	13,5	50	50	50
Slope, medium					62,31541933	62,44034908	49,67363133	37,50268199	74,83694338	13,40379736	13,28680289	13,40834398	13,4880545	13,48157514	13,48980077	49,9571392	49,89725841	49,89226054
Slope, low	16,16632444	16,52772074	74,13039014	39,67659138	61,90657084	62,33778234	49,57494867	37,48973306	74,71971253	12,73203285	12,96817248	12,93737166	13,4587269	13,44958932	13,46396304	50,0605749	49,95893224	49,5687885
25					2,621738893	0,426443615	-0,07435969	0,995488288	-1,29580165	-6,475858402	-22,0061857	2,503153006	0,13532791	1,51093965	0,497384866	1,72528777	-2,88808569	-4,29535934
22,5					1,800992299	0,267688436	-0,106412246	0,88004316	-1,0387649	-4,912917723	-18,8676788	0,421314562	0,06219823	0,204993183	0,308367366	3,31234426	-0,99790966	-0,62615026
20					0,819771779	0,108933257	-0,339778855	0,497950436	-1,04897583	-4,842091515	-12,7186658	-0,16891537	-0,0109315	-0,13667427	0,045219785	3,8985428	0,892266375	0,63787611
17,5					-0,32192267	-0,20997478	-0,371831412	0,115857713	-1,19281061	-4,025208071	-8,07490577	-1,50494956	-0,0840611	-0,18164048	-0,06966764	3,68405497	1,780383345	2,102334391
15					-0,1798257	-0,04842425	-0,001255864	0,267060181	-0,66852617	-3,208324628	-5,68902529	-3,586788	-0,0089115	-0,07825608	-0,0362949	3,26939556	2,468088503	2,765065118
12,5					-1,32152015	-0,04702658	-0,033308421	0,418262649	-0,41148941	-3,883555654	-4,05577131	-4,17701794	-0,0820412	-0,1973976	-0,15118232	3,05490774	2,554558223	2,826500179
10					-1,66084497	-0,20578176	0,135953075	0,302817521	-0,2880765	-3,812729446	-3,92777033	-4,76724787	-0,2293105	-0,31653913	-0,26606974	2,44007674	2,44061613	2,487071464
9,5					-1,72870993	-0,0133188	0,210068184	0,439717053	-0,12977008	-3,798564204	-3,60111954	-4,736133	-0,1994527	-0,31069731	-0,22974316	1,7966644	2,337662986	1,978235568
9					-1,79657489	-0,14116155	0,082869241	0,309968989	-0,10508749	-3,784398963	-3,27446874	-4,70501814	-0,1695948	-0,30485549	-0,26754666	1,35342366	2,234709843	2,070695334
8,5					-1,70396593	-0,10885144	0,156984351	0,180220925	0,053218933	-3,770233721	-2,19519144	-4,67390327	-0,2138766	-0,29901367	-0,23122008	0,91018292	1,730933074	1,962723213
8					-1,93230482	-0,23669419	0,029785408	0,050472861	0,077901515	-3,756068479	-2,62116715	-4,64278841	-0,1840187	-0,29317185	-0,19489351	0,46694217	1,828391743	1,453887315
7,5					-1,83969585	-0,20438408	0,103900518	0,187372393	0,102584097	-3,741903238	-1,54188985	-4,61167354	-0,1541609	-0,21315473	-0,15856693	0,42404461	1,525026787	1,345915195
7					-1,90756082	-0,33222683	-0,023298425	0,057624329	0,127266679	-2,981680761	-1,21523905	-4,58055868	-0,124303	-0,28148822	-0,19637043	-0,2193677	1,021250018	0,837079297
6,5					-1,97542578	-0,29991673	0,050816685	-0,07212373	0,151949261	-2,967515519	-0,88858826	-3,80363956	-0,1685848	-0,2756464	-0,16004385	-0,2622653	0,717885062	0,528675288
6					-1,88281682	-0,42775947	-0,076382258	-0,2018718	0,176631844	-2,207293042	-0,56193746	-3,7725247	-0,0645872	-0,19562927	-0,12371727	-0,705506	-0,18671533	0,220271278
5,5					-1,95068178	-0,55560222	-0,002267148	-0,33161986	0,201314426	-2,193127801	-0,23528667	-3,74140983	-0,0347294	-0,18978745	-0,08739069	-1,1487468	-0,28966848	0,112299158
5					-1,85807282	-0,52329212	0,071847961	-0,19472033	0,359620852	-1,432905324	0,09136413	-2,96449071	-0,0790112	-0,18394563	-0,12519419	-1,5919875	-0,79344524	-0,39653674
4,5					-1,76546385	-0,65113486	-0,055350981	-0,32446839	0,25067959	-1,418740082	1,170641429	-3,6791801	0,02498636	-0,10392851	-0,01473753	-1,4347135	-0,49557476	-0,50450886
4					-1,51238097	-0,61882476	0,018764128	-0,18756886	0,408986016	-2,150632076	1,497292225	-2,90226098	-0,0192954	-0,172262	-0,05254103	-1,4776111	-0,59852791	-0,81291287
3,5					-1,25929808	-0,58651465	-0,108434814	-0,31731693	0,433668598	-0,644352364	1,823943022	-2,87114612	-0,0635773	-0,16642018	-0,09034453	-1,9208518	-1,30271649	-1,32174877
3					-1,16668911	-0,7143574	-0,235633757	-0,44706499	0,324727337	-0,630187122	2,903220321	-2,094227	-0,1078591	-0,23475367	-0,12814803	-1,9637494	-1,40566963	-1,229289
2,5					-0,7531323	7,165442464	-0,161518647	-0,31016546	0,349409919	0,87609259	3,229871117	-2,06311213	-0,0780012	-0,15473654	-0,09182145	-2,0066469	-1,50862277	-1,33726112
2					-0,33957548	-0,48958434	0,113910614	-0,43991352	0,507716345	1,636315067	4,309148416	-1,28619301	-0,0481433	-0,14889472	-0,05549487	-2,2497161	-2,01239954	-1,64566513
1,5					-0,24696652	-0,77757994	-0,013288428	-0,56966159	0,398775084	1,650480309	5,388425715	-0,50927389	-0,0182855	-0,1430529	-0,09329837	-2,4927852	-1,71452906	-1,75363725
1					0,166590297	-0,74526983	-0,140487371	-0,69940965	0,423457666	2,410702786	7,220329517	-0,47815903	0,01157241	-0,06303677	0,017158284	-2,7369544	-1,81748221	-1,86160937
0,5					0,901094964	-0,55280687	-0,066372261	-0,56251012	0,581764092	4,663039733	8,299606816	-0,44704416	-0,0327094	-0,13136926	-0,02064522	-2,5705804	-1,92043535	-1,96958149
0,24	1,330433126	-2,80833023	0,551334432	0,031802303	-0,04858451	0,042401634	-0,031240939	0,073257565	-0,21109691	0,446214015	0,932837199	-1,00460281	0,03025703	0,018701161	0,04876378	-0,3536475	-0,17209549	-0,14426263
0,23	1,093293535	-2,41337433	0,607052339	0,023651184	-0,01778695	0,079903487	-0,039814853	0,006298781	-0,28176484	0,660793484	0,390599847	-0,77755734	-0,0099602	0,052128897	0,008951062	-0,3524375	-0,37308193	-0,55644159
0,22	1,474723739	-2,01841844	-0,821101616	0,015500065	0,013010598	0,11740534	-0,048388767	-0,06066	-0,21859928	0,875372954	-0,15163751	-1,32346639	0,02412374	0,01120492	0,043410681	-0,3512275	-0,37390396	-0,36340099
0,21	1,237584148	-2,22850665	-0,225793942	0,511424505	0,04380815	-0,00550917	-0,056962681	0,139120909	-0,15543372	1,089952423	0,077243818	-1,09642092	-0,0160935	-0,02971906	0,003597963	-0,1502594	-0,37472599	0,031379453
0,2	1,000444557	-1,83355075	-0,304973478	0,251235606	-0,08692804	0,031992687	-0,065536594	0,072162125	-0,09226816	0,519111362	0,306125142	-0,09642092	0,01799046	0,00370868	-0,03621475	0,06070859	0,024780792	0,022680199
0,19	0,763304966	-0,83355075	-0,249255571	0,243084487	-0,05613049	0,06949454	-0,074110508	0,005203341	-0,16293609	-0,051729699	0,535006466	0,130624554	-0,0222268	-0,0372153	-0,07602747	0,05191862	-0,17620564	0,013980944
0,18	-0,09240442	-1,04363896	0,076257219	0,486971148	-0,02533294	0,106996393	-0,082684422	-0,06175544	-0,09977053	0,16284977	-0,77834956	0,357670026	0,01185717	-0,00378756	0,032704484	0,05312865	0,023136731	0,00528169
0,17	0,289026784	-0,64868307	-0,002922316	-0,025255531	-0,15606912	-0,01591811	-0,091258336	-0,12871423	-0,03660497	-0,407991291	-0,54946824	0,584715499	-0,0283601	0,029640175	-0,00710823	0,25409668	0,222479107	0,198322287
0,16	0,670455989	-0,25372717	-0,082101852	-0,03340665	-0,12527157	0,021583741	0,101882533	0,071066685	0,026560589	-0,978832352	-0,32058692	0,811760971	0,00572389	-0,0112838	0,027351385	0,25530671	0,221657076	0,189623032
0,15	0,433316398	0,141228724	-0,296178829	-0,041557769	0,067059721	0,059085594	0,093308619	0,004107901	-0,04410734	-0,764252883	-0,09170559	0,265851917	-0,0344934	-0,05220778	-0,01246133	0,25651675	0,220835046	0,180923778
0,14	0,196176807	-0,06885949	-0,375358365	0,454366671	-0,06367647	0,096587447	0,084734706	-0,06285088	0,019058219	-0,549673413	0,137175732	1,265851917	-0,0004094	-0,01878004	-0,05227405	0,25772678	0,420177422	0,172224524
0,13	-0,040962784	0,326096409	-0,4545379	0,698253332	-0,03287892	-0,02632706	0,076160792	-0,12980967	0,082223779	-1,120514475	-0,40506162	1,492897389	-0,0406267	0,014647695	-0,01781443	0,05917882	0,419355391	0,36526512
0,12	-0,278102375	0,721052305	0,140769774	-0,066011127	-0,00208136	0,011174795	0,067586878	0,069971245	0,011555849	0,223107008	0,386093738	-0,11582414	-0,0049947	-0,02937427	-0,02822768	0,02293423	0,02237464	-0,00908761
0,11	-0,515241966	1,1160082	-0,208204645	-0,074162246	0,028716188	0,048676647	0,059012964	0,003012461	0,074721409	0,437686477	-0,15614361	-0,6617332	0,02908924	0,004053466	0,006231937	0,22390225	0,02155261	-0,01778687
0,1	-0,752381557	0,90591999	-0,017589297	-0,334351145	0,05951374	-0,07423786	0,050439051	-0,06394632	0,13788697	-0,133154584	0,072737709	0,338266804	-0,011128	0,037481202	0,040691556	0,02535429	0,02073058	-0,02648612
0,09	-0,989521148	1,300875885	-0,501461158	-0,342502264	0,090311292	-0,036736	0,041865137	0,135834589	0,067219039	0,081424885	0,301619033	-0,20764225	0,02295595	-0,00344277	0,000878838	-0,3729517	-0,18025586	-0,03518538
0,08	-1,226660739	1,090787675	0,093846516	-0,098615604	0,121108845	-0,15965051	0,033291223	0,068875804	0,1303846	-0,489416176	-0,24061832	0,019403222	-0,0172613	0,029984962	0,035338458	0,02777436	0,019086519	-0,04388463
0,07	-1,46380033	2,69583178	0,554256748	-0,358804503	0,151906397	-0,12214866	0,024717309	0,00191702	0,19355016	-0,274836707	-0,011737	-0,52650583	0,01682267	-0,01093901	-0,00447426	-0,1707736	0,018264488	0,149155965
0,06	-1,700939921	3,090787675	0,475077213	-0,618993401	0,182703949	-0,0846468	0,016143396	-0,06504176	0,256715721	-0,060257237	-0,55397435	-0,29946036	0,05090664	0,022488721	0,029985359	0,03019443	0,017442458	-0,06128314
0,05	-1,938079512	2,880699466	0,261000235	-0,375106741	0,05196776	-0,20756131	0,007569482	-0,13200055	0,319881281	0,154322232	-0,32509303	-0,07241489	0,01068938	-0,01843526	-0,00982736	0,03140446	0,016620427	-0,06998235
-0,05	-1,83519624	3,805037893	0,548384416	-0,456617932	0,036875798	-0,1533755	-0,078169656	-0,0013693	0,28236943	-0,056144666	-0,34963582	0,652130783	-0,019977	0,018435255	-0,03659285	0,04350479	0,008400123	0,044764913
-0,06	-1,453766036	2,989905578	0,873897206	-0,716806831	0,06767335	-0,11587364	0,114971213	-0,06832808	0,211701499	0,158434804	-0,12075449	0,106221728	0,01410694	-0,02248872	-0,00213323	-0,1550432	0,007578093	0,036065655
-0,07	-1,072335831	1,569729159	0,524922787	-0,472920171	-0,06306284	-0,07837179	-0,095317483	0,131452828	0,141033568	0,373014273	0,108126831	0,333267201	-0,0261103	0,010939015	-0,04194595	0,04592485	0,006756062	-0,17437345
-0,08	-1,309475422	1,359640949	0,175948368	-0,48107129	0,129268454	-0,04086994	-0,103891397	0,064494044	0,204199129	-0,197826788	0,337008155	0,560312674	0,00797365	-0,02998496	-0,00748633	0,24689288	0,005934032	0,220407001
-0,09	-0,928045218	1,149552739	-0,03812861	-0,237184629	-0,00146773	-0,00336808	-0,112465311	-0,00246474	0,133531198	0,016752681	0,565889478	0,014403619	-0,0322436	0,003442774	0,026973288	-0,1514131	0,005112002	0,009967896
-0,1	-0,546615013	0,93946453	0,017589297	-0,245335748	-0,13220392	0,034133768	0,080675558	-0,06942352	0,062863267	0,231332151	-0,74746655	0,241449091	0,00184037	-0,0374812	-0,01283943	0,04955495	0,004289971	0,001268641
-0,11	-0,165184809	1,334420425	0,073307203	-0,253486868	0,06012737	-0,08878074	-0,129613138	-0,13638231	-0,00780466	-0,339508911	0,252533449	-0,30445996	-0,0383769	-0,00405347	0,021620189	0,05076499	0,003467941	-0,00743061
-0,12	0,216245396	0,51928811	0,263922552	-0,009600207	-0,07060882	-0,05127888	0,063527731	0,063398603	0,055360897	-0,124929441	0,481414773	-0,07741449	-0,0042929	0,02937427	-0,01819253	0,05197502	0,00264591	-0,01612987
-0,13	-0,020894195	-0,2958442	0,184743016	-0,269789106	-0,03981127	-0,01377703	0,054953817	-0,00356018	0,118526458	-1,039391985	-0,62309661	1,212443457	-0,0460581	-0,00845172	-0,01313238	0,29039767	0,3979826	0,139084507
-0,14	0,360536009	0,099111691	-0,164231403	-0,025902445	-0,00901372	0,023724822	0,046379903	-0,07051896	0,047858527	-0,824812515	0,376903386	0,666534402	-0,0119741	0,024976018	0,021327243	0,2916077	0,196996164	0,130385253
-0,15	0,123396418	-0,11097652	-0,108513497	0,470021995	0,021783837	0,061226675	0,037805989	0,129261947	0,111024087	-0,610233046	-0,16533397	0,893579875	0,1707123	-0,01594796	-0,01848547	0,29281774	0,196174133	0,121685998
-0,16	0,504826623	-0,32106473	0,216999294	0,209833096	-0,10895235	0,098728527	0,029232076	0,062303163	-0,09347733	-0,395653576	0,063547357	0,34767082	-0,0181074	0,017479777	0,015974144	0,09426978	0,195352103	0,314726595
-0,17	0,267687032	-0,53115294	0,2727172	0,201681977	-0,0781548	-0,02418598	0,020658162	-0,00465562	-0,03031177	-0,181074107	-0,47869	0,574716292	-0,0583247	-0,0234442	-0,02383857	0,2952378	0,194530073	-0,09745238
-0,18	0,649117236	-0,74124115	-0,346052103	0,697606417	-0,04736726	0,013316876	0,012084248	-0,07161441	-0,10097971	0,033605362	-0,24980867	0,028807238	-0,0242407	0,009983637	0,010621046	0,09668984	-0,20662077	0,095688238
-0,19	0,411977645	-0,95132936	-0,290334197	0,437417518	-0,0165597	0,050817728	0,003510334	-0,13857319	-0,17164764	0,248084832	-0,02092735	1,028807238	0,00984326	-0,03094044	-0,02919167	-0,1018581	-0,00727839	0,086888981
-0,2	0,79340785	-1,76646167	-0,369513732	0,177228619	0,014237856	0,088319581	-0,00506358	0,061207723	-0,10848208	0,462664301	0,207953976	-0,29005634	0,04392723	0,002487296	0,005267947	-0,1006481	-0,00810042	-0,12355012
-0,21	1,174838054	-1,97654988	-0,853385593	0,1690775	0,045035408	0,125821434	-0,013637493	-0,00575106	-0,17915001	0,677243771	0,436835299	-1,60891993	0,00370998	0,035915032	0,039727566	-0,0994381	-0,20908686	0,069490472
-0,22	0,937698463	-2,18663809	0,011716965	-0,091111399	-0,08570078	0,002906929	-0,022211407	-0,07270985	-0,24981794	0,106402709	-0,10540205	-1,38187445	0,03779395	-0,00500894	-8,5151E-05	-0,297986	-0,4100733	-0,34268848
-0,23	1,319128668	-2,3967263	0,067434871	0,152775262	-0,05490323	0,040408782	-0,030785321	0,127071067	-0,18665238	0,320982179	0,123479271	-1,15482898	-0,0024233	0,028418792	0,034374468	-0,296776	-0,21073092	-0,35138774
-0,24	1,081989077	-2,60681451	-0,281539548	0,396661923	0,137428064	0,077910635	-0,039359235	0,060112283	-0,25732031	1,320982179	0,352360594	-0,92778351	-0,0426406	-0,01250518	-0,00543825	-0,4953239	-0,21155295	-0,15834714
-0,5					1,407260743	-0,48818666	0,081857958	-0,55535865	0,631129256	5,437427451	10,45816141	2,598402591	0,02700634	0,028664991	0,052007942	-2,8645471	-2,12634164	-1,98509385
-1					1,499869706	-0,29572371	-0,045340985	-0,41845912	-2,01666503	6,197649928	10,78481221	4,121125967	0,05686421	0,034506809	0,088334521	-2,9074447	-2,02888297	-2,09306597
-1,5					1,752952595	-0,2634136	0,028774125	-0,54820718	0,68049442	6,957872405	11,1146301	4,898045088	0,08672208	0,040348628	0,050531021	-2,7501706	-1,9314243	-2,0006062
-2					1,845561558	-0,2311035	-0,098424818	-0,41130765	0,571553159	7,718094882	11,4381138	4,929159952	0,11657995	0,120365756	0,160987679	-2,7930682	-2,03437744	-1,90814643
-2,5					1,938170521	-0,03864054	0,177004344	-0,27440812	0,729859585	7,732260124	11,0121381	6,451883329	0,14643782	0,126207574	0,197314258	-2,4356226	-1,73650696	-1,81568668
-3					1,870305558	-0,16648329	-0,151508651	-0,40415618	0,620918324	7,00036813	11,33878889	7,228802449	0,17629569	0,132049393	0,159510758	-2,2783466	-1,63904829	-1,52279501
-3,5					1,962914521	0,02597967	0,123920511	-0,26725665	0,645600906	7,760590607	10,91281318	8,070525809	0,20615356	0,212066521	0,195837337	-2,5214177	-1,54158962	-1,63076713
-4					2,055523484	0,058289775	0,19803562	-0,39700471	0,536659645	7,028698613	10,48683748	7,291032178	0,23601143	0,292083648	0,232163916	-2,1639721	-1,24371914	-1,13744358
-4,5					1,987658521	0,09059988	0,07083677	-0,26010518	0,561342227	7,78892109	10,05086177	8,067951299	0,26586929	0,297925467	0,194360416	-2,0066981	-1,14626047	-1,2454157
-5					1,919793558	0,122909995	0,144951787	-0,12320565	0,586024809	7,803006332	10,38751257	7,353261908	0,22158749	0,229591977	0,156556916	-1,849424	-1,24921361	-0,75209216
-5,5					1,851928595	0,15522009	0,219066896	-0,25295371	0,610707391	7,071194339	9,96153686	7,384376772	0,25144536	0,235435795	0,192883495	-1,4919784	-1,15175495	-0,4592005
-6					1,784063632	0,187530195	0,091867954	-0,11605418	0,50176613	6,339302345	9,535661152	7,415491637	0,20716355	0,241275614	0,155079995	-1,1345328	0,148174599	-0,36674074
-6,5					1,876672595	0,2198403	0,165983063	0,020845351	0,526448712	6,353467587	9,109585445	6,700802246	0,16288174	0,172942124	0,117276495	-0,9772588	0,44604508	0,12658280
-7					1,808807632	0,252150405	0,038784121	-0,10890271	0,551131295	5,621575593	7,930893235	6,73191711	0,19273961	0,252959252	0,153603074	-0,6198132	0,543603749	0,41947446
-7,5					1,740942669	0,28446051	0,314213282	0,027996819	0,575813877	4,8896836	7,505007528	6,017227719	0,1484578	0,184625761	0,115799573	-0,2623676	0,640962418	0,71236612
-8					1,673077706	0,316770615	0,18701434	-0,10175125	0,600496459	4,903848841	6,326405318	6,048342584	0,17831567	0,19046758	0,077996073	0,09507806	0,9388329	0,80482588
-8,5					1,605212743	0,34908072	0,261129449	0,035148287	0,491555198	4,171956848	5,147803108	5,333653193	0,13403386	0,12213409	0,040192573	0,45252368	1,236703381	1,09771754
-9					1,376873854	0,381390825	-0,067383545	0,172047819	0,382613937	3,440064954	3,969200898	4,618963802	0,08975206	0,127975909	0,076519152	1,01014089	1,33416205	1,19017731
-9,5					1,309008891	0,41370093	0,208045616	0,308947351	0,407296519	2,708172861	2,790596688	3,904274411	0,11960992	0,133817727	0,038716652	1,16741491	1,632032532	1,48306897
-10					1,080670001	0,12570533	0,080846674	0,179199287	0,164731415	1,230223632	1,611996478	3,18958502	0,07532812	0,139659546	0,000912152	1,92520371	1,929903014	1,77596062
-12,5					0,420397334	0,127103003	0,250108169	0,330401755	0,202896639	-0,937121865	-2,02313606	1,107746676	0,15047778	0,243043949	0,108414968	2,51140225	1,415137296	2,43869135
-15					-1,20271889	-0,03165218	-0,184572491	0,214956628	-0,65743351	-3,850524698	-10,1740256	-0,97409187	0,0773481	0,198077733	0,067657625	2,69725761	1,702018828	2,60012641
-17,5					-1,54204371	-0,19040736	-0,216625048	0,366159096	-1,06851597	-8,256041801	-20,5827957	-5,29334308	-0,0699213	0,078936209	-0,0472298	4,2843141	1,788488548	2,16069769
-20					-2,3627903	-0,34916253	-0,449991657	0,517361564	-1,47959843	-11,91550177	-30,2389393	-8,86679004	-0,2913303	-0,04020532	-0,16211722	4,47016945	1,474134643	1,42040520
-22,5					-3,02306297	-0,18761201	-0,280730161	0,935211628	-1,75705705	-16,32101897	-43,6582153	-14,6776498	-0,36446	-0,01099622	-0,12874448	4,25568164	-0,24310195	-0,12161484
-25					-3,84380956	-0,34636719	-0,312782718	1,086414097	-2,16813952	-21,47259341	-9,66202173	-19,7427052	-0,6600087	-0,72354022	-0,31776198	2,63999268	-0,75786767	-2,66579433

Table 4: Measured data for linearity analysis. Linearity relative to expected output with a 1A input current, in percent. To find linearity relative to other currents, please divide each value in the table with the desired value. Red numbers, se Table 1.

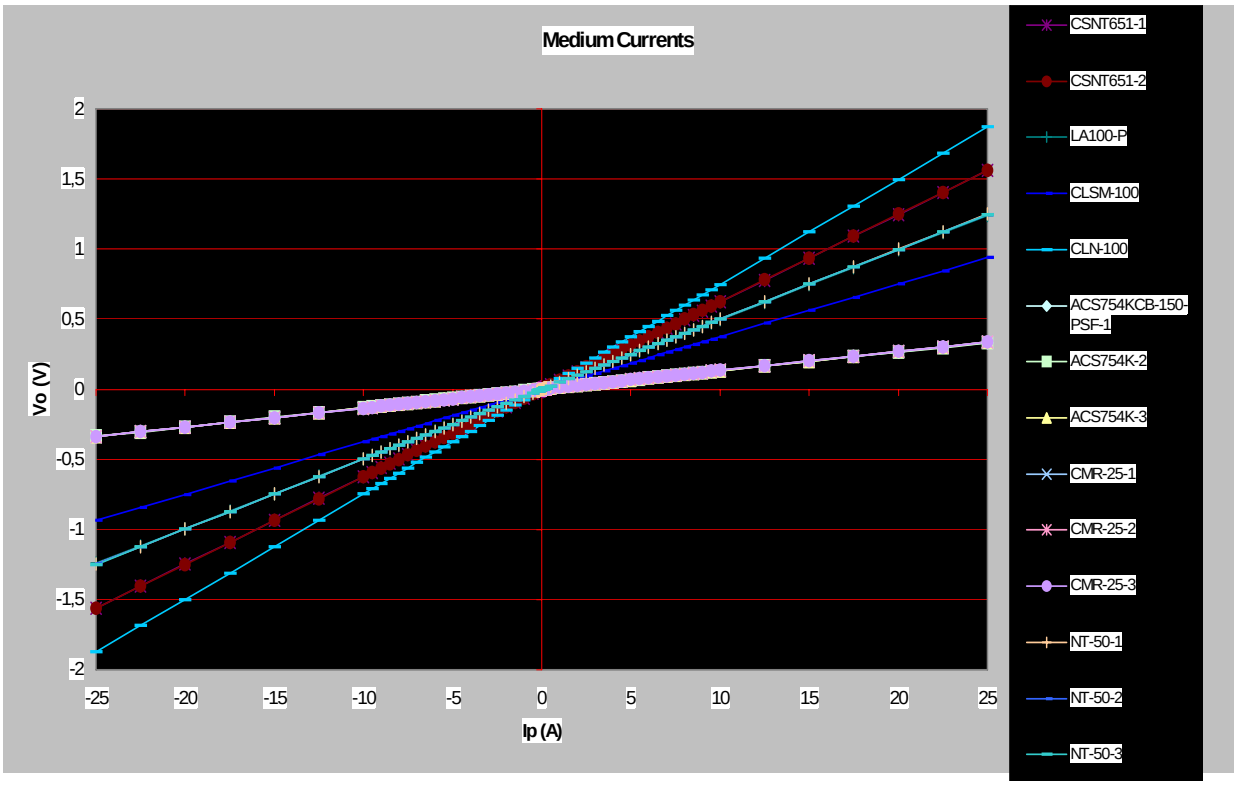

Figure 26: Medium current linearity measurements.

All components except OL.

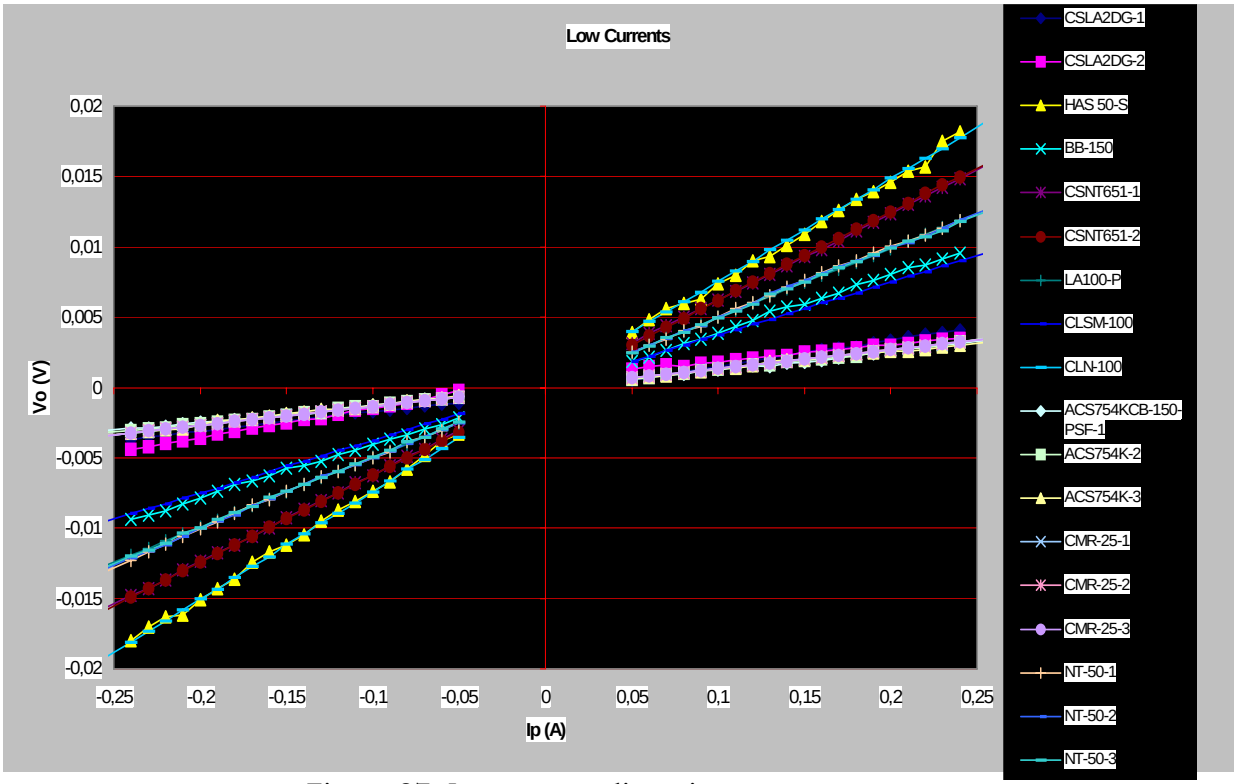

Figure 27: Low current linearity measurements.

All components.

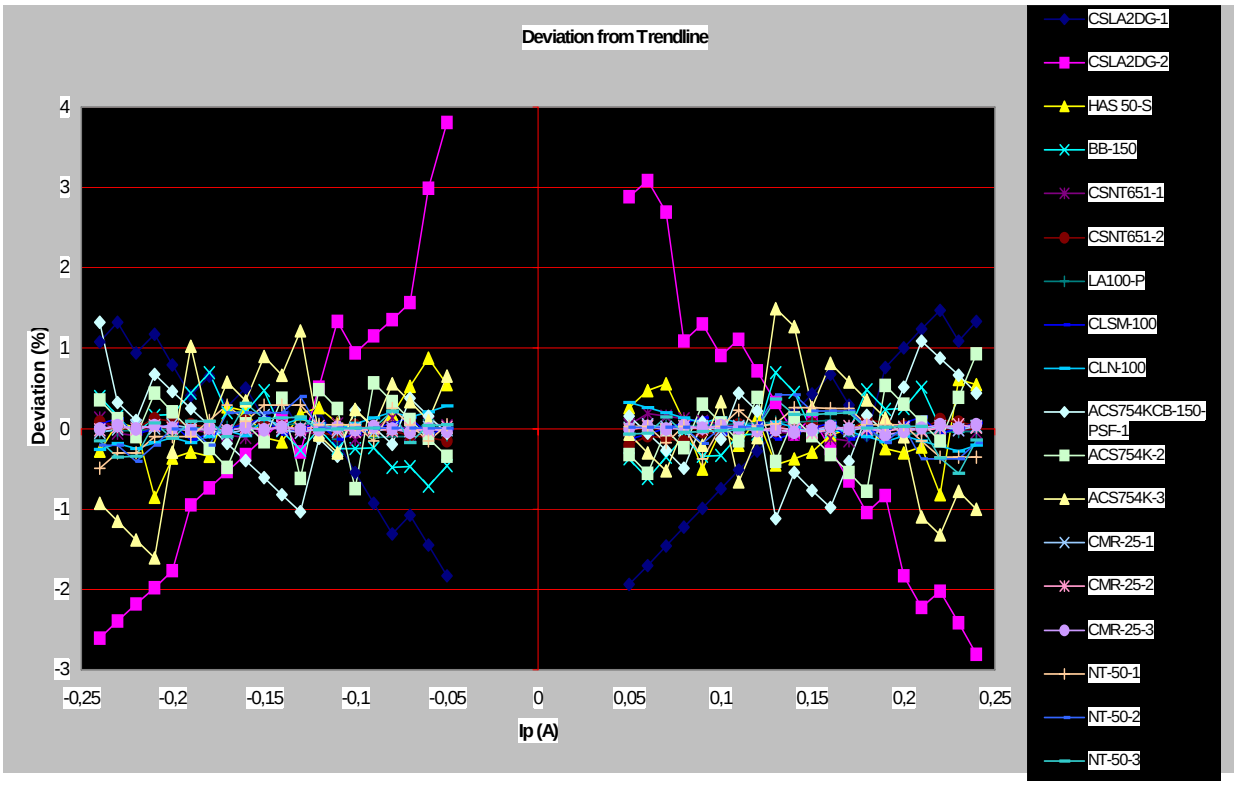

Figure 28: Low current linearity measurements in percent of output with a 1A input current. All components.

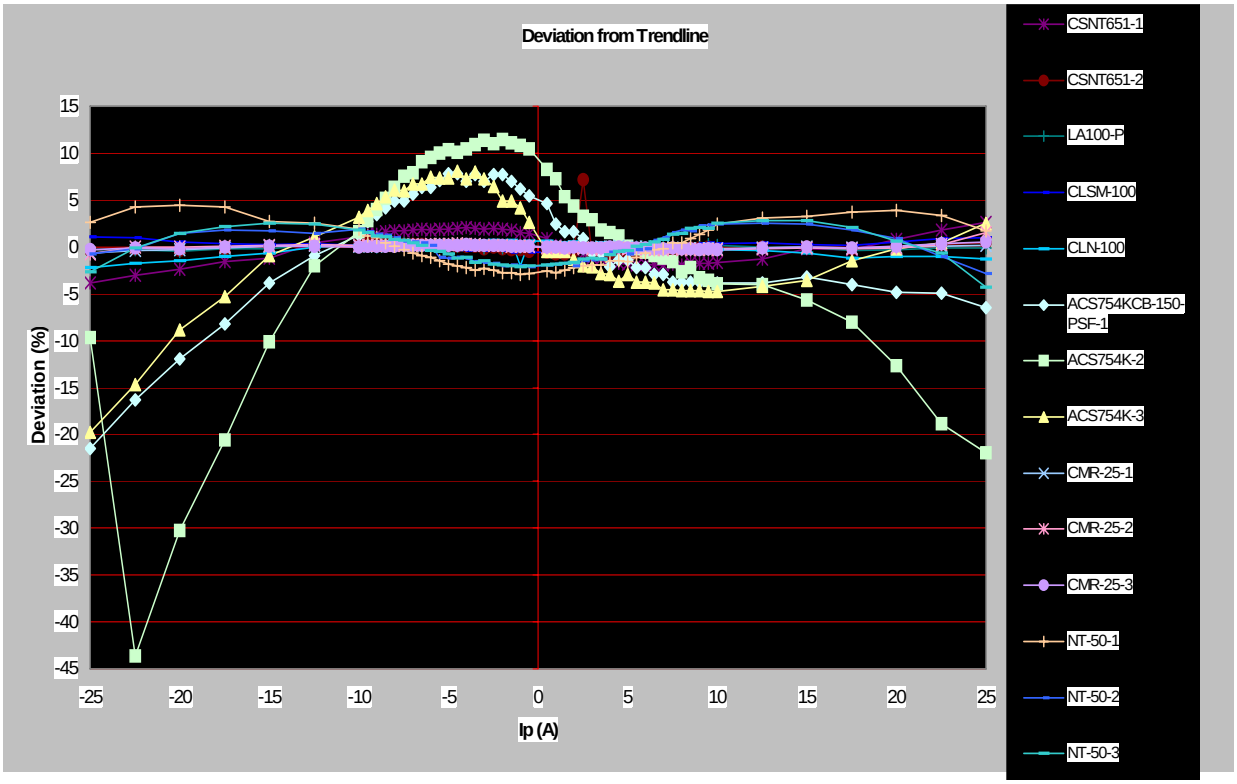

Figure 29: Medium current linearity measurements in percent of output with a 1A input current. All components except OL.

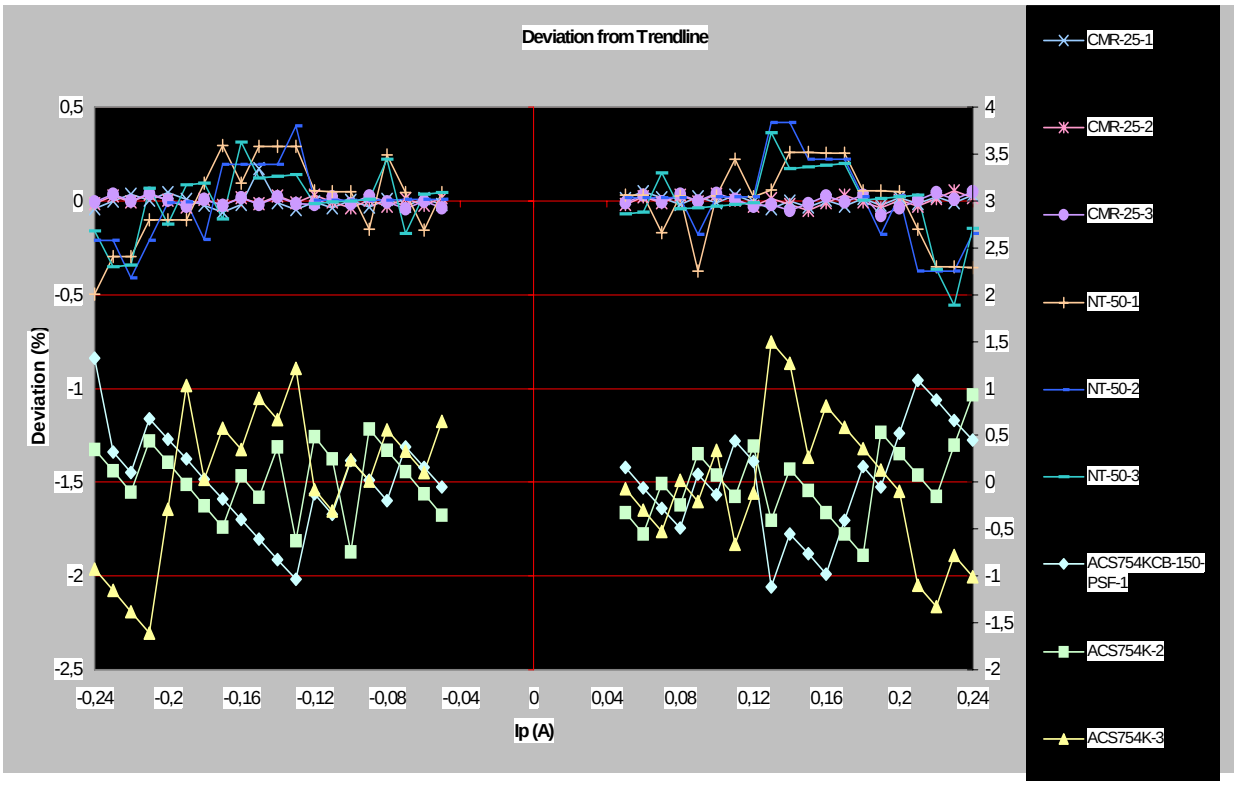

Figure 30: As Figure 28 but without OL and CL. Compare results below and above 0,12mA. CMR-25 and NT-50 are related to the left axis and ACS754K to the right axis.

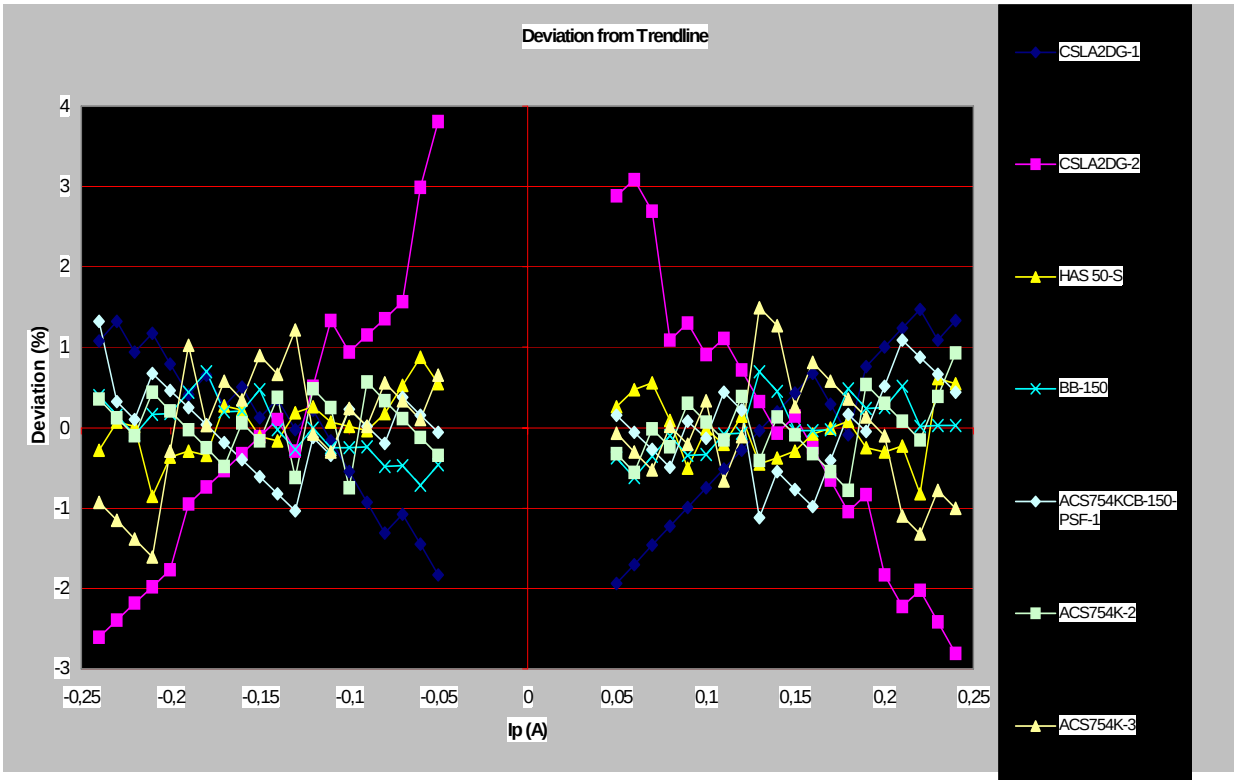

Figure 31: As Figure 28 but only components with highly fluctuating linearity.

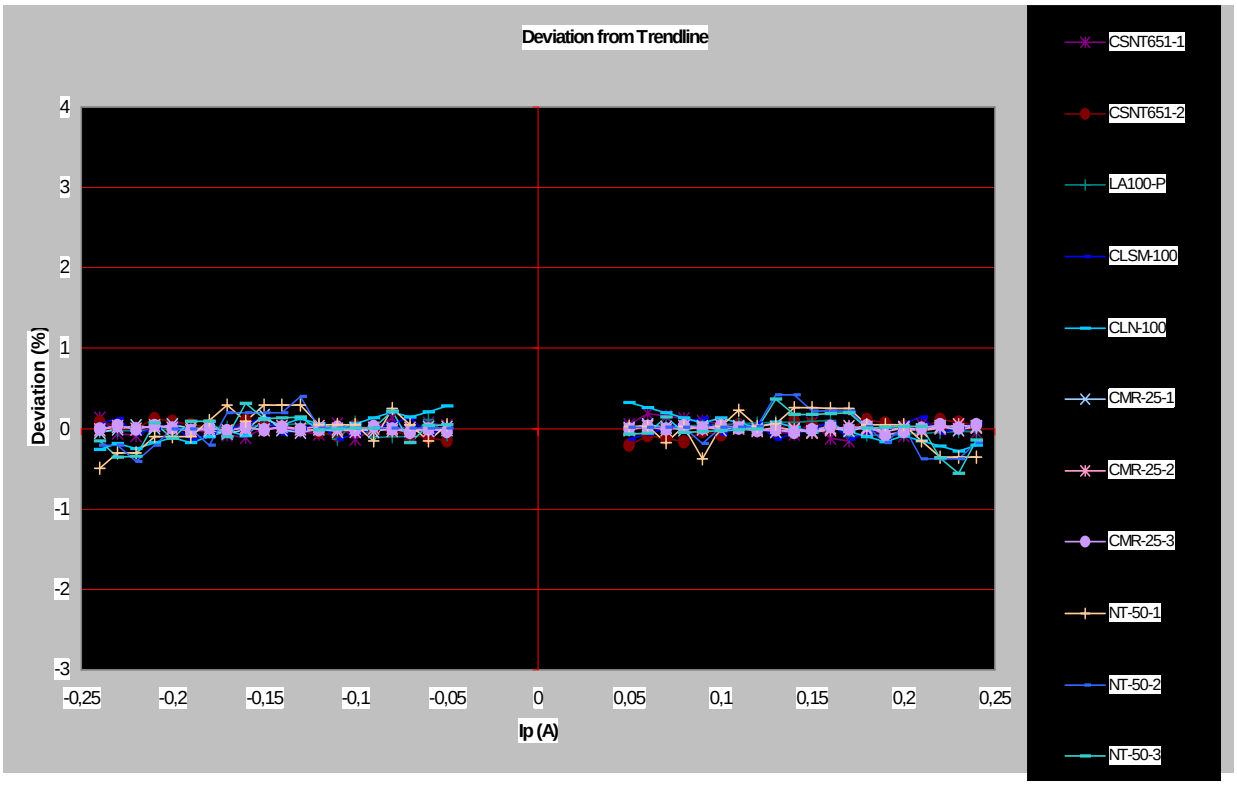

Figure 32: As Figure 28 but only components with less fluctuating linearity.

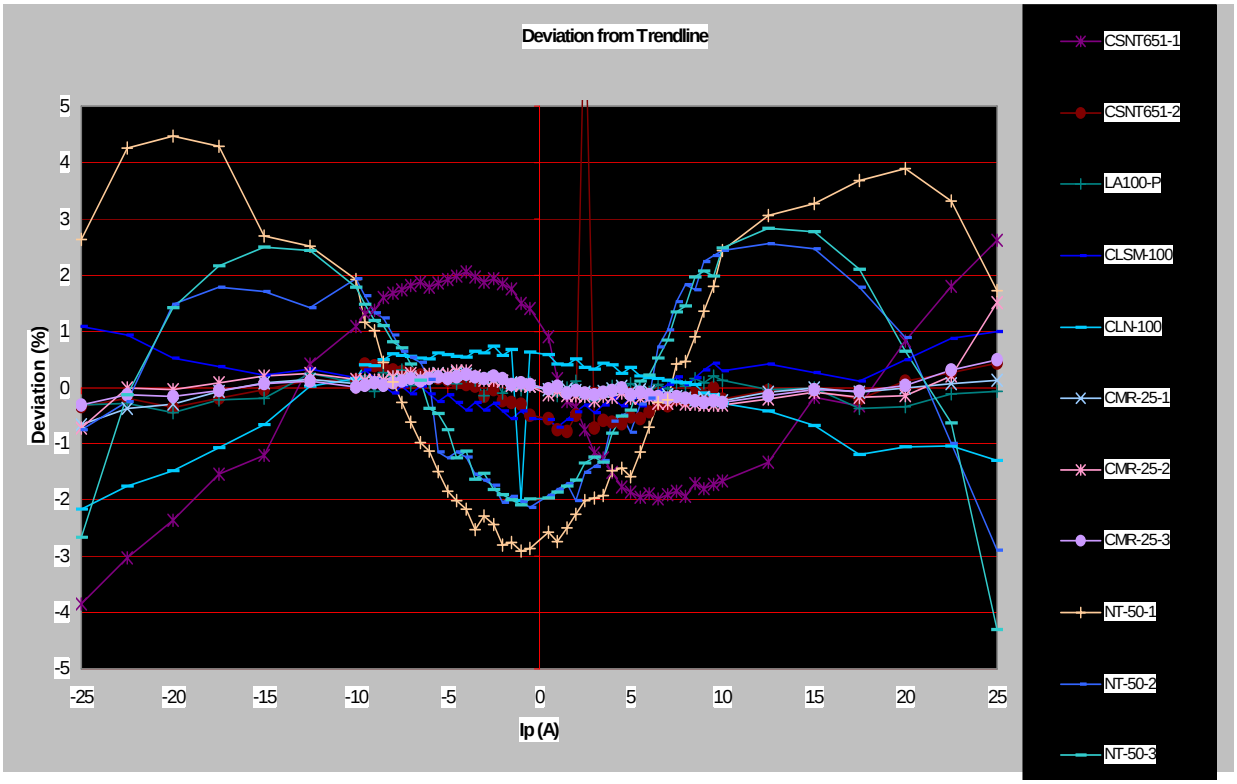

Figure 33: As Figure 29 but only components with less fluctuating linearity.

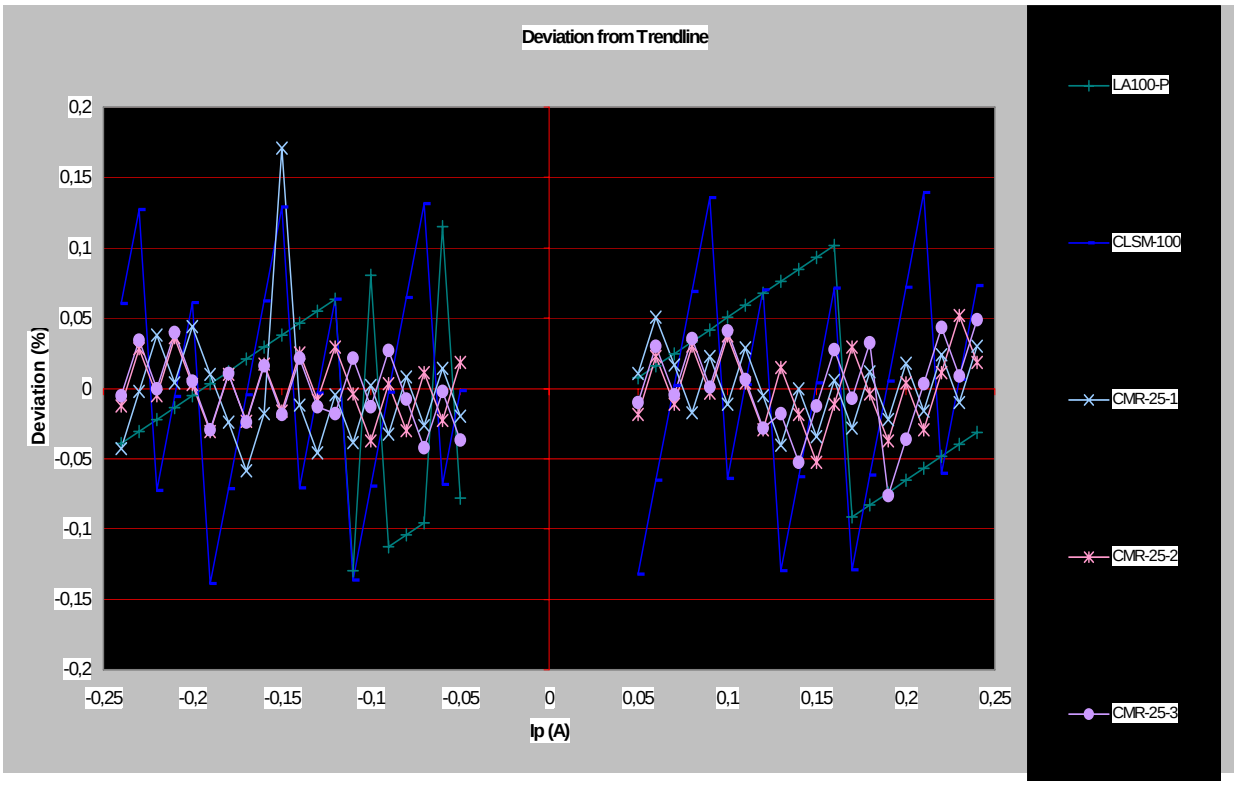

Figure 34: Best alternatives, low currents.

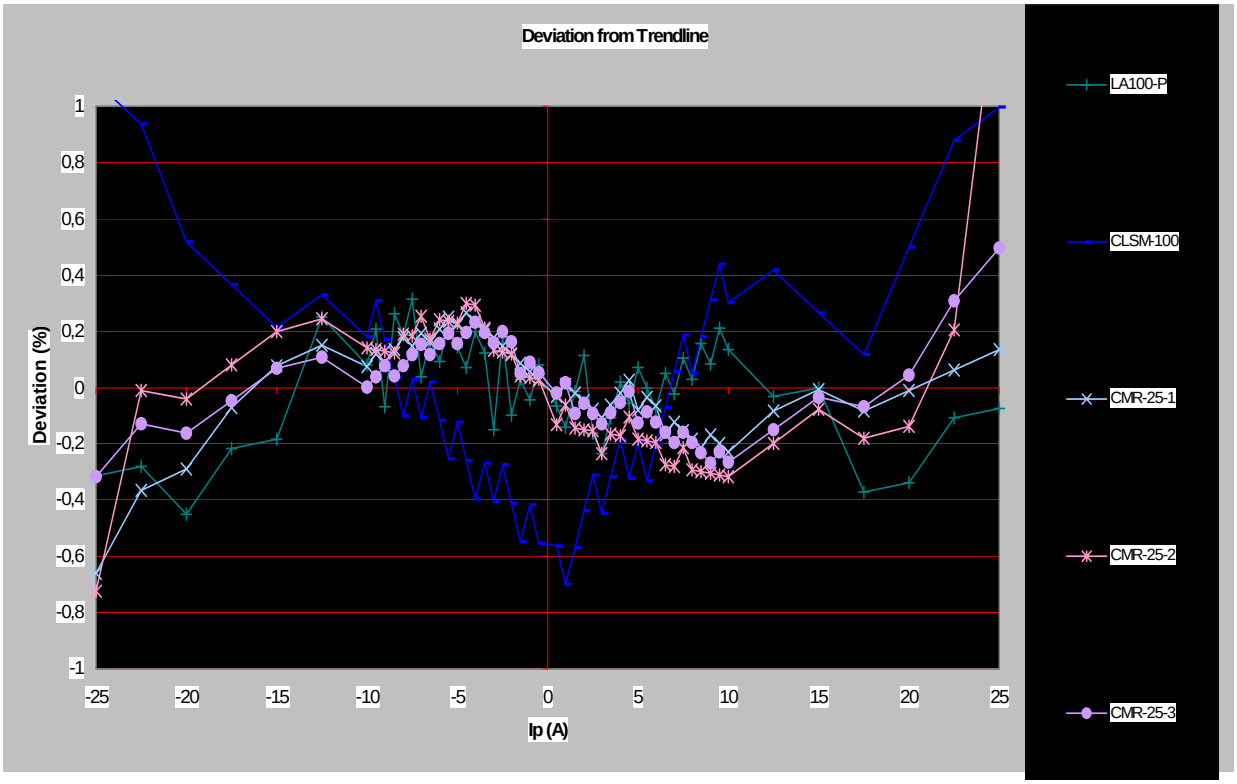

Figure 35: Best alternatives, medium currents.

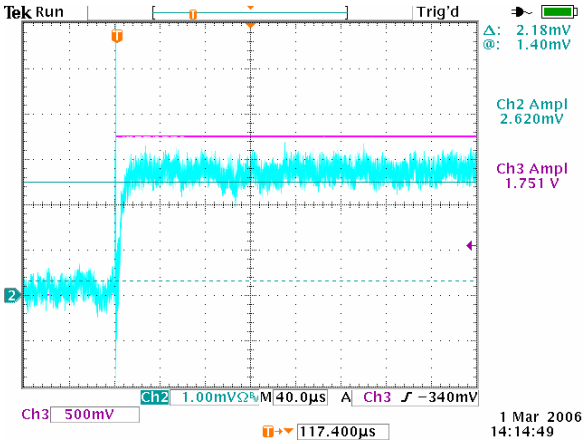

Figure 36: ACS754KCB-150-1 Up

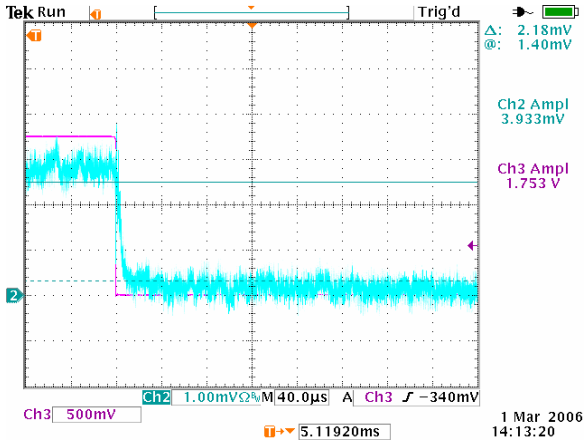

Figure 37: ACS754KCB-150-1 Down

The ACS754KCB has a 2,5V offset on the output, and to get a reasonable resolution I measured relative a reference 2,5V so that zero measured output refer to zero input.

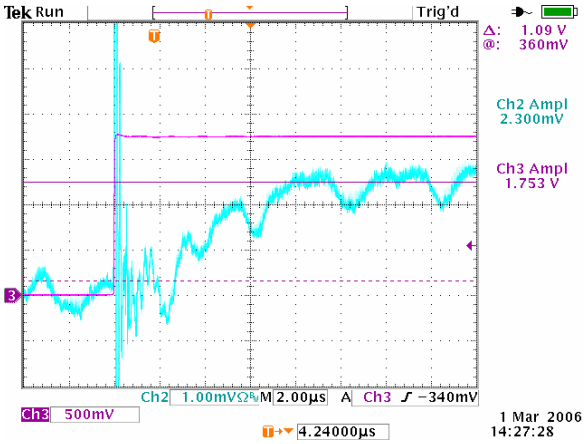

Figure 38: ACS754KCB-150-1 Zoom

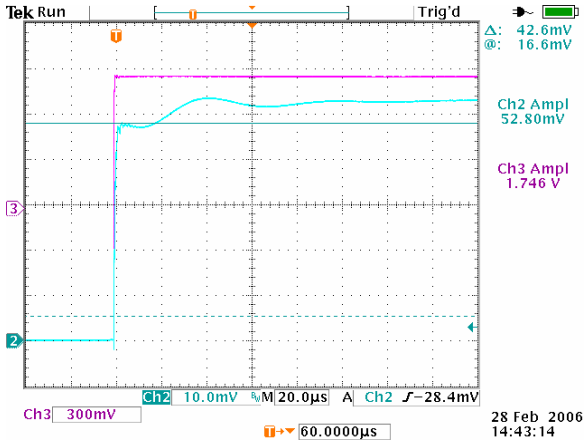

Figure 39: CLN 100 Up

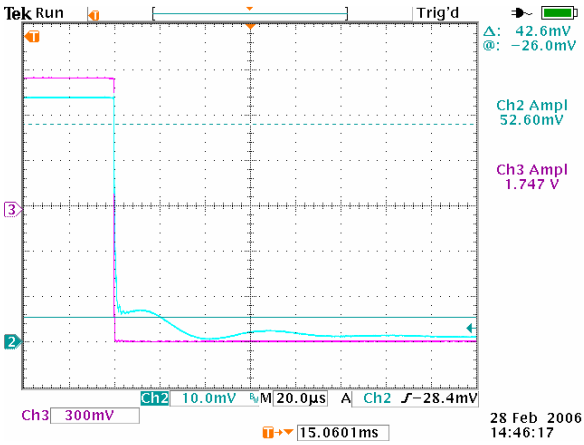

Figure 40: CLN 100 Down

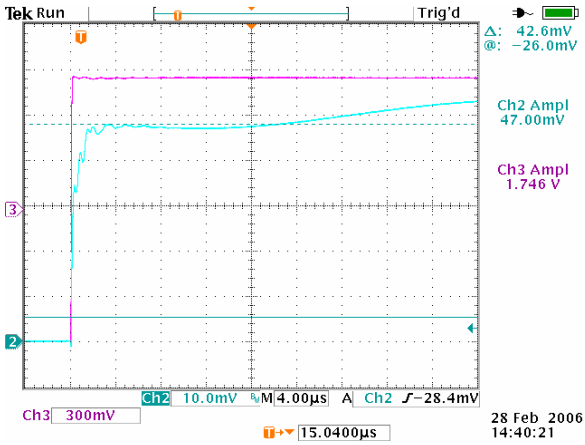

Figure 41: CLN 100 Zoom

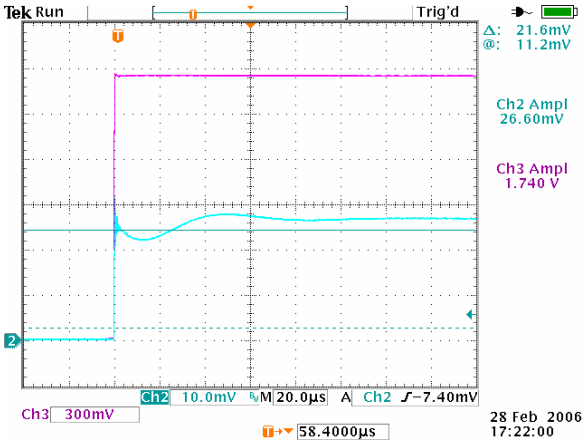

Figure 42: CLSM 100 Up

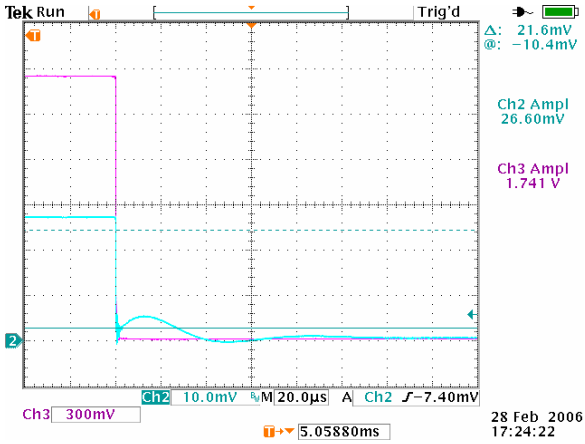

Figure 43: CLSM 100 Down

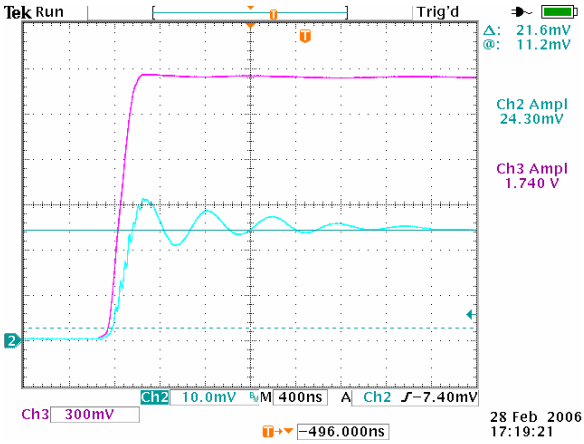

Figure 44: CLSM 100 Zoom

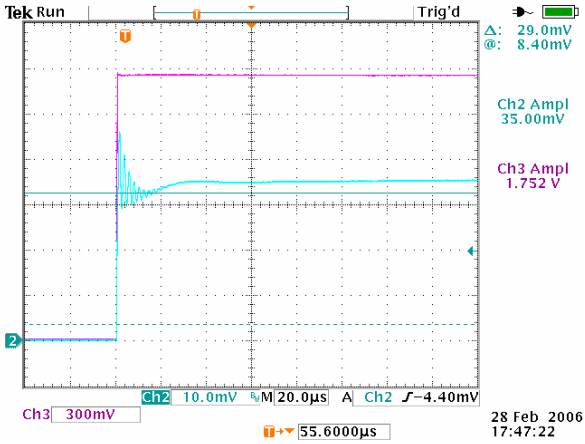

Figure 45: LA 100-P Up

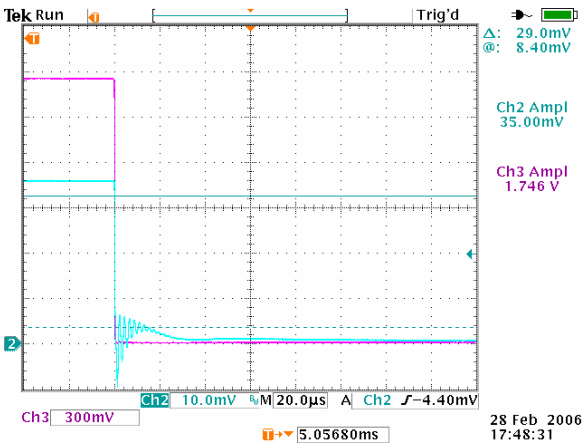

Figure 46: LA 100-P Down

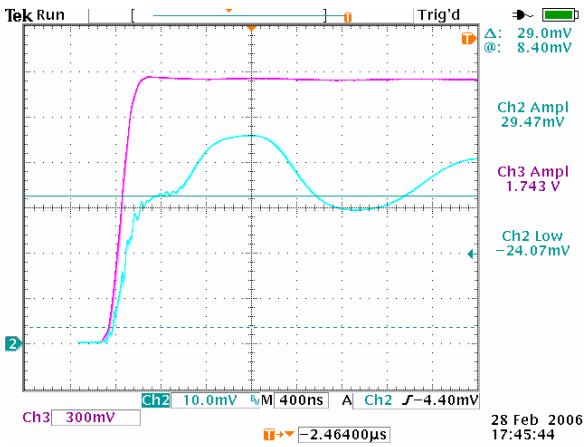

Figure 47: LA 100-P Zoom

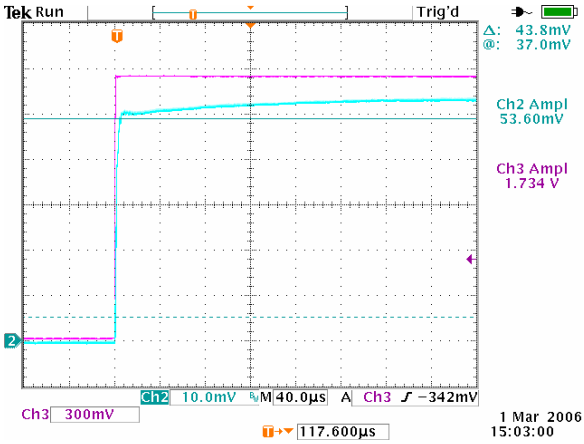

Figure 48: HAS 50-S Up

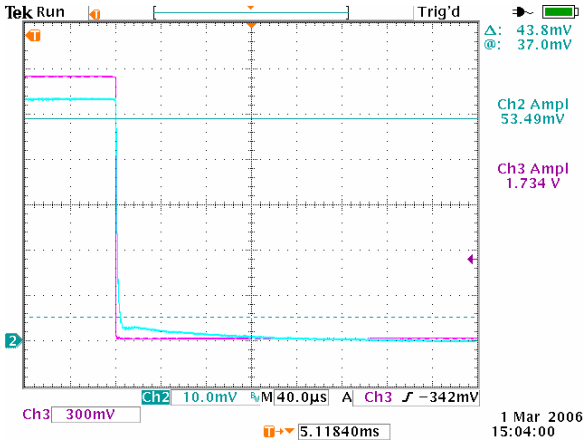

Figure 49: HAS 50-S Down

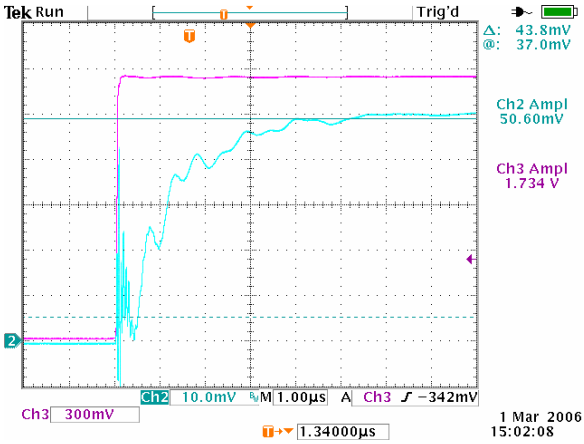

Figure 50: HAS 50-S Zoom

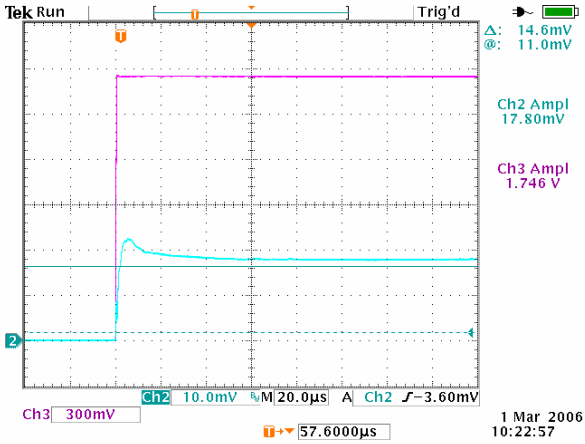

Figure 51: NT-50-3 Up

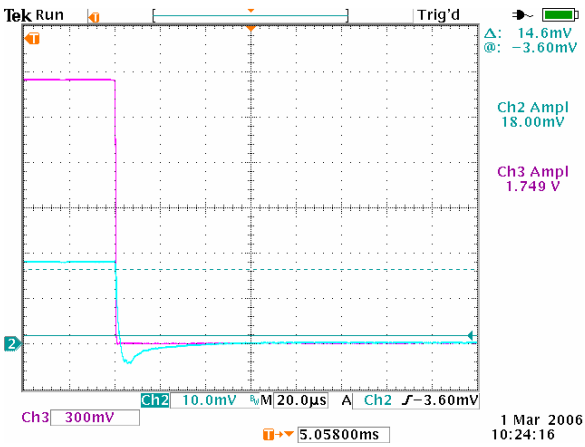

Figure 52: NT-50-3 Down

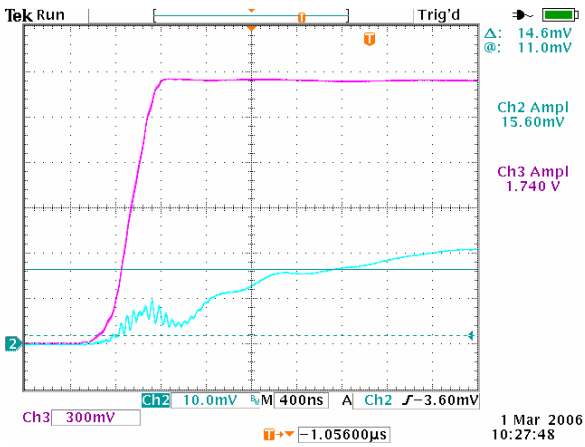

Figure 53: NT-50-3 Zoom

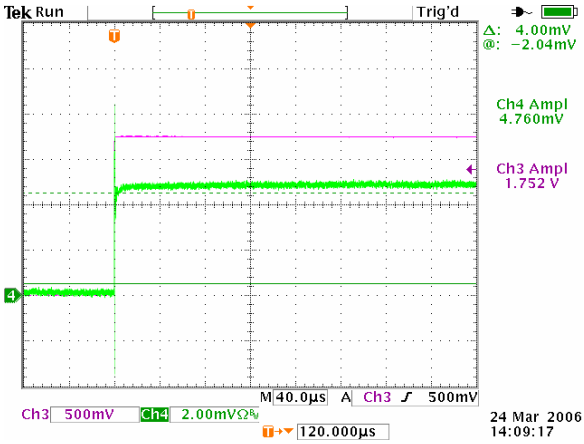

Figure 54: CMR-25-1 Up

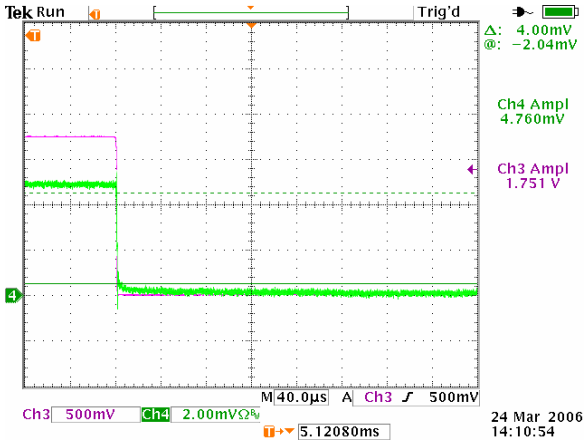

Figure 55: CMR-25-1 Down

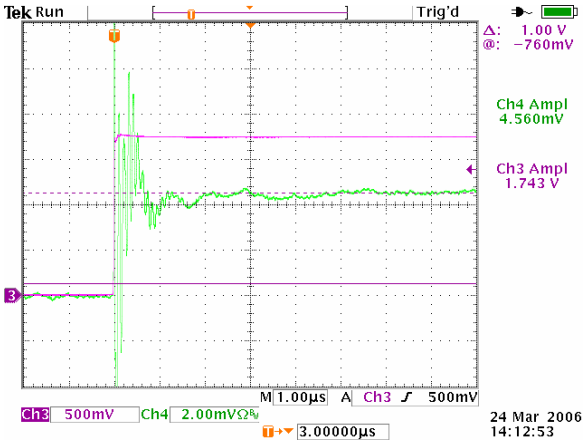

Figure 56: CMR-25-1 Zoom

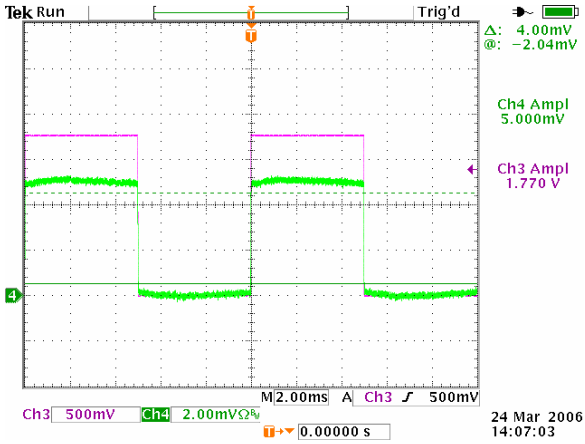

Figure 57: CMR-25-1 Square

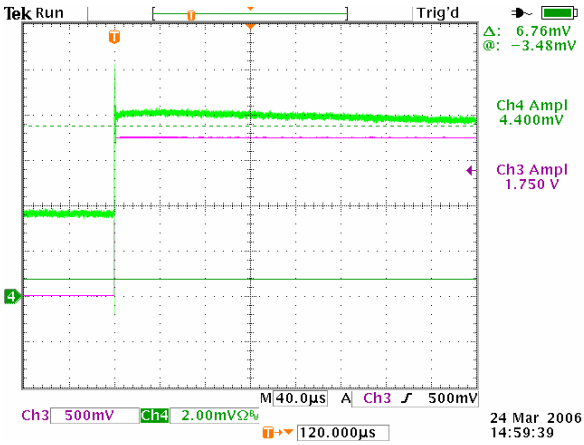

Figure 58: CMR-25-3 Up

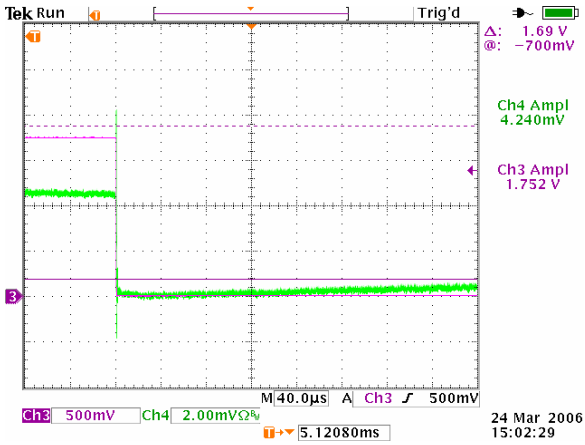

Figure 59: CMR-25-3 Down

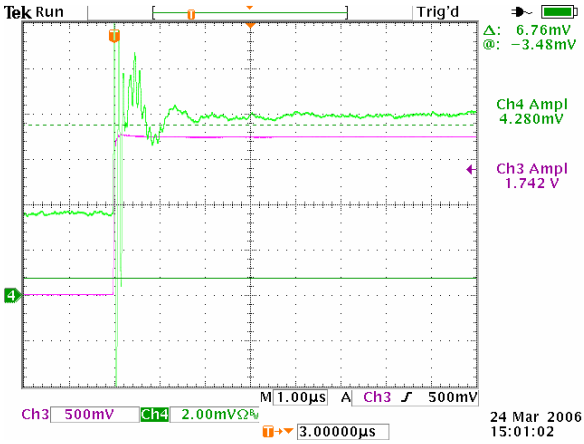

Figure 60: CMR-25-3 Zoom

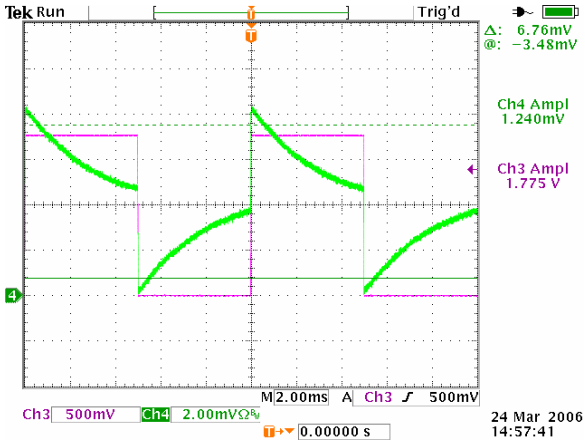

Figure 61: CMR-25-3 Square

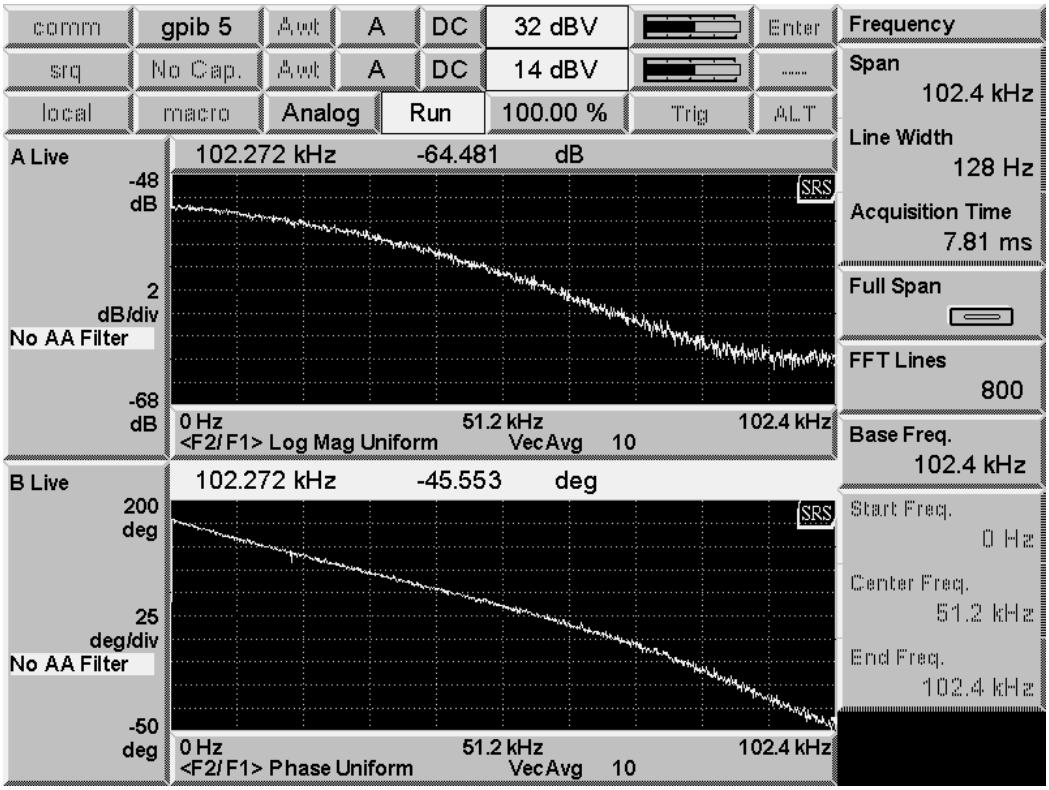

Figure 62: ACS754KCB-150-1: 13 dB, 230 deg.

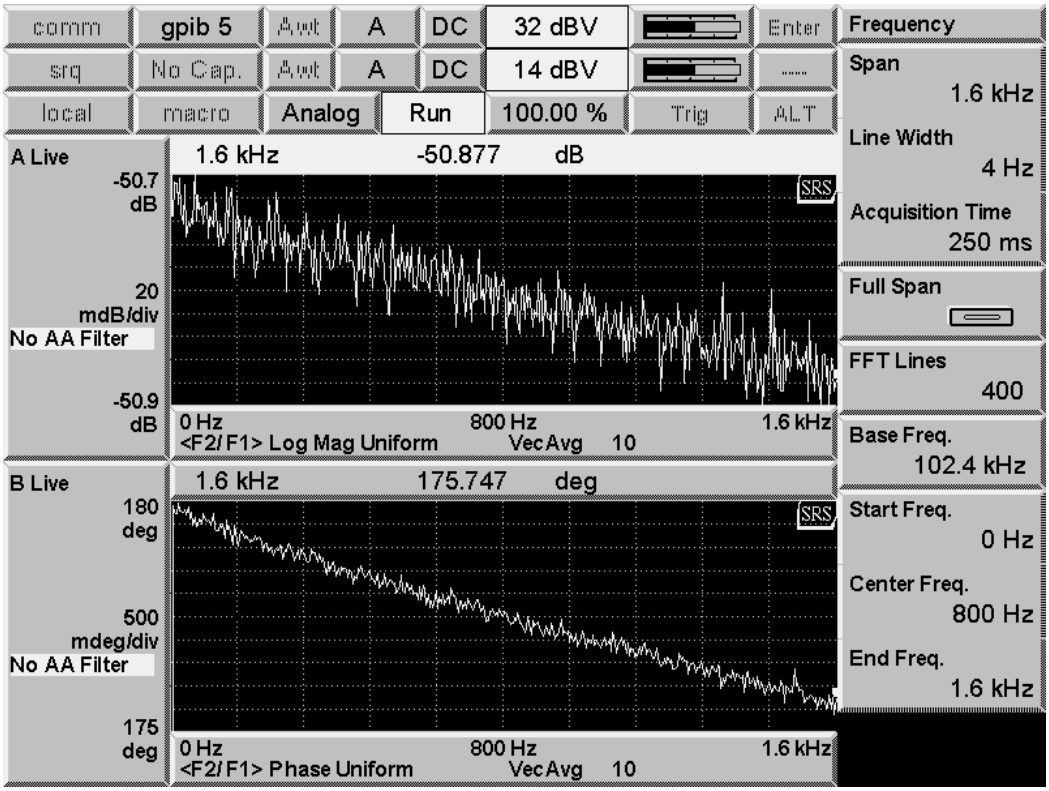

Figure 63: ACS754KCB-150-1 Zoom

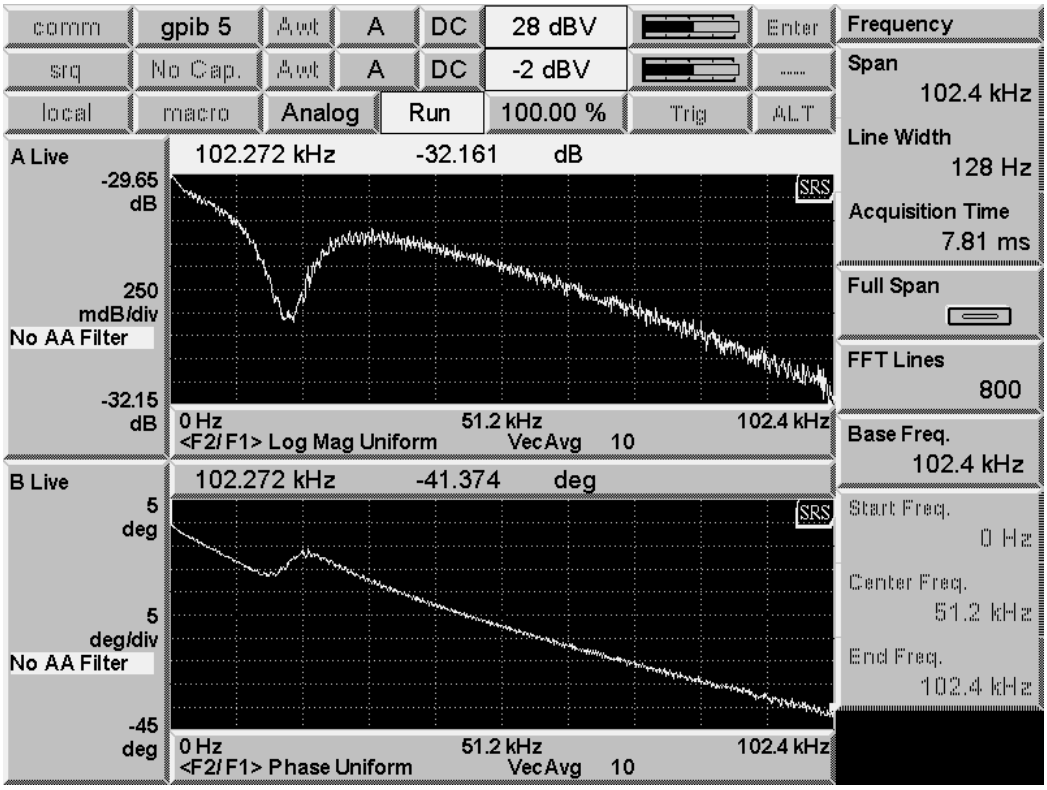

Figure 64: CLN-100: 2,5 dB, 42 deg.

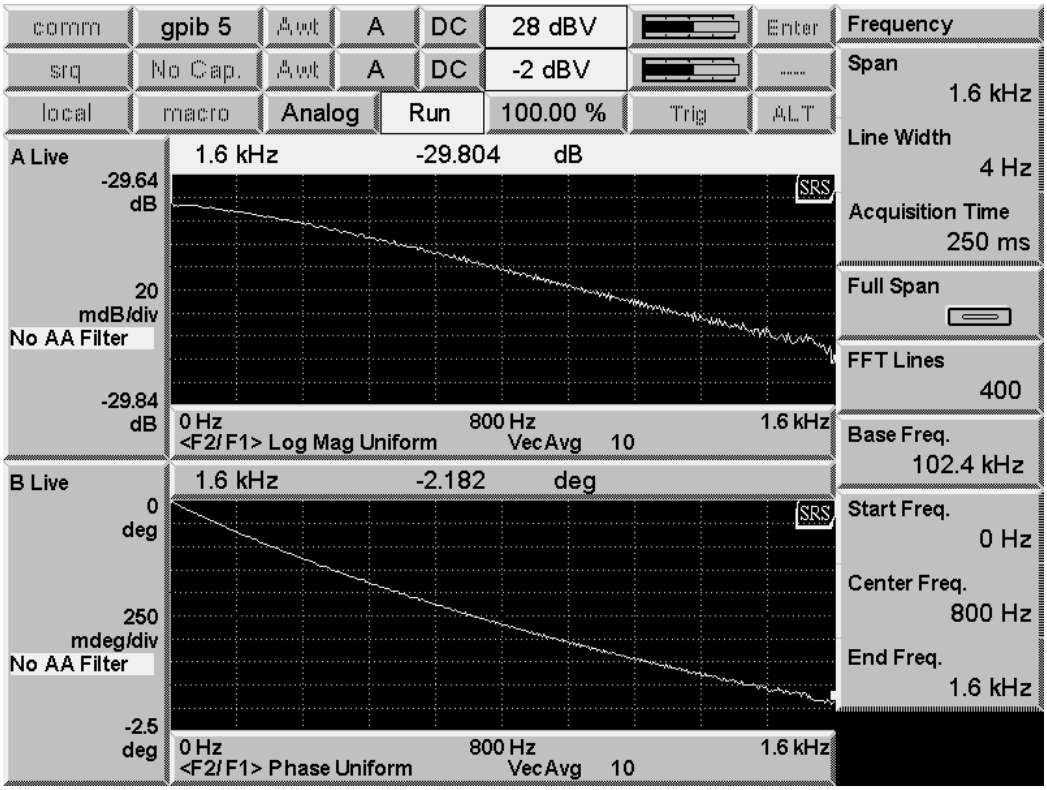

Figure 65: CLN-100 Zoom

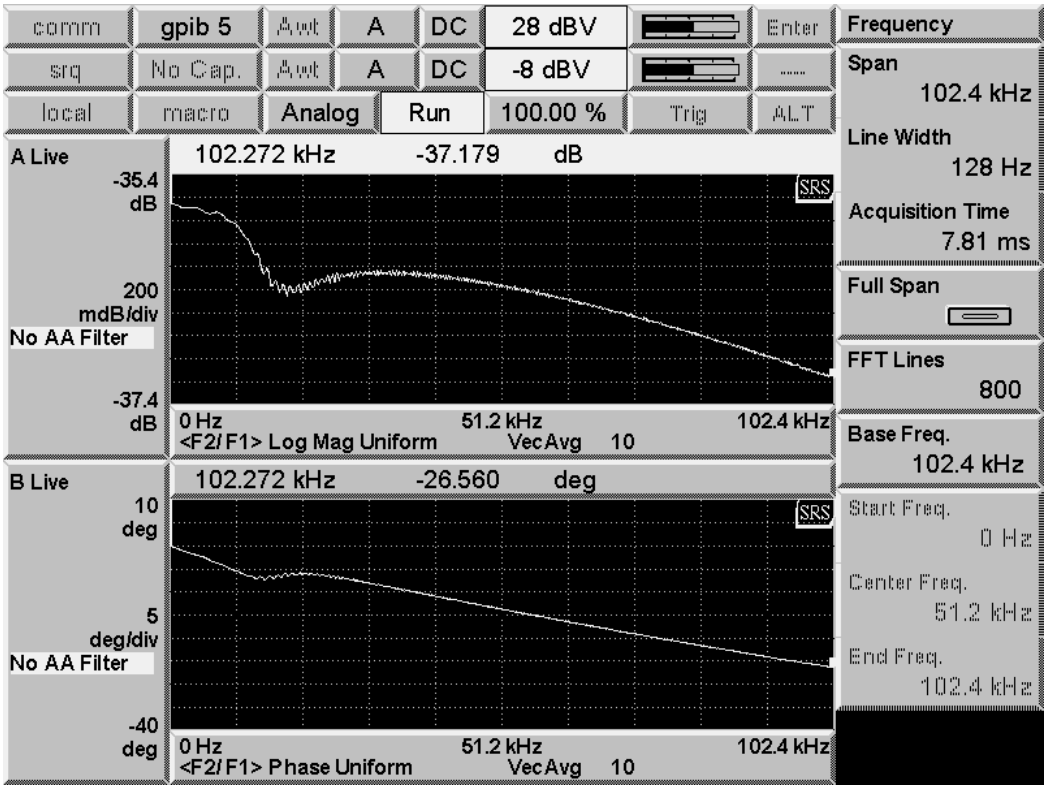

Figure 66: CLSM-100: 1,5 dB, 27 deg.

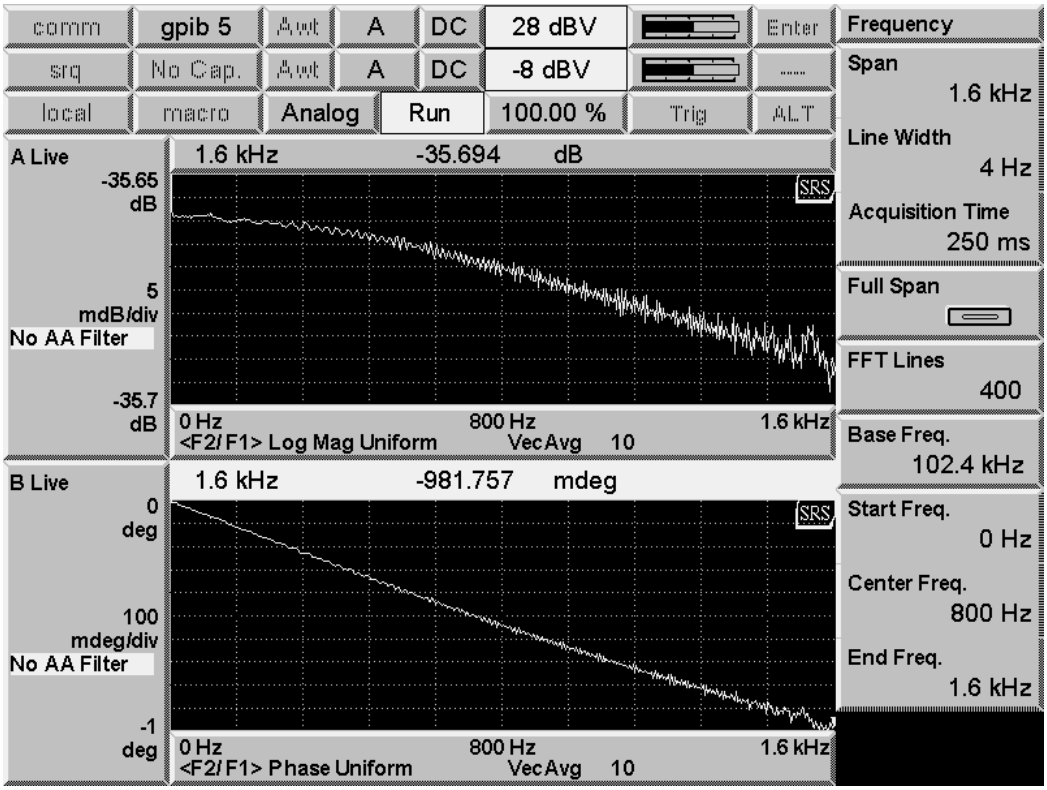

Figure 67: CLSM-100 Zoom

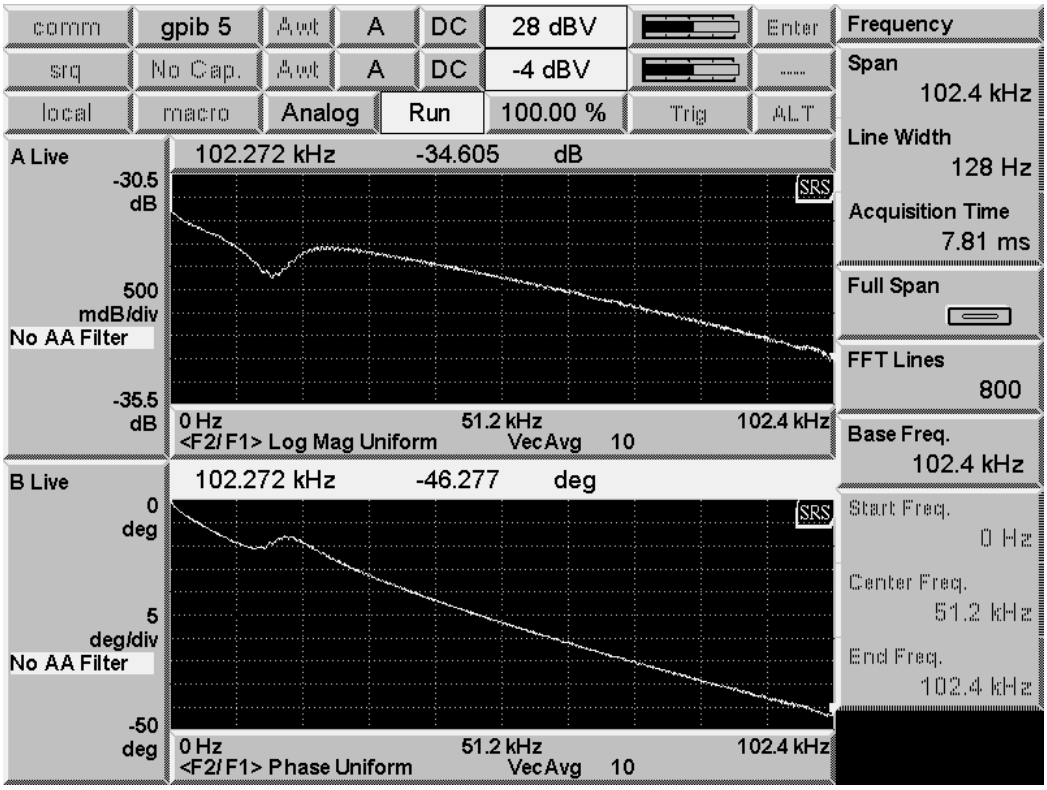

Figure 68: CSNT651-1: 3,2 dB, 47 deg.

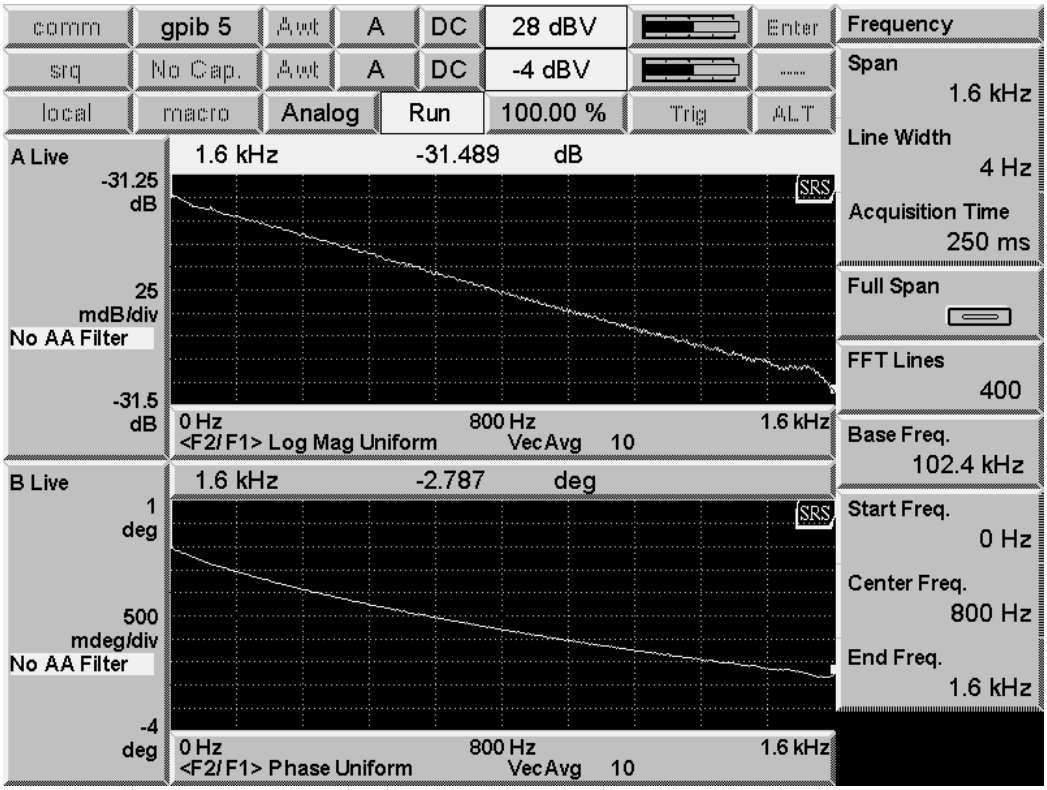

Figure 69: CSNT651-1 Zoom

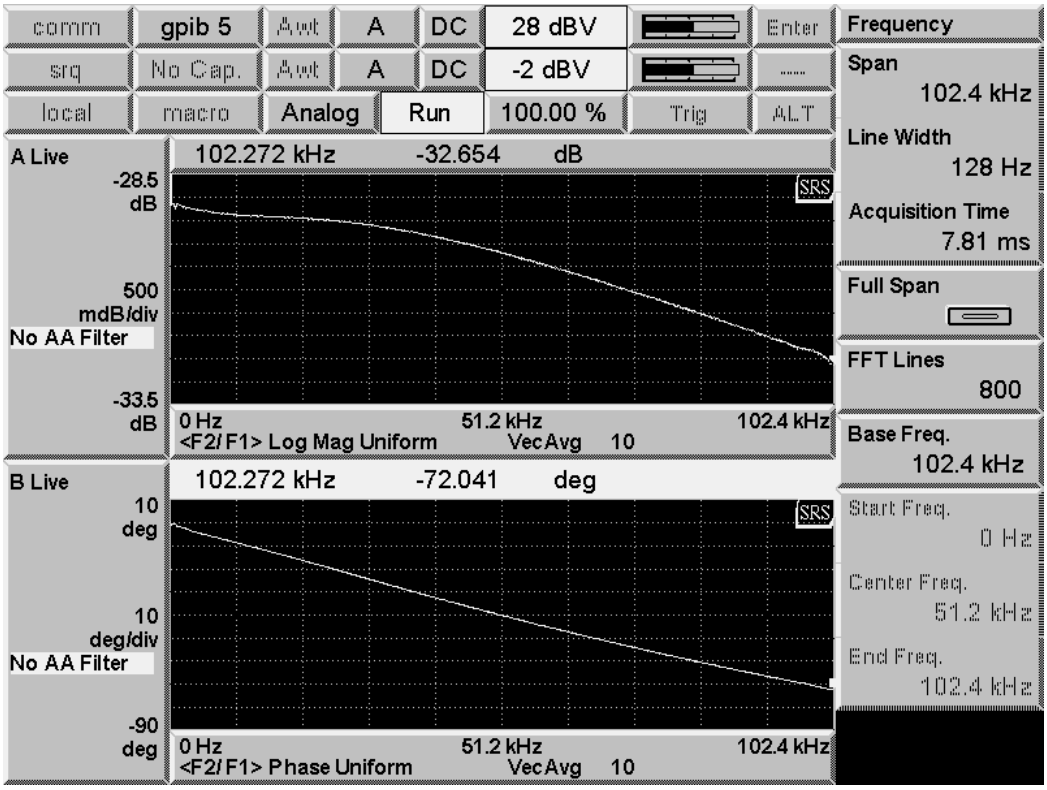

Figure 70: HAS 50-S: 3,5 dB, 72 deg.

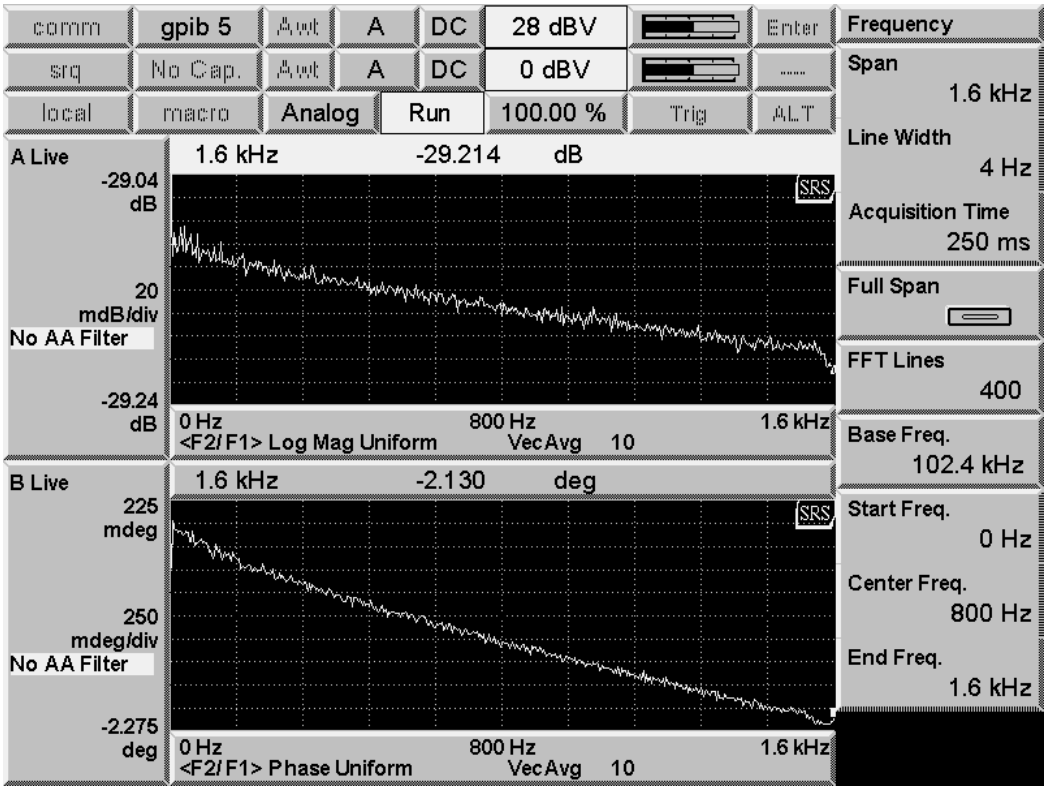

Figure 71: HAS 50-S Zoom

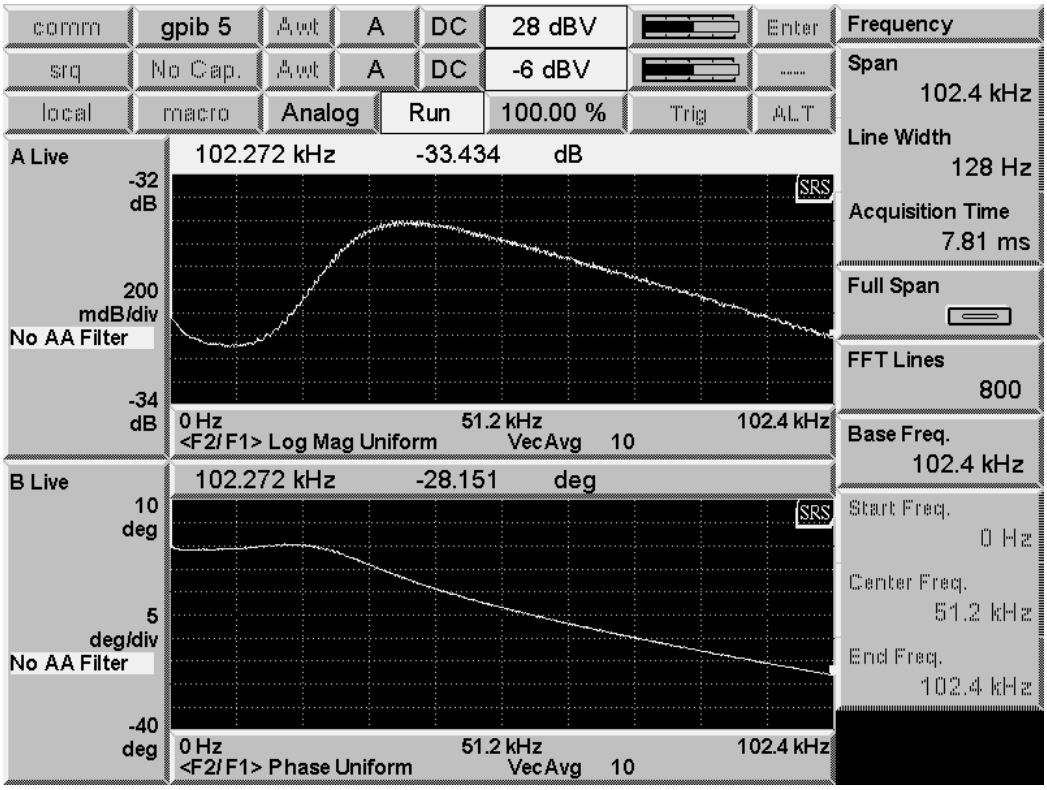

Figure 72: LA 100-P: 0,2 dB (ptp 1,1 dB), 27 deg.

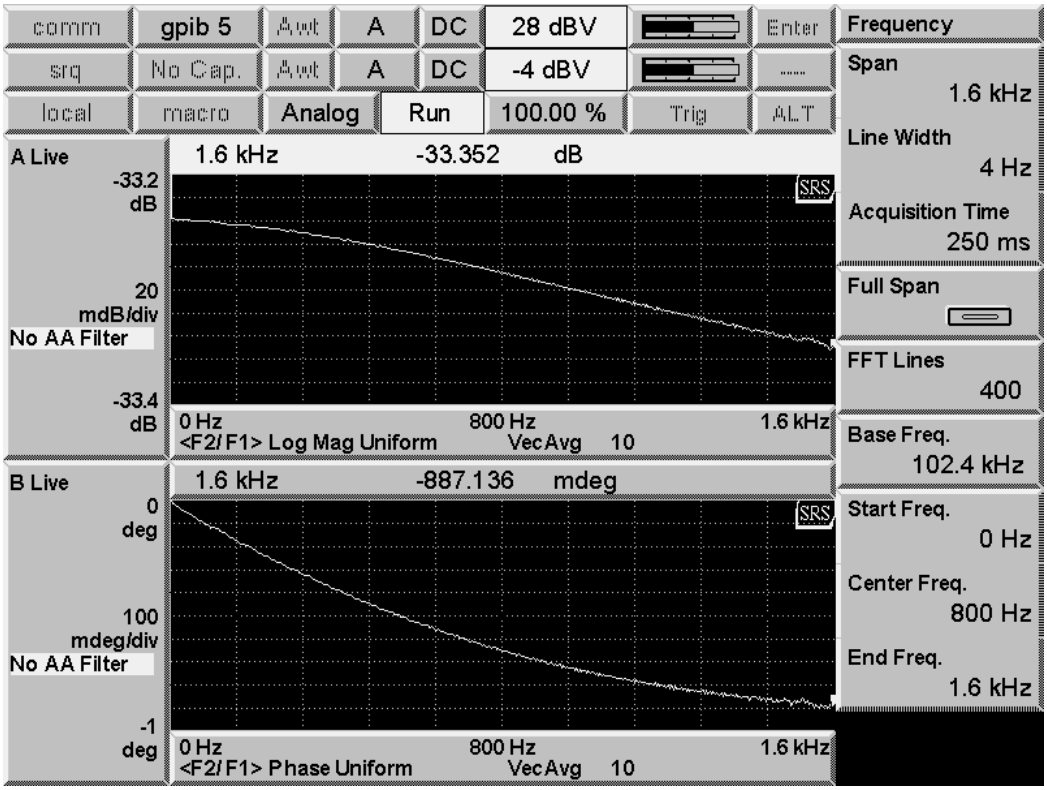

Figure 73: LA 100-P Zoom

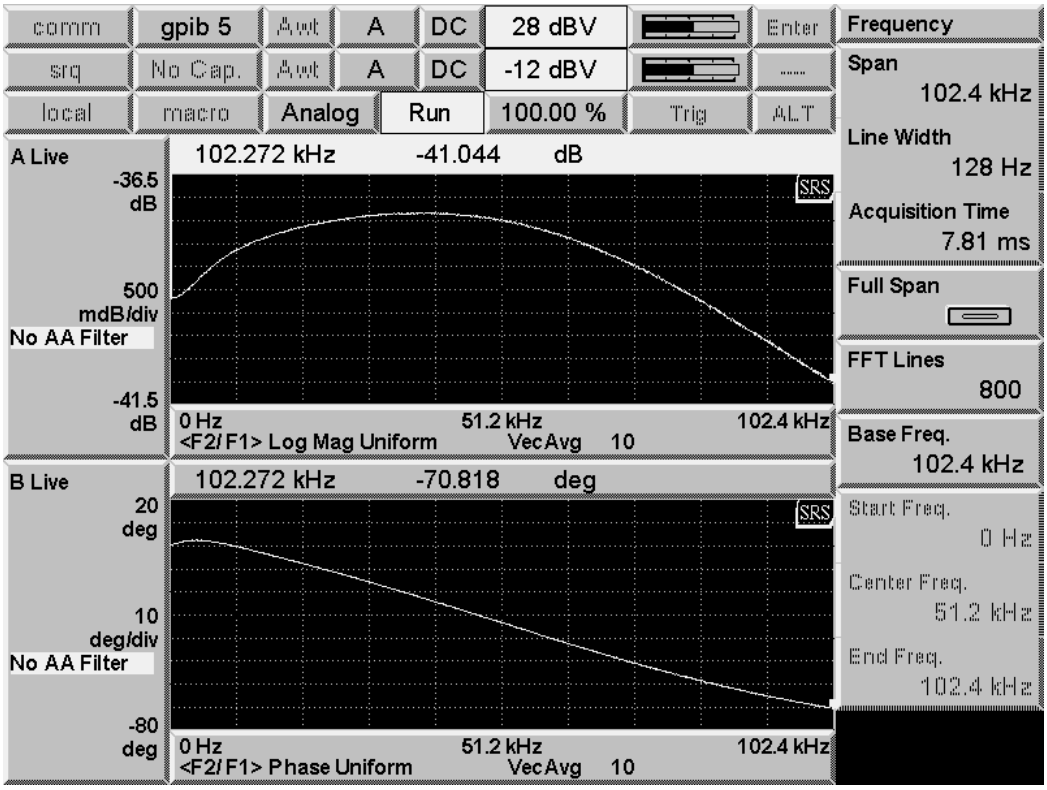

Figure 74: NT-50-3: 1,7 dB (ptp 3,6), 70 deg.

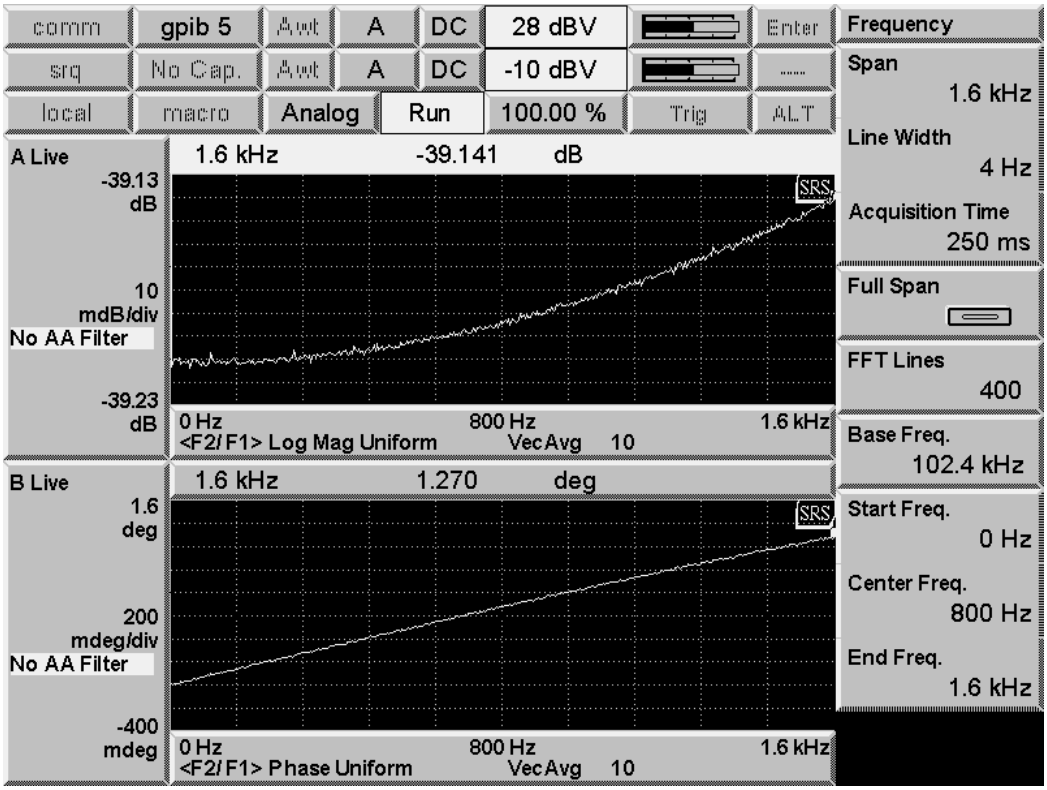

Figure 75: NT-50-3 Zoom

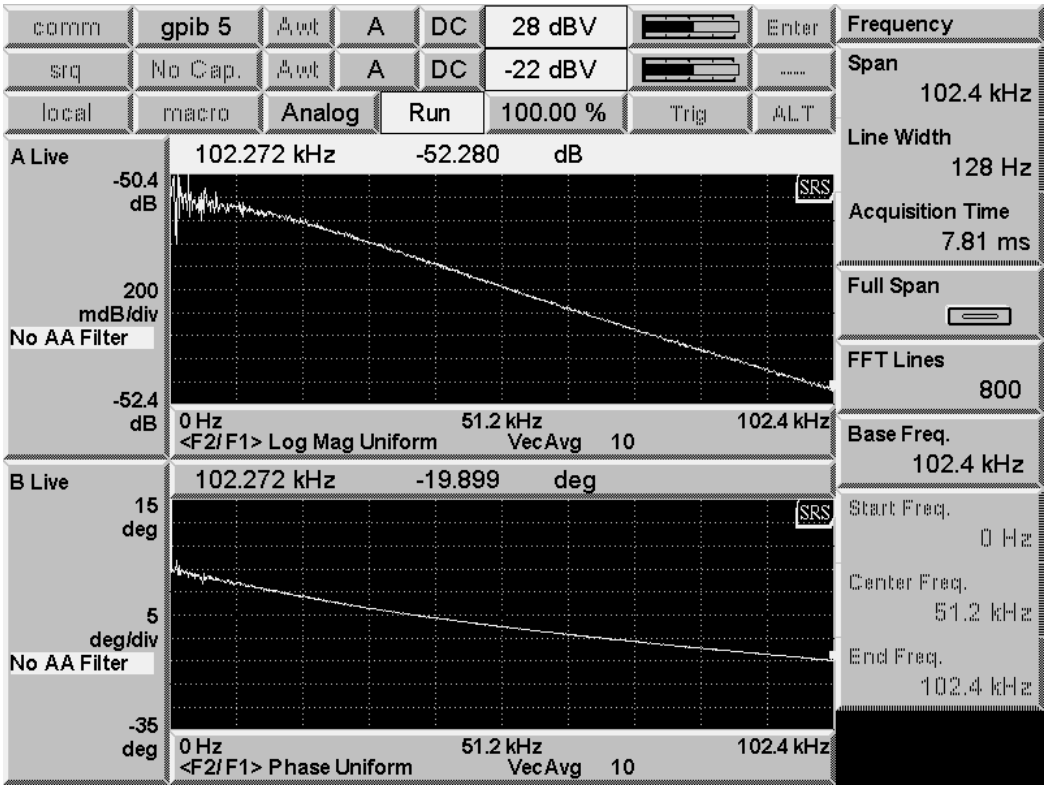

Figure 76: CMR-25-1: 1,6 dB, 20 deg.

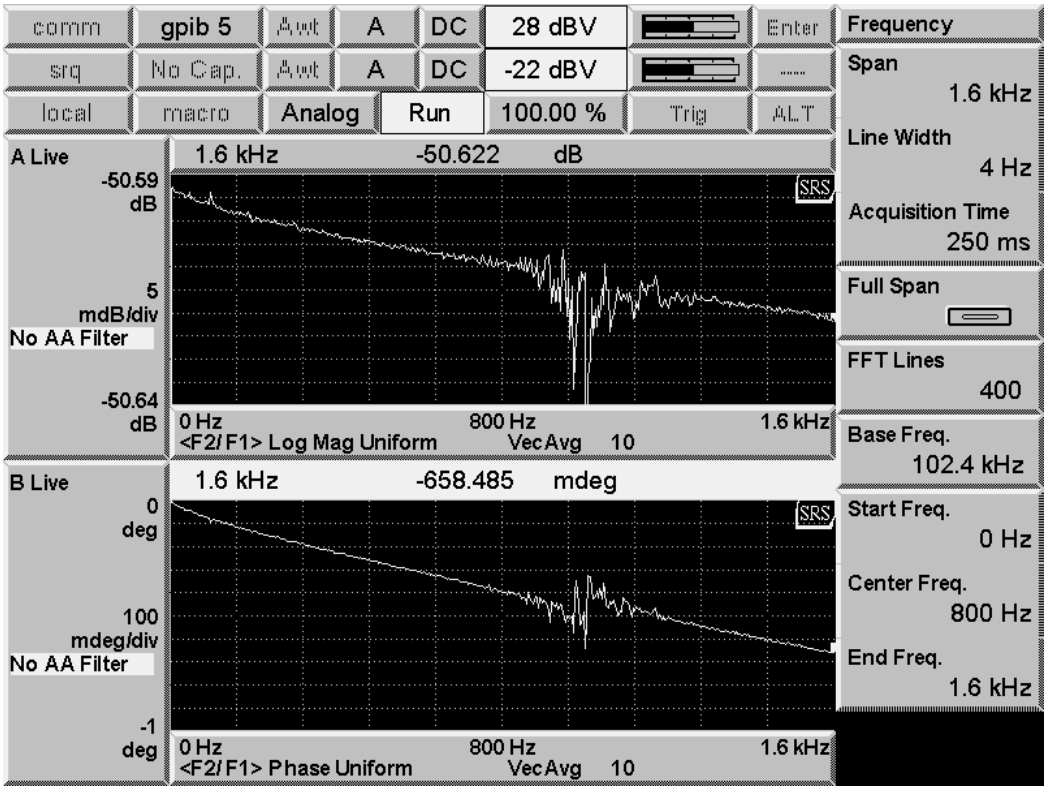

Figure 77: CMR-25-1 Zoom

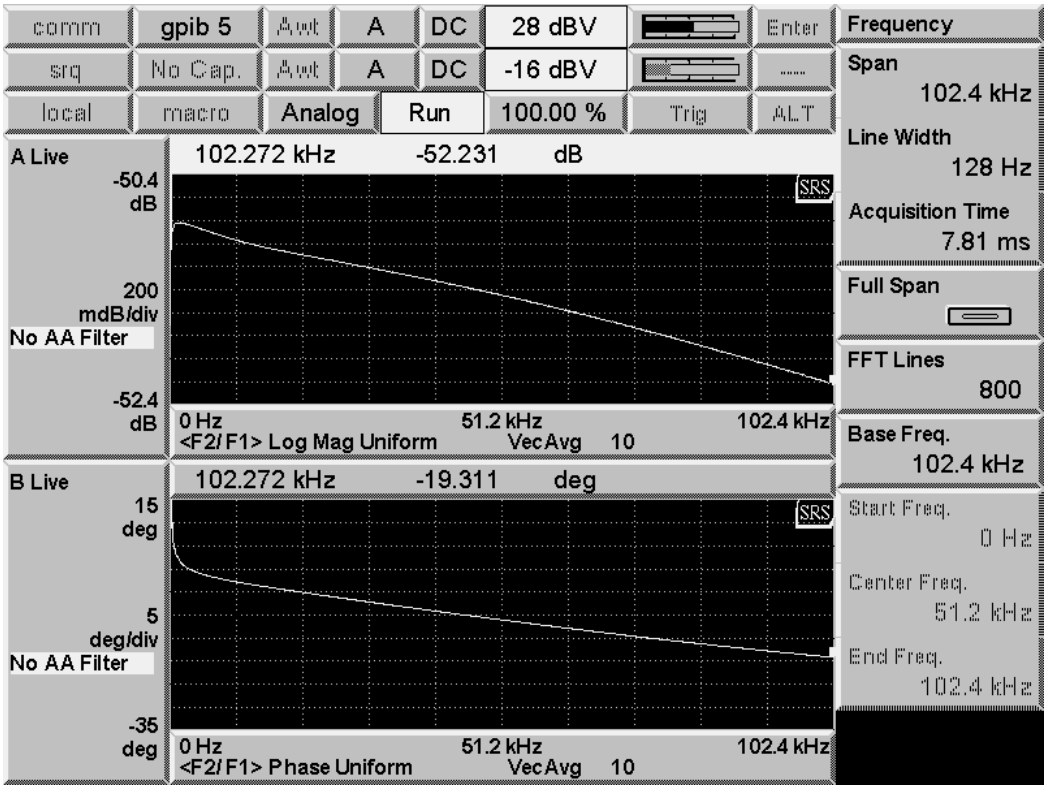

Figure 78: CMR-25-3: 1,4 dB, 100 deg.

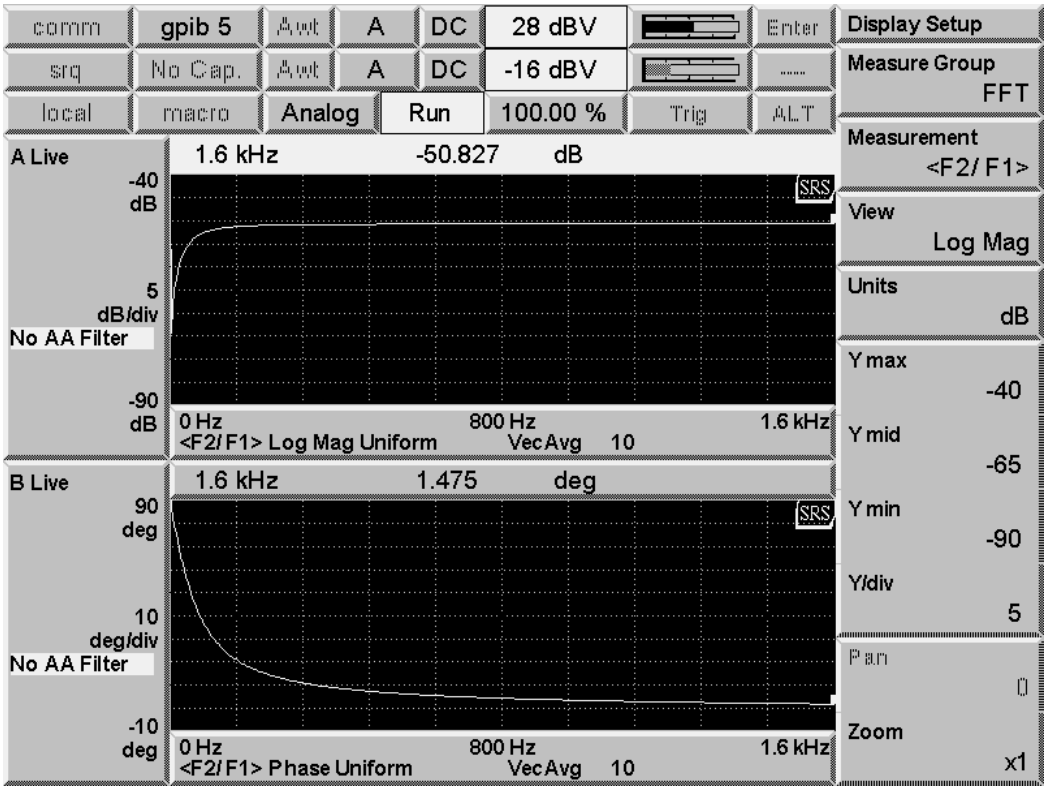

Figure 79:CMR-25-3 Zoom

BIBLIOGRAPHY

[1] Honeywell International Inc. *Hall Effect Sensing and Application.* http://content.honeywell.com/sensing/prodinfo/solidstate/technical/hallbook.pdf, 2005-11-07.

[2] Nordling, Carl; Österman, Jonny. *Physics Handbook for Science and Engineering.* Studentlitteratur, 2002.

[3] Lorrain, Paul; Corson Dale R. *Electromagnetism, Principles and Applications*, 2d ed. W.H. Freeman and Company, 1997.

[4] Ramsden, Ed. *5 Ways of Monitoring Electrical Current.* http://www.sensorsmag.com/articles/0799/26/main.shtml, 2005-11-07.

[5] Honeywell. *Magnetic Current Sensing.* http://www.ssec.honeywell.com/magnetic/datasheets/an209.pdf, 2005-11-15.

[6] Emerald, *Paul. 'Non-intrusive' Hall-effect current-sensing techniques provide safe, reliable detection and protection for power electronics.* http://www.allegromicro.com/techpub2/stp/stp98-1.pdf, 2005-11-18.

[7] Checkelsky, Joe. *Anisotropic Magnetoresistance of* $Fe_xCo_{1-x}S_2$. Harvey Mudd College 2004-04-30. http://www2.hmc.edu/~eckert/research/JCHECKELSKY.pdf, 2005-11-30.

[8] Popovic, Radivoje S.; Drljaca, Predrag M.; Schott, Christian; Racz, Robert. *Integrated Hall sensor/Flux Concentrator Microsystems.* Sentron, 2001-10. http://www.sentron.ch/support/techpapers.htm, 2005-12-07.

[9] Caruso, Michael J.; Bratland, Tamara ; Smith, Carl H.; Schneider, Robert. *Anisotropic Magnetoresistive Sensors Theory and Applications*, 1999-03. http://www.sensorsmag.com/articles/0399/0399_18/main.shtml, 2005-12-08.

[10] Philips Semiconductors. *Magnetoresistive Sensors for Magnetic Field Measurement*, 200-09-06. http://www.zmd.de/pdf/magnetoresistive.pdf, 2005-12-08.

[11] Lemme, Helmuth; Friedrich, Andreas P.; Victor, Alfred. *The Universal Current Sensor*, 200-05. http://www.sensitec.de/downloads/122/97/Universal_Current_Sensor_E.pdf, 2005-12-09.

[12] Drafts, Bill. *New Magnetoresistive Current Sensor Improves Power Electronics Performance*, 1999-09. http://www.sensorsmag.com/articles/0999/84/main.shtml, 2005-12-12.

[13] Honeywell. *Set/Reset Function for Magnetic Sensors*. http://www.ssec.honeywell.com/magnetic/datasheets/an213.pdf, 2005-12-13.

[14] Caruso, Michael J.; Bratland, Tamara ; Smith, Carl H.; Schneider, Robert. *A New Perspective on Magnetic Field Sensing*. http://www.ssec.honeywell.com/magnetic/datasheets/new_pers.pdf, 2005-12-14.

[15] Charlton, Timothy R. *Growth, Characterization, and Properties of Co/Re Superlattices*. http://www.as.wvu.edu/phys/mbe/theses/charlton.pdf, 2006-02-20.

[16] Harris, Randy. *Nonclassical Physics, beyond Newton's view*. Addison-Wesley, 1998.

[17] Blundell, Stephen. *Magnetism in Condensed Matter*. Oxford Univ. Press, 2001.

[18] Polman, Perry A. *Magnetoresistance (MR) Transducers: And How to Use Them as Sensors*, 1st ed, Honeywell International Inc, 2004. http://content.honeywell.com/sensing/prodinfo/solidstate/technical/mr_appbook.pdf, 2006-02-22.

GLOSSARY

AMR Anisotropic MagnetoResistance

ASIC Application Specific Integrated Circuit

CL Closed Loop, the output are connected to the input. In this thesis CL refer to Closed Loop components with toroidal core.

HED Hall-Effect Device

HVDC High Voltage Direct Current. A power transmission technique using DC current instead of AC.

IC Integrated Circuit

IMC Integrated Magnetic Concentrator

MACH2 Modular Advanced Control HVDC. The second generation of MACH™, a control and protection system for HVDC Stations.

OL Open Loop, the output are not connected to the input. In this thesis OL refer to Open Loop components with toroidal core.

PCB Printed Circuit Board

PTPS Power Technologies Power Systems

Ratiometric The sensitivity are proportional to power supply.

Scattering In this context, the term "scattering" refers to the change in direction of a particle because of a collision with another particle or system.

Thin film Very thin layer of a material. Thickness of microscopic dimensions. Often somewhat different material characteristics then with bulk dimensions.